# SECOND WORKSHOP ON STABILITY AND OPERATIONAL SAFETY OF SHIPS

PREPRINT DRAFT PAPERS

NOVEMBER 18−19, 1996

OSAKA UNIVERSITY

Department of
Naval Architecture and Ocean Engineering

2-1 Yamada-oka, Suita, Osaka 565, Japan

SECOND WORKSHOP ON STABILITY
AND
OPERATIONAL SAFETY OF SHIPS

ORGANIZING COMMITTEE

Prof. Masami Hamamoto
(Coordinator)
Osaka University

Prof. Dracos Vassalos
University of Strathclyde

Prof. Michael Thompson
University College London

Prof. Yoshiho Ikeda
Osaka Prefecture University

Dr. Iwao Watanabe
Ship Research Institute

Dr. Naoya Umeda
National Research Institute of Fisheries Engineering

SECOND WORKSHOP ON STABILITY
AND
OPERATIONAL SAFETY OF SHIPS

PREPRINT DRAFT PAPERS

INTACT STABILITY

A Study on Capsizing Phenomena of a Ship in Waves
by Sa-Young Hong, Chang Gu Kang and S.W. Hong (Korea Research Institute of Ships and Ocean Engineering)

DAMAGE STABILITY

SESSION 4 CAPSIZE MODEL EXPERIMENTS WITH A DAMAGED SHIP
MODEL
Discussion Leader : Dr. Tor Egil Svensen (Det Norske Veritas)

Damage Stability with Water on Deck of a Ro-Ro Passenger Ship in Waves
by Shigesuke Ishida, Sunao Murashige, Iwao Watanabe, Yoshitaka Ogawa and Toshifumi
Fujiwara (Ship Research Institute)

Characteristics of Roll Motion for Small Fishing Boats
by Kiyoshi Amagai (Hokkaido University), Kimihiko Ueno (Tokyo University of Fisheries)
and Nobuo Kimura (Hokkaido University)

SESSION 5 DYNAMICS OF SHIP CAPSIZE WITH FLOODED INTERNAL
SPACE INCLUDING CARGO SHIFT
Discussion Leader : Prof. Apostolos Papanikolaou (National Technical University
Athens)

Assessment of Survival Time for Damaged Passenger/Ro-Ro Vessels
by Dracos Vassalos (University of Strathclyde)

Dynamics of a Ship with Partially Flooded Compartment
by Jan O de Kat (Marine Research Institute Netherlands)

The Use of Physical Models to Predict the Capsize of Damaged Ships in Waves
by David Molyneux (National Research Council Canada)

SESSION 6 PROBABILISTIC APPROACH TO DAMAGE STABILITY AND
SURVIVABILITY ASSESSMENT
Discussion Leader : Dr. Iwao Watanabe (Ship Research Institute)

by Robert Tagg (Herbert Engineering Co., USA)

About Safety Assessment of Damaged Ships
by Roby Kambisseri and Yoshiho Ikeda (Osaka Prefecture University)

PARTICIPANTS FOR SECOND WORKSHOP
NOVEMBER 18 – 19, 1996

1 Prof. Kiyoshi Amagai
   Dept. Fishing Vessel Technology,
   Faculty of Fisheries,
   Hokkaido University,
   3-1-1 Minatomachi, Hakodate-shi,
   Hokkaido 041, Japan
   Tel. +81-138-40-8836
   Fax +81-138-43-5015

2 Mr. Aage Damsgaard
   Danish Maritime Institute
   Hjortekaersvej 99,
   2800 Lyngby, Denmark
   Tel
   Fax

3 Mr. Takashi Enomoto
   Dept. of Naval Architecture and
   Ocean Engineering, Osaka University,
   2-1 Yamada-oka, Suita,
   Osaka 565, Japan
   Tel. +81-6-877-5111 Ext. 3504
   Fax +81-6-878-5364
   Email:enomoto@naoe.eng.osaka-u.ac.jp

4 Prof. Alberto Francescutto
   Dept. of Naval Architecture
   Univ. of Trieste, Via A. Valerio 10
   34127 Trieste, Italy
   Tel. +39-40-6763425,
   Fax +39-40-6763443
   Email:francesc@univ.trieste.it

5 Prof. Masataka Fujino
   Dept. of Naval Architecture and
   Ocean Engineering, Univ. of Tokyo,
   7-3-1 Hongo, Bunkyo-ku
   Tokyo 113, Japan
   Tel. +81-3-3812-2111 Ext. 6540
   Fax +81-3-3815-8360

6. Dr. Stefan Grochowalski
   National Research Council,
   Montreal Road, Bldg. M-22,
   Ottawa, Ont. KIA OR6, Canada
   Tel. +1-613-993 8958
   Fax +1-613-998 5701
   Email:STEFAN.GROCHOWALSKI@nrc.ca

7 Prof. Masami Hamamoto
   Dept. of Naval Architecture and
   Ocean Engineering, Osaka University,
   2-1 Yamada-oka, Suita,
   Osaka 565, Japan
   Tel. +81-6-879-7587, Fax +81-6-878-5364
   Email:hamamoto@naoe.eng.osaka-u.ac.jp

8 Prof. Kazuhiko Hasegawa
   Dept. of Naval Architecture and
   Ocean Engineering, Osaka University,
   2-1 Yamada-oka, Suita,
   Osaka 565, Japan
   Tel. +81-6-879-7588, Fax +81-6-878-5364
   Email:hase@naoe.eng.osaka-u.ac.jp

9 Dr. Masayoshi Hirano
   Mitsui Akishima Laboratory,
   1-50 Tsutsujiga-oka 1-Chome,
   Akishima City, Tokyo 196, Japan
   Tel. +81-425-45-3111,
   Fax +81-425-45-3113

10 Prof. Tsugukiyo Hirayama
   Yokohama National University,
   Tokiwadai-156, Hodogaya-ku,
   Yokohama, Japan
   Tel. +81-45-335-1451 Ext. 2792
   Fax +81-45-335-0496

11 Mr. H-s Gao
   China Ship Scientific Centre
   P.O Box 116,
   Wuxi, Jangsu 214082,
   People Republic of China
   Tel. (0510) 580 2131 - 589,
   Fax (0510) 580 1164

12 Dr. Sa-Young Hong
   Korea Research Institute of Ships a).
   and Ocean Engineering
   P.O Box 1, Taeduk Science Town,
   Tel. +82-42-868-7260,
   Fax. +82-42-868-7711

13 Dr. Do Chun Hong
   Director of Hydrodynamic Group,
   Maritime Research Institute,
   Hyundai Heavy Industry Co., Ltd.,
   1, Cheonha-Dong, Dong-ku, Ulsan, Korea
   Tel. +82-522-30-2063, 32-0223
   Fax +82-522-30-3410/(82,522) 30-3410

14 Prof. Yoshiho Ikeda
   Osaka Prefecture University,
   1-1 Gakuen-cho, Sakai,
   Osaka 593, Japan
   Tel. +81-722-52-1161 ext. 3369,
   Fax +81-722-59-3340
   Email:ikeda@marine.osakafu-u.ac.jp

15 Prof. Kinzo Inoue
   Kobe University of the Mercantile Marine,
   5-1-1 Fukaeminami-machi,
   Higashinada-ku, Kobe 658, Japan
   Tel. +81-78-431-6251, Fax +81-78-431-6254

16 Prof. Yoshiyuki Inoue
   Yokohama National University,
   Tokiwadai-156, Hodogaya-ku,
   Yokohama, Japan
   Tel. +81-45-335-1451, Fax +81-45-335-0496

17 Mr. Shigesuke Ishida
   Ship Research Institute,
   6-38-1 Shinkawa, Mitaka-city, Tokyo 181, Japan
   Tel. +81-422-41-3057
   Fax +81-422-41-3056

18 Mr. Kinya Ishibashi
   Dept. of Naval Architecture and
   Ocean Engineering, Osaka University,
   2-1 Yamada-oka, Suita,
   Osaka 565, Japan
   Tel. +81-6-877-5111 Ext. 3504
   Fax +81-6-878-5364
   Email:kinya@naoe.eng.osaka-u.ac.jp

19 Dr. Jan O. de Kat
   a) Marin, The Netherlands
   P.O Box 28, 6700AA Wageningen,
   Netherlands
   Tel. +31-317-493-405,
   Fax +31-317-493-245

   b) David Taylor Model Basin,
   NSWC, Carderock Division
   Seakeeping Department, Code 5500
   Building 18, Rm. 101A
   Bethesda, MD 20084-5000, USA
   Fax +1-301-227 3197
   Email:jdkat@baanvx.marin.nl

20 Prof. Keiichi Karasuno
   Dept. of Fishing Technology,
   Faculty of Fisheries,
   Hokkaido University,
   3-1-1 Minatomachi, Hakodate-shi,
   Hokkaido 041, Japan
   Tel. +81-138-40-8836
   Fax +81-138-43-5015

21 Mr. Masuo Kikusui
   Nippon Kaiji Kyoukai,
   4-7 Kioi-cho, Chiyoda-ku,
   Tel. +81-3-3230-1201
   Fax +81-3-3230-2232

22 Mr. Hyun Seok Kim
   Dept. of Ship and Marine Technology
   University of Strathclyde,
   100 Montrose Road, Glasgow G4 OLZ
   Scotland, UK
   Tel. +44-141-552-4400 ext. 3462
   Fax +44-141-552-2879
   Email:clhr@ccsun.strath.ac.uk

23 Mr. Toru Katayama
   Osaka Prefecture University,
   1-1 Gakuen-cho, Sakai,
   Osaka 593, Japan
   Tel. +81-722-52-1161 Ext. 3369
   Fax +81-722-59-3340
   Tel. +81-722-52-1161 Ext. 3369
   Fax +81-722-59-3340

24 Dr. Masashi Kashiwagi
   Research Institute for Applied Mechanics,
   Kyushu University, Kasuga City,
   Fukuoka 816, Japan
   Tel.   Fax

25 Dr. Yoon-Soo Kim
   Shipbuilding and Offshore Division,
   Koje Shipyard, Samsung Heavy Industry,
   530 Jangpyung-RI, Sinhyun-Up,
   Koje-Gun, Kyungnam, Korea 656 800
   Tel. +82-558-30-4731,
   Fax +82-558-30-4956

26 Prof. Takeshi Kinoshita
   Institute of Industrial Science,
   University of Tokyo,
   7-22-1 Roppongi, Minato-ku,
   Tokyo 106, Japan
   Tel. +81-3-3402-6231 ext. 2295
   Fax +81-3-3479-0294

27 Prof. Katsuro Kijima
   Kyushu University,
   6-10-1, Hakozaki, Higashi-ku,
   Fukuoka City, Fukuoka 812, Japan
   Tel. +81-92-641-1101,
   Fax +81-92-632-1560

28 Prof. Sun-Hong Kwon
   Pusan National University,
   30, Jang Jun-dong, Dong Raer-ku,
   Pusan, 609-735, Korea
   Tel. +82-51-510-2347,
   Fax +82-51-512-8836

29 Prof. Seung-Joon Lee
   Dept. of Naval Architecture and
   Ocean Engineering, College of Engineering,
   Chungnam National University,
   Daeduk Science Town 305-764, Korea
   Tel. +82-42-821-6627, Fax +82-42-823-5437
   Email:sjlee@naoe.chungnam.ac.kr

30 Prof. Gyoung-Woo Lee
   Faculty of Engineering and
   Naval Architecture,
   Mokpo National Maritime University,
   571, Jukgyo-dong, Mokpo,
   Chonnam 530-729, Korea
   Tel.
   Fax +82-631-42-5176

31 Mr. Luca Letizia
   Dept. of Ship and Marine Technology,
   University of Strathclyde,
   100 Montrose Street, Glasgow G4 OLZ,
   Scotland, UK
   Tel. +44-141-552-4400,
   Fax +44-141-552-2879

32 Prof. Hisaaki Maeda
   Institute of Industrial Science,
   University of Tokyo,
   7-22-1, Roppongi, Minato-ku,
   Tokyo 106, Japan
   Tel. +81-3-3402-6231 ext. 2295
   Fax +81-3-3479-0295

33 Mr. Akihiko Matsuda
   National Research Institute of
   Fisheries Engineering,
   Ebidai, Hasaki-machi,
   Ibaraki, 314-04, Japan
   Tel. +81-479-44-5943,
   Fax +81-479-44-6221

34 Dr. Jerzy Matusiak
   Helsinki University of Technology,
   Laboratory of Naval Architecture,
   Otakaari 4, SF-02150 Espoo,
   Helsinki, Finland
   Tel. +358-0-451-3480,
   Fax +358-0-451-3419
   Email:Jerzy.Matusiak@hut.fi

35 Dr. Sunao Murashige
   Ship Research Institute
   6-38-1, Shinkawa, Mitaka City,
   Tokyo 181, Japan
   Tel. +81-422-41-3058,
   Fax +81-422-41-3056

36 Mr. David Molyneux
National Research Council of Canada,
Institute for Marine Dynamics,
P.O Box 12093, Postal Stat. "A",
St. John's Newfoundland - A1B 3XS
Canada,
Tel.   Fax

37 Prof. Shigeru Naito
Dept. of Naval Architecture and
Ocean Engineering, Osaka University,
2-1 Yamada-oka, Suita,
Osaka 565, Japan
Tel. +81-6-879-7572, Fax +81-6-878-5364
Email:naito@naoe.eng.osaka-u.ac.jp

38 Prof. Emeritus Kensaku Nomoto
Dept. of Naval Architecture and
Ocean Engineering, Osaka University,
2-1 Yamada-oka, Suita,
Osaka 565, Japan
Tel. +81-6-879-7588, Fax +81-6-878-5364

39 Mr. James P. Panjaitan
Dept. of Naval Architecture and
Ocean Engineering, Osaka University,
2-1 Yamada-oka, Suita,
Osaka 565, Japan
Tel. +81-6-877-5111, Fax +81-6-878-5364
Email:panjaita@naoe.eng.osaka-u.ac.jp

40 Prof. Apostolos Papanikolaou
Lab. Of Ship Design,
Dept. of Naval Architecture and
Marine Engineering, National Technical
University Athens, Greece
Tel.   Fax
Email:papa@deslab.ntua.gr

41 Prof. Makoto Ohkusu
Research Institute for Applied Mechanics,
Kyushu University
Kasuga City, Fukuoka 816, Japan
Tel.   Fax

42 Dr. M.R Renilson
Australian Maritime College,
P.O Box 986, Launceston,
Tasmania 7250, Australia
Tel. +61-03-260-768,
Fax +61-03-266-261
Email:renilson@mariner.amc.edu.au

43 Prof. Key Pyo Ree
Dept. of Naval Architecture and
Ocean Engineering,
Seoul National University,
Seoul 151-742, Korea
Tel. +82-2-880-7325 ext. 3369,
Fax +82-2-888-9298

44 Mr. K.K Roby
Osaka Prefecture University
1-1 Gakuen-cho, Sakai,
Osaka 593, Japan
Tel. +81-722-52-1161 ext. 3369
Fax +81-722-59-3340

45 Prof. Hiroyuki Sadakane
Kobe University of the
Mercantile Marine,
5-1-1 Fukaeminami-machi,
Higashinada-ku, Kobe 658, Japan
Tel. +81-78-431-6250,
Fax +81-78-431-6361

46 Mr. Wataru Sera
Dept. of Naval Architecture and
Ocean Engineering, Osaka Univ.
2-1 Yamada-oka, Suita,
Osaka 565, Japan
Tel. +81-6-877-5111 ext. 3504
Fax +81-6-878-5364

47 Mr. Rubin Sheinberg
Naval Engineering Division,
U.S Coast Guard,
707 E. Ordnance Road, Baltimore,
MD 21226-1741, USA
Tel. +1-410-863-5620
Fax +1-410-863-5605

48 Prof. Chan Ik Shin
Nagasaki Institute of Applied
Science,
536 Aba-machi, Nagasaki 851-01,
Japan
Tel. +81-958-38-5161,
Fax +81-958-38-3548

49 Prof. Kyoung-Ho Sohn
   Korea Maritime University,
   1, Dongsam-dong, Youngdo-ku,
   Pusan 606-791, Korea
   Tel. +82-51-410-4303, Fax +82-51-404-3986

50 Dr. K. J. Spyrou
   M.Alexandrou 30,
   Piraeus 18533,
   Greece
   Tel.
   Fax +30-1-9714 657

51 Prof. Yutaka Suzuki
   Dean, Faculty of Engineering
   Osaka University
   2-1 Yamada-oka, Suita,
   Osaka 565 Japan
   Tel.   Fax

52 Dr. Tor Svensen
   Det Norske Veritas Pte Ltd
   10 Science Park Drive
   DNV Technology Centre
   Singapore 118224
   Tel. +65-779-1266, Fax +65-779-7949
   Email: TESV@osl1.dnv.no

53 Dr. Ken takagi
   Dept. of Naval Architecture and
   Ocean Engineering, Osaka University,
   2-1 Yamada-oka, Suita,
   Osaka 565, Japan
   Tel. +81-6-879-7571, Fax +81-6-878-5364

54 Dr. Matao Takagi
   17-16 Maruyama-cho, Suita,
   Osaka 564, Japan
   Tel   Fax

55. Prof. Mikio Takaki
   Hiroshima University,
   1-4-7 Kagamiyama, Higashi-Hiroshima,
   Japan
   Tel. +81-824-24-7775,
   Fax +81-824-22-7194

56 Mr. Robert Tagg
   Herbert Engineering Corp.,
   98 Battery St. Suite 500,
   San Fransisco, CA 94111, USA
   Tel. +1-415-296-9700, Fax +1-415-296-9763

57 Prof. Yoshifumi Takaishi
   Nihon University,
   7-28-10 Jindaiji-higashicho,
   Chofu, Tokyo 182 Japan
   Tel. +81-424-84-2857,
   Fax +81-424-84-2857

58 Dr. Steven R. Bishop
   UCL Centre for Nonlinear Dynamics
   and Its Applications,
   University College London,
   Torrington Place, London ,
   WC1E 6BT, UK
   Tel. +44-171-380-7729,
   Fax +44-171-380-0986

59 Mr. Michael Tsangaris
   Dept of Ship and Marine Technology,
   University of Strathclyde,
   100 Montrose Street, Glasgow
   G4 OLZ, Scotland, UK
   Tel. +44-141-552-4400 ext. 3462,
   Fax +44-141-552-2879

60 Dr. Osman Turan
   Dept of Ship and Marine Technology,
   University of Strathclyde,
   100 Montrose Street, Glasgow,
   G4 OLZ, Scotland, UK
   Tel. +44-141-552-4400,
   Fax +44-141-552-2879

61 Dr. Naoya Umeda
   National Research Institute of
   Fisheries Engineering, Ebidai,
   Hasaki-machi, Ibaraki,
   314-04, Japan
   Tel. +81-479-44-5942,
   Fax +81-479-44-6221

62 Prof. Dracos Vassalos
   Dept. of Ship and Marine Technology,
   University of Strathclyde,
   100 Montrose Street, Glasgow
   G4 OLZ, Scotland, UK
   Tel. +44-141-552-4400,
   Fax. +44-141-552-2879
   Email:d.vassalos@ccsun.strath.ac.uk

63 Mr. A.W Vredeveldt
    TNO, The Netherlands

64 Dr. Iwao Watanabe
    Ship Research Institute,
    6-38-1 Shinkawa, Mitaka-city, Japan
    Tel. +81-422-41-3058
    Fax +81-422-41-3056

65 Mr. Yasuyuki Yamakoshi
    National Research Institute of
    Fisheries Engineering,
    Ebidai, Hasaki-machi,
    Ibaraki, 314-04, Japan
    Tel. +81-479-44-5942
    Fax +81-479-44-6221

66 Mr. Norio Yuda
    Dept. of Naval Architecture and
    Ocean Engineering, Osaka University,
    2-1 Yamada-oka, Suita,
    Osaka 565, Japan
    Tel. +81-6-877-5111, Fax +81-6-878-5364
    E-mail::yuda@naoe.eng.osaka-u.ac.jp

67 Prof. Toshio Iseki
    Tokyo Univ. of Mercantile Marine,
    2-1-6, Kotoku Echujima
    Tokyo 135 Japan

68 Mr Yoshiro Ichikawa
    Ministry of Transport,
    2-1-3 Kasumigaseki, Chiyoda-ku
    Tokyo 100, Japan

GEOMETRICAL ASPECTS OF
BROACHING-TO INSTABILITY

Kostas Spyrou

Centre for Nonlinear Dynamics and its Applications, University College London

ABSTRACT

Recent developments towards the clarification of the dynamics of the broaching-to mode of ship instability are reported. A multi-degree nonlinear mathematical model of the automatically steered ship in astern seas, is taken as the basis of the investigation. A basic novelty of the approach lies in the fact that it unifies contemporary methodologies of ship controllability and transverse stability studies, within the framework of modern dynamical systems' theory. Specific nonlinear phenomena are identified as responsible for the onset of broaching behaviour. Steady-state and transient responses are investigated and it is shown how capsize is incurred during the forced turn of broaching. A classification of broaching mechanisms has been developed, concerning frequencies of encounter near zero, where surf-riding plays the dominant role, as well as frequencies of encounter away from zero, where, the instability is inherent of the overtaking-wave periodic mode.

INTRODUCTION

The broaching-to mode of dynamic instability is considered as one of the most enigmatical types of unstable behaviour. Although there seems to exist a consensus about what constitutes broaching (sudden "loss" of heading, felt as quick increase of heading deviation, sometimes ending with capsize, in spite of efforts to regain control), until recently we were lacking a satisfactory description of the fundamental dynamical phenomena that underpin the onset of such undesirable behaviour. Earlier research has offered valuable insights about the horizontal-plane stability of steered or unsteered ships in astern seas, particularly at zero frequency of encounter, [1], [2], [3], [4], [5]. It is known for example that, yaw instability is more likely to arise when the ship centre rests at the down-slope of long waves and, particularly, nearer to the trough where the wave yaw moment tends to turn the ship towards the beam sea condition; or that around the crest it is likely to encounter instability in surge. The common denominator for many earlier approaches is the concentration on local stability and linearized dynamics something that, in the spirit if 50's or 60's, was basically the result of necessity rather than choice. However, in recent years there has been increased interest for what was seen as a daunting task in the past, the study of large-amplitude motions where system response is shaped by nonlinear effects. Consideration of motion nonlinearity can open new

horizons in at least two different ways: At first, it can often explain the instability of the linearized system as the fingerprint of the presence of some bifurcation phenomenon. Secondly, it can reveal the existence of new, qulitatively different types of responses that were not accounted for by the linearized model. Perhaps the best known (and verified) examples of nonlinear behaviour in ship dynamics are, the roll response curve near resonance and the spiral curve of a directionally unstable vessel, see Fig. 1. It is felt that a similar, simple geometrical representation of system dynamics is what is urgently needed for the broaching problem.
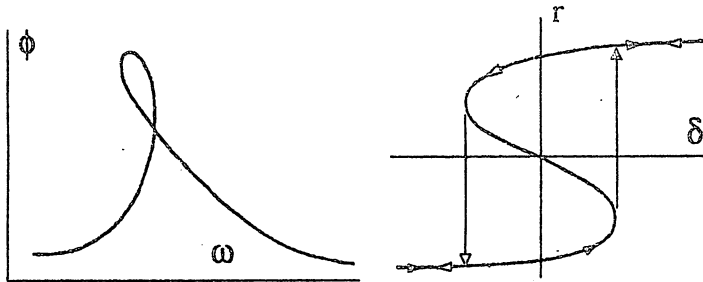

Fig. 1: The transition to resonant roll (left) and the phenomenon of directional instability of ships (right) are typical manifestations of nonlinear behaviour. For the latter, linear analysis predicts instability when the rudder is set amidships. Nonlinear analysis shows however the existence of a set of three states (two stable and one unstable in the middle) organized according to a classical cusp pattern. [6]

Geometrical considerations lie at the "heart" of a nonlinear dynamics approach and they can be also very helpful in the process of selecting a suitable mathematical model. If for example the main question asked is *what are the origins of broaching behaviour*, the answer should contain, in broad terms, a qualitative description of the underlying geometry that organizes our system's state and control spaces. This description should be built primarily "around" specific bifurcation phenomena (notably, for typical configurations only a limted number of distinctive bifurcations can take place) and associated transient dynamic effects. On the other hand, the pursue of quantitative accuracy will become meaningful only once a specific reference "landscape" has been established for our problem.

So effects which do not alter significantly the character of system response may, at first instance, be neglected. This last observation is especially comforting for the development of a mathematical model for broaching given that still, little confidence exists about the accuracy of theoretical predictions of the hydrodynamic forces that act on moving ships in large waves.

In a series of recent papers, broaching was examined from such a nonlinear viewpoint with consideration of multi-degree dynamics, [7], [8], [9], [10], [11], [12]. Other contemporary approaches may be found for example in [13], [14], [15]. The emphasis on the multi-degree nature of the problem is very important because, from the outset, it is known that broaching can involve (although not as a necessity) instabilities in at least three differents directions: Instability in surge that is connected with the surf-riding condition, instability of yaw that triggers the uncontrolled turning motion, and, instability in roll that leads to capsize. In ship studies, the systematic treatment of different instabilities within a single framework is rather unusual. However such an approach offers distinctive advantages, because it allows to see how one instability is possible to be preparing the ground for another. By exploring the intimate connection between these dynamic effects, and also some others that are less obvious, we have developed a classification of broaching mechanisms, [10], organized in two groups : Broaching that involves surf-riding (basically at high Froude number) and also, directly from periodic motion. In the following we shall review some of the most important earlier results and furthermore, we shall present some more recent findings.

PHENOMENA OF INSTABILITY RELATED WITH SURF-RIDING IN QUARTERING SEAS

(a) General features

It is rather well known that, a small ship sailing with high speed in an environment of large quartering waves with length at least equal to the ship length can be forced to advance with speed equal to the wave celerity, a mode of behaviour usually referred-to as, the surf-riding condition. The range of headings where surf-riding can arise covers a band around the purely following sea course and its onset is characterized by two speed thresholds: The first signals the existence of a pair of points of static equilibrium, that are "born" at the middle of the wave's down slope; with further increase of Fn they tend to move away from each other, towards the wave crest and trough. However the overtaking-wave oscillatory pattern remains in existence and it is a matter of the initial condition of the ship whether it will be engaged in the one or in the other type of behaviour. The second threshold flags the occurrence of a homoclinic connection, a bifurcation that is accountable for the abrupt disappearance of the oscillatory pattern, Fig. 2. Considering the arrangement in state-space, the limit-cycle corresponding to the periodic motion tends to come nearer to the saddle of crest, driving the inset and outset of the saddle to be orientated almost parallel to the limit-cycle.

Fig. 2: Geometry of the homoclinic connection

As soon as the saddle "touches" the limit-cycle, the latter breaks and the oscillatory motion can no longer exist (from the previous description it becomes perhaps obvious why this bifurcation is also called "saddle-loop"). Thereafter a zone of headings emerges featuring stationary behaviour, due to the point of static equilibrium near trough that is stabilizable with proper selection of the proportional gain of the autopilot. The width of this zone increases at higher Fn. From certain initial conditions periodic motions may still be possible but the prescribed heading should lie at the outskirts of this zone, Fig. 3. At very high Fn the periodic pattern comes into existence again but in the present study we are not interested in that range of very high Fn.

In principle, the surf-riding states form a closed curve, [7], [8]. However diffraction effects have been shown to place heavy demand for larger rudder angles. Sometimes, the maximum rudder deflection is reached and, as a matter of fact, the curve cannot close, [9], [10]. If the ship is steered with control law that includes heading-proportional gain, the prescribed heading ψ_r is linked with the actual heading ψ with the relation:
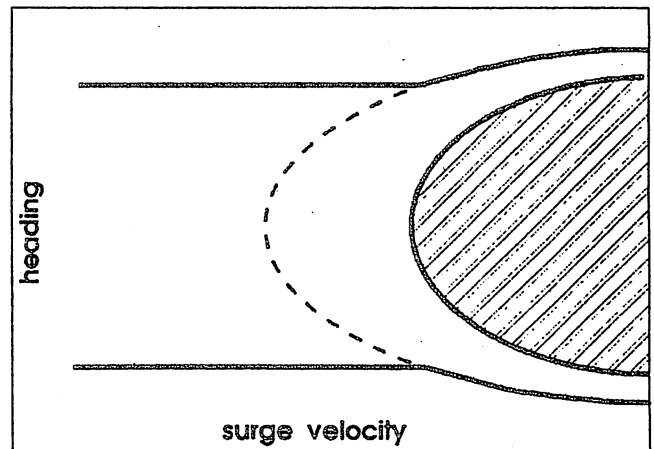
Fig. 3: Development of the initial conditions domain that is associated with surf-riding. The hatched region corresponds to Fn between the two surf-riding thresholds. The grey area shows a typical surf-riding domain when the higher surf-riding threshold is exceeded.
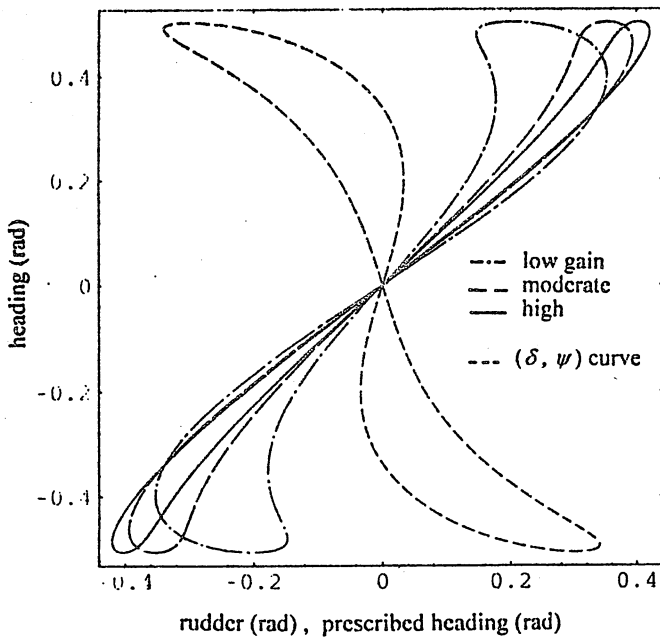
Fig. 4: Effect of proportional gain on surf-riding

$\psi_r - \psi = -\delta / a_\psi$ that involves only the rudder angle δ (to find it however requires solution of the algebraic system of motion equations at steady-state) and the gain a_ψ, that is normally defined in advance. Obviously with higher gain, ψ_r and ψ tend to coincide although how exactly this happens depends on the specific form of motion equations that are "represented" through δ. The specific geometry of the (ψ_r, ψ) relation with increasing a_ψ is shown in Fig. 4. However the relation between ψ_r and δ is independent of the gain value.

The condition of surf-riding should not be confused with the asymmetric oscillatory motion (known as "large-amplitude surging", [16]) that precedes the first appearance of surf-riding. In terms of our system's state-space arrangement, as the limit-cycle that represents the oscillatory motion approaches the saddle of crest, the ship tends to create the impression that it remains for a while almost stationary at the crest of the wave, [10]. In a dynamical sense, this condition is significantly different from true surf-riding, where the ship remains stationary in the region of the wave trough .

(b) Broaching at the encounter of surf-riding

Surf-riding can arise either with gradual increase of the nominal Froude number, or, as the result of a change concerning the wave parameters that represent the exogenous controls of our system. For "small" control parameter perturbations, a ship initially in overtaking-wave periodic motion will be eligible to "surf" only if it operates in the proximity of the higher surf-riding threshold; because only there the inset of the saddle of crest, that is the separatrix of stationary and periodic motion, is approached by the periodic orbit, [10] . Supposing that this threshold was, for some reason, exceeded, stable surf-riding will be realized only if the following two additional conditions are fulfilled: (a) at the prescribed heading the static equilibrium of the trough is stable, and, (b) the applied perturbation causes inward crossing of the boundary of the attracting domain of this stable equilibrium . When the condition (a) is not satisfied it is possible to experience surf-riding for limited time as a transient effect. As soon as the periodic motion disappears and given that stable surf-riding is not possible, the ship is left with no other option that turning towards the beam-sea, because no other stable steady-state (stationary or periodic) exists at the prescribed heading.

(c) Oscillatory surf-riding

Under certain circumstances, particularly when the heading is not very near to zero, it is possible to experience also an oscillatory-type surf-riding that is born due to a supercritical Hopf-bifurcation, Fig. 5. Moreover,

Hopf supercritical

Hopf subcritical

surge velocity (m/s)

6.8

6.6

6.4

6.2

-3   -2.5   -2   -1.5

position on the wave (m)

Fig. 5: The two types of Hopf bifurcation.
The supercritical one was found in surf-
-riding.

Fig. 6: The self-sustained oscillations can grow until
they reach the saddle of trough where they
disappear in a blue-sky situation.

the region of headings where oscillatory surf-riding is encountered can be host to period-doubling bifurcations, that lead sometimes to chaotic behaviour, [8], [11]. Generally, such behaviour was met only in very narrow ranges of control parameter values. Therein, the ship wanders at a slow rate on the down slope of a single wave, in an apparently erratic manner. Finally, there seem to exist different possible scenarios about the exit from oscillatory surf-riding, [10]. For example, the self-sustained oscillations can turn unstable at a fold, or, they can disappear in a blue-sky fashion due to a new homoclinic connection, if they collide with the saddles of trough, Fig. 6.

(d) Voluntary escape

Another possibility is to attempt to escape voluntarily from surf-riding by setting a different propeller rate or heading, with desired destination the overtaking-wave periodic mode. For these manoeuvres, we derived the complete arrangement of domains of surf-riding, periodic motion, broaching and capsize, for the

nominal Froude number

0.5

0.4

0.3

0   0.05   0.1   0.15   0.2   0.25   0.3

heading (rad)
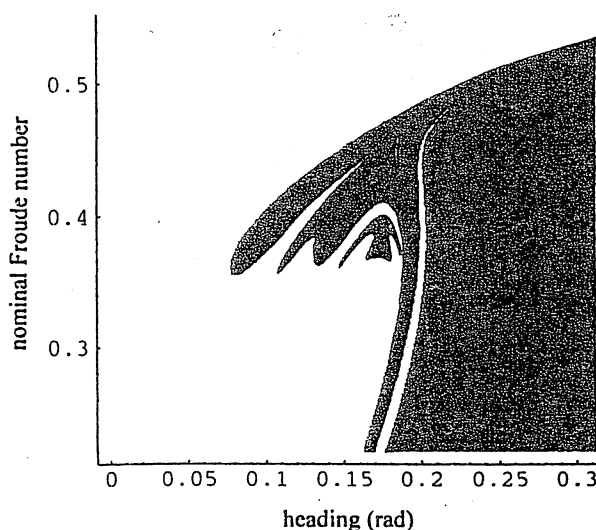
Fig. 7: Capsize due to sudden reduction of propeller
rate. The ship was initially at steady surf-riding
condition (initial $Fn=0.56$, $\lambda/L=2.0$, $H/\lambda=1/20$,
$GM=1.51m$).

state/control parameters' plane (ψ, Fn). The characteristic layout of the capsize domain that corresponds to an abrupt reduction of propeller rate, is shown in Fig. 7. Here should be noted that, on the basis of the value ψ one can derive easily also the values of the other state-vector components.

BROACHING DIRECTLY FROM PERIODIC MOTIONS

(a) Loss of stability of periodic motion

For larger vessels, surf-riding is rather unlikely to happen due to limitations of wave length, λ, and operational Froude number. However it is well known that broaching can occur also at frequencies of encounter that are not very near to zero (where the constraints set on λ and Fn do not need to hold). Often, this is the reflection of a change in the stability of the overtaking-wave periodic motion. It is quite common in dynamics, as periodic motions grow larger and nonlinear effects become more pronounced, to encounter phenomena such as, birth of new periodic states and exchanges of stability, coexistence of multiple periodic states, and, dynamic transitions from

control : $t_\delta = 3$, $a_\psi = 3$, $b_r = 1$

$\lambda/L=2.0$, $H/L=1/20$, $Fn=0.289$, $GM=1.51$ m
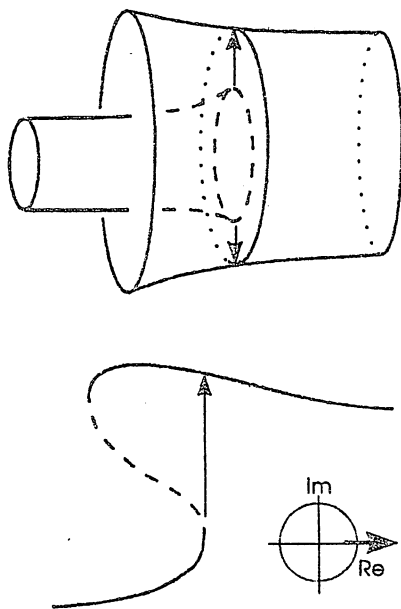
Fig. 8: Geometric representation of the the jump associated with the cyclic-fold
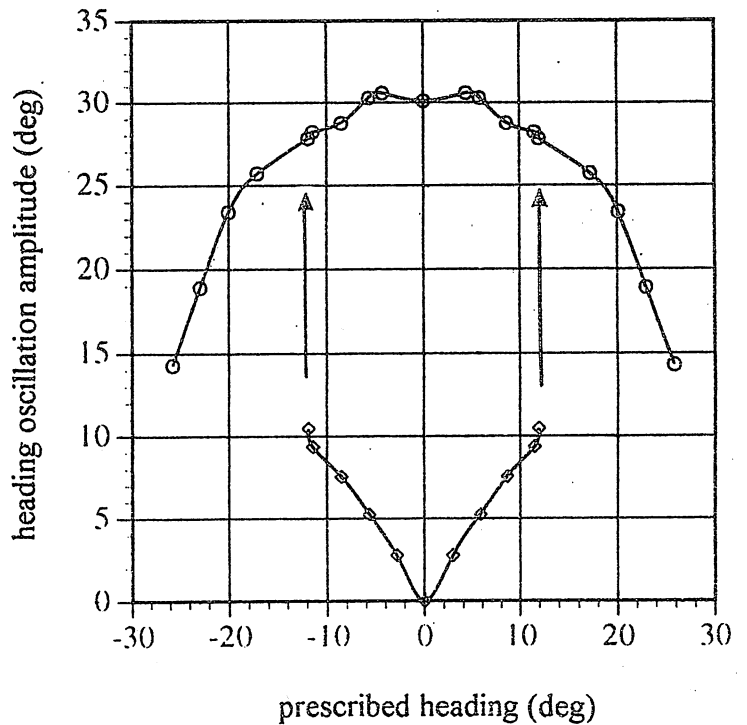
Fig. 9: Amplitude continuation for the two coexisting types of periodic motion showing how the jump from the ordinary towards the resonant oscillation comes about at a fold. With reduced GM the jump occurs at lower prescribed heading. The reference vessel is the same purse-seiner of earlier studies

—15—

one periodic state to another. As discussed in detail in [17], in the presence of extreme excitation, periodic ship motions show a tendency to "fold" in the qualitative way shown in Fig. 8. This generates coexistence of two stable oscillatory-type motions; the one corresponds to what should be seen as the customary, relatively low amplitude, response, whereas the second represents the condition of resonance, Fig. 9. The autopilot gains, particularly the differential one, have a serious effect on the specific dynamics. It is interesting that, in many cases the resonant oscillation cannot exist in a practical sense because it extends beyond the usual rudder limits. If, with gradual increase of the prescribed heading the state is reached where the ordinary oscillation looses stability, a transient arises that is felt as a progressive, oscillatory-type, build-up of yaw and rudder deviations. Broaching behaviour is, in this case, the manifestation of a classical transition to resonance.

(b) Excessive rudder oscillation

This route is rather simple to perceive, and has been discussed to some length in [8] and [10]: At a certain combination of ψ_r, λ and H, the one end of the rudder's oscillatory motion reaches its physical limit. Thereafter, if the wave characteristics are fixed and higher headings are prescribed (or, if the wave characteristics are altered in a sense that the yaw excitation on the ship is increased for the same ψ_r), the preservation of the oscillatory motion requires rudder moments which however are not available due to system constraints. This scenario is meaningful when the rudder maintains considerable lift-producing capability up to large angles, something that often happens for fishing vessels.

CONCLUDING REMARKS

The association between well known nonlinear phenomena and broaching behaviour, together with the concurrent treatment of different, yet inherently connected, instabilities, provide a new perspective for the study of a problem that has remained at the centre of research interest for nearly fifty years.

In earlier studies of broaching it was often tacitly assumed that, even in large waves, a small ship approaches the zero-encounter-frequency condition in a smooth, basically "linear" manner. As we have seen however, this takes place in fact in a much more dynamic fashion where, at a certain stage, the ship is accelerated up to a speed as high as the wave celerity (a typical transition is from *Fn=0.35* or *0.40* to *Fn=0.56* for wave length that is two times the ship length). Moreover, such transitions seem to concern only a limited range of headings "around" the following-sea course and there exists a sharp boundary that separates, in state-space, this from the domain of ordinary overtaking-wave response. The fact that this transition is abrupt in nature puts in question also the effectiveness of the customary examination of yaw-sway stability at zero frequency of encounter where, after all, properly selected autopilot gains are known to remove thit type of instability. The problem however should be in reality considerably more complex since we are dealing here with a change of state where the initial (periodic) and the final (stationary) state of the ship are dynamically unrelated. One question that immediately comes to mind is, whether the autopilot gains that seem adequate for maintaining stable periodic motion can be equally effective for the stationary mode [17].

Of course, it cannot be forgotten that real ship operation will present several differences from the idealized system that was considered here. For example, long maintained regular waves are rather rarely encountered in nature. Moreover, control systems and strategies may be considerably more complex from the simple model of control assumed here; and of course it is not unlikely that, for certain circumstances, some other important effects are not catered for by our mathematical model. Nevertheless, the understanding that a number of specific phenomena govern, to a large extent, the behaviour of the system in a physical sense, provides the solid basis on which future improvements can be specified and assessed.

It is believed finally that a similar know-how should be developed soon as regards experimental techniques since only through the physical verification of the predicted modes of behaviour we can expect that, one day, such knowledge will be integrated effectively in the customary design and operational procedures of ships.

REFERENCES

[1] RYDILL, L.J., "A linear theory for the steered motion of ships in waves", Trans. RINA, 101, 1959.

[2] WAHAB, R. AND SWAAN, W.A., "Coursekeeping and broaching of ships in following seas". Journal of Ship Research, 7, 4, 1964.

[3] EDA, H., "Directional stability and control of ships in waves", Journal of Ship Research, 16, 3, 1972.

[4] MOTORA, S., FUJINO, M. AND FUWA, T., "On the mechanism of broaching-to phenomena". *Proceedings,* Second International Conference on Stability of Ships and Ocean Vehicles", Tokyo, Oct. 1982.

[5] RENILSON M.R. AND DRISCOLL, A., "Broaching - An investigation into the loss of directional control in severe following seas". *Trans*. RINA, 124, 1982.

[6] SPYROU, K.J. "A new approach for assessing ship manoeuvrability based on dynamical systems' theory". PhD Thesis, Univ. of Strathclyde, Dept. of Ship and Marine Technology, Glasgow, Dec.1990

[7] SPYROU, K., "Surf-riding, yaw instability and large heeling of ships in following/quartering waves". Ship Technology Research/Schiffstechnik, 42, 2, 1995.

[8] SPYROU, K.J., "Surf-riding and oscillations of a ship in quartering waves". Journal of Marine Science and Technology, 1, 1, Springer-Verlag, Tokyo, 1995.

[9] SPYROU, K.J. AND UMEDA, N., "From surf-riding to loss of control and capsize: A model of dynamic behaviour of ships in following/quartering seas". Proceedings of the 6th International Symposium on Practical Design of Ships and Mobile Units, PRADS '95, Seoul, Sept. 1995.

[10] SPYROU, K.J., "Dynamic instability in quartering waves: The behavior of a ship during broaching". Journal of Ship Research, 40, 1, 1996.

[11] SPYROU, K.J., "Homoclinic connections and period doublings of a ship advancing in quartering waves". CHAOS, American Institute of Physics, 6, 2, 1996.

[12] SPYROU, K.J., "Dynamic instability in quartering waves: Part II - Analysis of ship roll and capsize for broaching". Journal of Ship Research, 40, 4, 1996 (forthcoming).

[13] RUTGERSON, O. AND OTTTOSON, P., " Model tests and computer simulations - An effective combination for investigation of broaching phenomena". *Trans.* SNAME, 95, 1987.

[14] ANANIEV, D.M AND LOSEVA, L., "Vessel's heeling and stability in the regime of maneuvering and broaching in following seas". *Proceedings*, Fifth International Conference on Stability of Ships and Ocean Vehicles, Melbourne, Florida, Nov. 1994.

[15] UMEDA, N. & VASSALOS, D., "Nonlinear periodic motions of a ship running in following and quartering seas". Journal of the Society of Naval Architects of Japan, 179, 1996.

[16] KAN, M., "Surging of large amplitude and surf-riding of ships in following seas". Selected Papers in Naval Architecture and Ocean Engineering, The Society of Naval Architects of Japan, 28, 1990.

[17] SPYROU, K.J., "Nonlinear effects on periodic motions" (to be published).

Some Remarks on Broaching Phenomenon

Naoya UMEDA

National Research Institute of Fisheries Engineering
Ebidai, Hasaki, Ibaraki, 314-04, Japan

Summmary

Based on partly-captive model experiments, the author provides views for a desirable mathematical model for analysing broaching and remarks on estimations of hydrodynamic coefficients in the model. Then, by reviewing his recent analytical and numerical works utilising the proposed mathematical model, a qualitative explanation has been obtained for broaching in the light of non-linear dynamical system approach. Furthermore, a simple method for predicting broaching without repeating numerical simulation is proposed for a practical use and well compared with existing free running model experiments.

Introduction

Broaching is a phenomenon that a ship cannot maintain her desired course in spite of the maximum steering effort and then suffers a violent yaw motion. While the directional instability can be dealt with a linear theory, non-linear theory, which has not yet fully developed, is essential to explain broaching. Although a few high-speed craft may experience broaching in still water, the most realistic threat of broaching exists for a ship running in quartering seas with somewhat high speed. To precisely realise this running condition in a model scale, it is indispensable to use a large scale seakeeping and manoeuvring basin with an X-Y towing carriage. These significant difficulties in both theory and experiment have left an investigation of broaching unsolved till now.

At the previous workshop, the author (1995) discussed the methodology for investigating a broaching phenomenon with non-linear dynamical system approach. In particular, he pointed out the importance of steady state of both surf-riding equilibria and periodic motions and then proposed a procedure to identify critical condition for broaching based on a concept of "sudden change" of operational parameters as well as an invariant manifold analysis.

Following his paper as a part of the UK-Japan co-operative research project, the author and Vassalos (1996) carried out an investigation of periodic motions, their stability and invariant manifolds. Combining it with the previous results for surf-riding equilibria (Umeda and Renilson, 1992, 94), this paper remarks features of broaching phenomenon in the light of non-linear dynamical system approach.

Apart from these works, Spyrou (1995-96) intensively has been investigating the same topic with a similar method. However, some qualitative conclusions in his investigation do not fully agree with those of the author's because of difference in the mathematical model. This indicates that the mathematical model itself should be examined. Therefore, by comparing results of captive model experiments and hydrodynamic predictions, the author and his colleagues carried out the experimental validation of mathematical model. Based on this validation, this paper remarks on a suitable mathematical model of broaching.

Mathematical model for investigation of broaching

1) 6 degrees-of-freedom or 4 degrees-of-freedom?

For the investigation of capsizing due to broaching, 6 degrees-of-freedom models, surge-sway-heave-roll-pitch-yaw models, and 4 degrees-of-freedom models, surge-sway-roll-yaw models, have been utilised with an auto pilot model. When the investigation is limited to broaching, 3 degrees-of-freedom models also have been utilised. If critical condition for broaching with the 4 degrees-of-freedom model can approximate to that with the 6 degrees-of-freedom model within practical accuracy, the use of the 4 degrees-of-freedom should be recommended. Because, increase in the number of degrees-of-freedom makes non-linear dynamical system analysis extremely difficult. A thought of usefulness of the 4 degrees-of-freedom model for broaching is as follows. (Umeda, 1995)

When a ship runs in quartering seas with somewhat high speed, the encounter frequency of the ship in waves becomes much smaller than the natural frequencies in heave and pitch. Therefore, heave and pitch motions can be approximated by simply tracing their static equilibria. Hence, it is sufficient to examine surge, sway, yaw and roll motions, whose restoring terms are zero or small.

To establish the above thought, qualitative examination is essential with both model experiments and numerical calculations. Thus, the authors (Umeda, Yamakoshi and Suzuki, 1995) carried out partly-captive model experiments of a small trawler in a seakeeping and manoeuvring basin named "Marine Dynamics Basin" of National Research Institute of Fisheries Engineering. The model was free in heave and pitch and
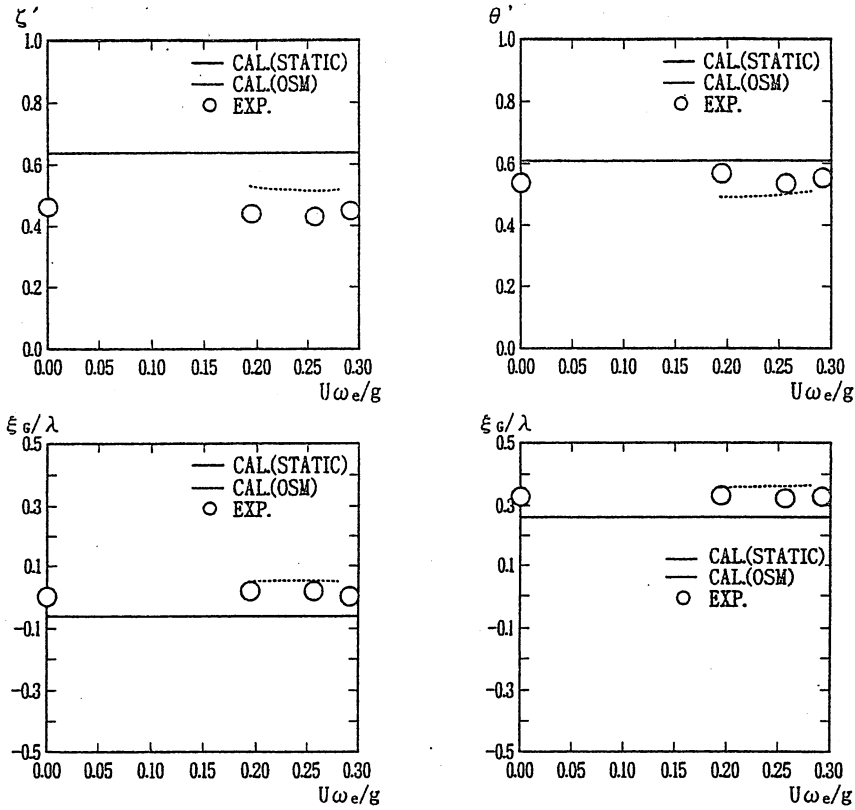
Fig. 1   Non-dimensional heave (ζ) and pitch (θ) motions of a small trawler
(H/λ=1/20, λ/L=1.6, χ=30 degrees) (Matsuda, Umeda & Suzuki, 1996)
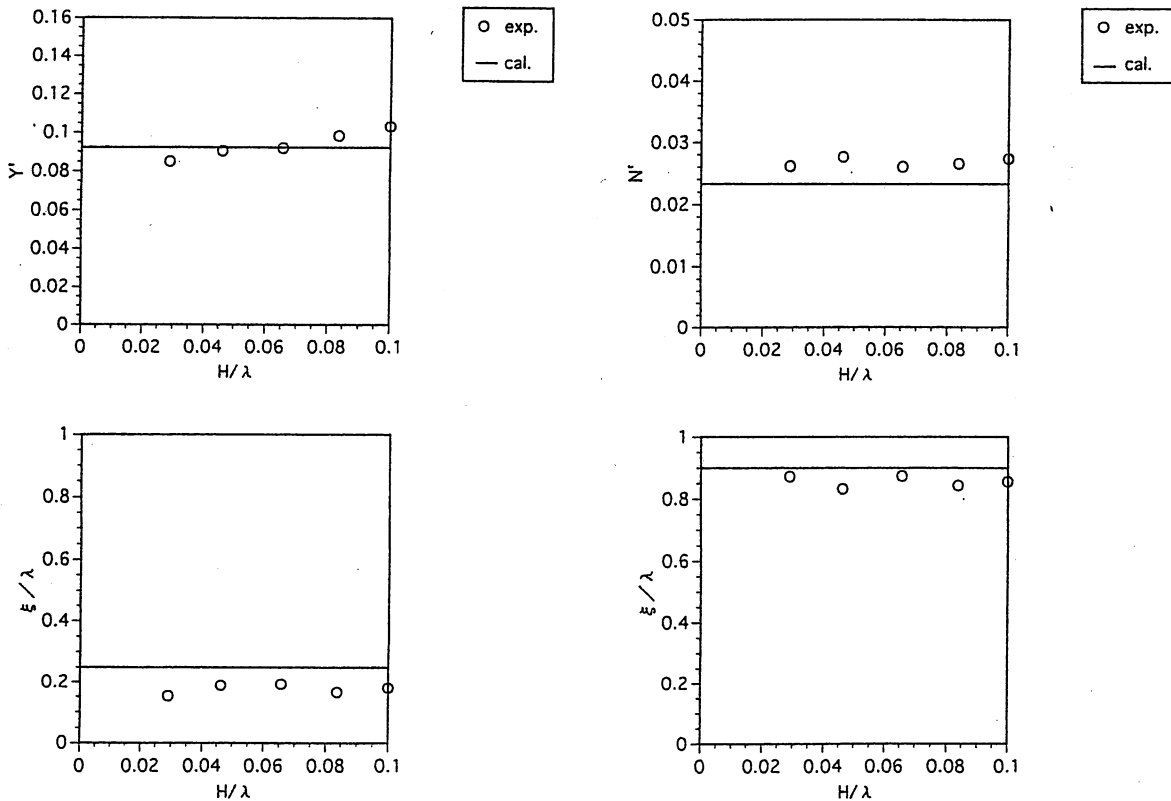
Fig. 2   Non-dimensional sway force (Y) and yaw moment (N) of a small trawler
(Fn=0.478, λ/L=1.6, χ=30 degrees) (Umeda et al., 1995)

was fitted with an X-Y towing carriage. The surge force, sway force, yaw moment and roll moment were detected by a dynamometer. The model was towed in quartering seas with low encounter frequency, which covers the range of motions relating to broaching.

As shown in Fig. 1 , the measured heave and pitch were compared with two prediction methods: One is to calculate a static equilibrium with the Froude-Krylov components (Static); the other is a strip method (OSM). (Matsuda, Umeda and Suzuki, 1996) In these experiments with very low encounter frequency, the measured amplitude and phase lag do not depend on the encounter frequency. This results support the fore-mentioned thought. The calculated results with the "static" method agree with the measured results to some extent and those with the strip method show better agreement. It is note-worthy that the results with the strip method do not depend on the encounter frequency very much. These conclusions were also validated for the experiments with extreme wave steepness H/λ=1/10.

2) Can we predict hydrodynamic terms in the mathematical model?

It is necessary to predict hydrodynamic terms in the 4 degrees-of-freedom mathematical model. They are functions of wave steepness, drift angle, non-dimensional yaw rate and so on. Obviously the wave steepness is at least up to 1/7. The drift angle and non-dimensional yaw rate are less than 0.2 even during broaching because of large forward velocity. (Fuwa et al., 1983) As a result, the leading hydrodynamic terms in the mathematical model can be only the wave forces without ship lateral motions and linear manoeuvring hydrodynamic forces in still water. Here the latter includes resistance and propulsive forces.

For the wave forces, the author and his colleagues (Umeda, Yamakoshi and Suzuki, 1995) had already concluded with their partly-captive model experiments that a linear slender body theory with no free surface effect can predict them within practical accuracy up to the wave steepness 1/10. Some examples are shown in Fig. 2. As the model was free in heave and pitch, the measured wave forces are suitable for the 4 degrees-of-freedom model.

For the linear manoeuvring hydrodynamic derivatives with respect of drift angle and yaw rate in still water, a captive model experiment such as a circular motion test can be expected. Although several empirical formulae have been developed with experimental data of tankers, cargo ships and so on, it should be underlined that these ships have no relevant to broaching. Except for the wave effect on rudder forces, the mathematical model that the author and his co-workers used is basically the 3 or 4 degrees-of-freedom model with the first-order hydrodynamic terms obtained by the above recommended methods. Because, the non-linearity that characterised broaching is due to the effects of

surge and sway displacement, this model can explain basic feature of broaching phenomenon.

If we intend to improve prediction accuracy, it is necessary to consistently take higher order terms into account. That is, wave effects on linear manoeuvring derivatives, wave effects on transverse restoring moment, non-linear manoeuvring derivatives in still water, non-linear restoring and damping roll moment in still water and so on. Renilson (1982) examined directional instability with the first higher order component obtained by a slender body theory. Son and Nomoto (1983) treated directional instability with the first two components obtained by a PMM test. Spyrou (1995-96) investigated broaching with the second, third and fourth components. Nevertheless, it has not yet been established how these higher order terms influence critical conditions of broaching.

For some of the wave effects on linear manoeuvring forces, several theoretical methods have been proposed so far. (Hamamoto, 1971, Renilson, 1982, Fujino et al., 1983, Ananiev, 1995) In the near future, it is expected that theoretical prediction methods for all of linear manoeuvring coefficients, including rudder and propeller contributions, will be established with experimental validations based on captive model experiments.

For non-linear manoeuvring forces in still water we have two major problems. One is that no theoretical or empirical method for relevant ships is available. The other is that extrapolation of non-linear function that obtained empirically may induce unrealistic results in the process of non-linear dynamical system approach.

Considering the above situations, unless reasonable prediction methods are provided, it sounds a premature attempt to consider higher order terms in the mathematical model in broaching.

Non-linear dynamics on broaching

1) What is broaching?

A ship running in quartering waves, whose length is comparable with her length, is usually overtaken by waves with periodic motions whose period is equal to the encounter period. Linear seakeeping theories such as a strip theory deal with mainly this harmonic motion and can reasonably well predict it. However, when the encounter frequency tends to zero, a linear theory leads to infinite amplitudes of surge and sway as shown in Figs. 3-4. This is because no restoring forces in surge and sway exist in a linear theory. Obviously, it is not reasonable that analysis based on the small amplitude assumption results in infinite amplitudes. Therefore the author and Vassalos (1996) applied an averaging method to the non-linear 4 degrees-of-freedom mathematical model. As a result of this analytical procedure, virtual restoring terms were obtained from wave forces that
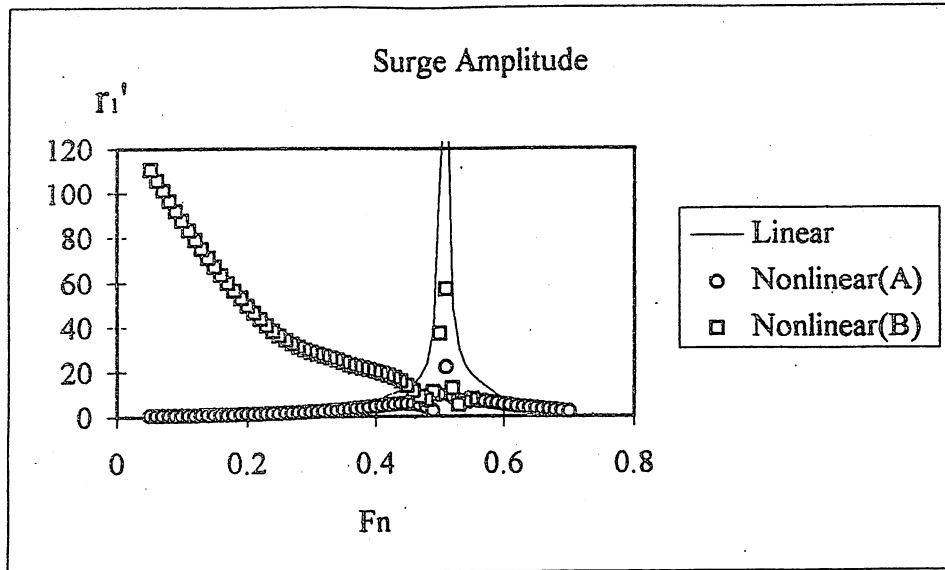
Fig. 3 Surge Amplitude of a purse seiner (H/λ=1/15, λ/L=1.5, χ=15 degrees, K_p=1.0, T_D=0) (Umeda and Vassalos, 1996)


Fig. 4 Sway Amplitude of a purse seiner (H/λ=1/15, λ/L=1.5, χ=15 degrees, K_p=1.0, T_D=0) (Umeda and Vassalos, 1996)

Maximum of Real Part of Eigenvalues

{Re(σ')}max

Fig. 5   Maximum of real part of nondimensional eigenvalues multiplied by
the absolute value of encounter frequency for a purse seiner
($H/\lambda=1/15$, $\lambda/L=1.5$, $\chi=15$ degrees, $K_p=1.0$, $T_D=0$)

(Umeda and Vassalos, 1996)

### Critical Conditions
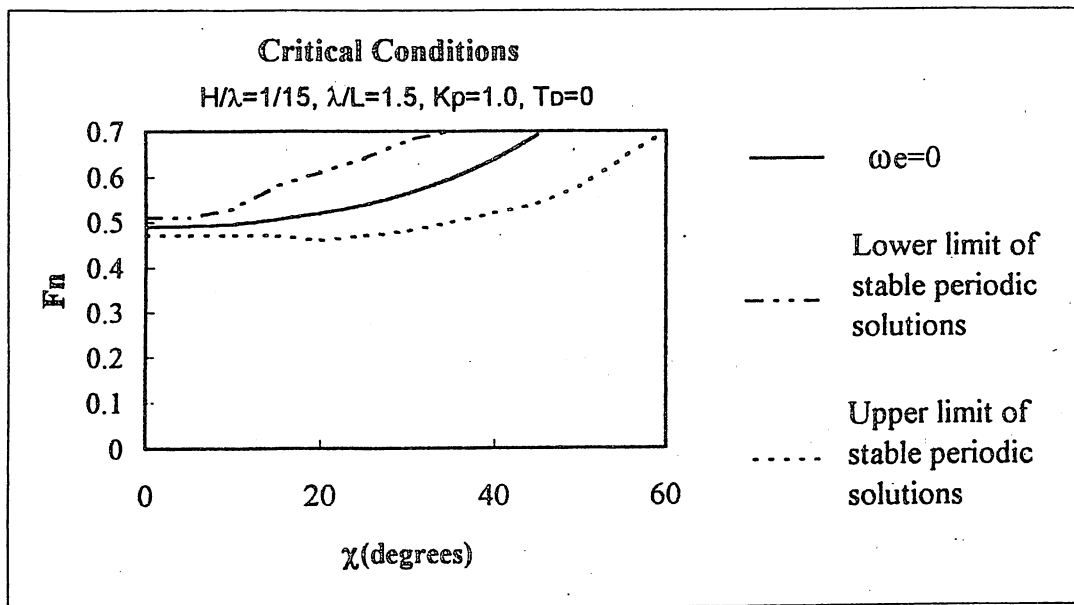
$H/\lambda=1/15$, $\lambda/L=1.5$, Kp=1.0, TD=0

Fig. 6   Critical condition for stable periodic motions   of a
purse seiner   ($H/\lambda=1/15$, $\lambda/L=1.5$, $K_p=1.0$, $T_D=0$)

(Umeda and Vassalos, 1996)

depend not only time but also horizontal displacements. Hence finite amplitudes in surge and sway appear as a steady state.

Non-linearity results in co-existence of steady states, besides finiteness of amplitudes. As shown in Fig. 5, one of them behaves stably in high encounter frequency regions as the linear periodic motion but in a low encounter frequency region its stability decreases and finally it becomes unstable. Fig. 6 shows that the region where no stable periodic motion is found exists only in the vicinity of the zero encounter frequency.

How does a ship behave in the region where a periodic motion is unstable or slightly stable? The answer should be related to another type of steady state, that is, the surf-riding equilibrium. This equilibrium point indicates that a ship runs with a drift angle, heading angle, rudder angle and no relative velocity to a wave. Thus an existing condition of this equilibrium can be easily calculated by solving an equation of static balance of forces. However, if the propeller revolution increases up to this condition, the surf-riding does not occur. Thus this condition is only a necessary condition for broaching. In following seas two equilibria can exist within one wave length. An unstable equilibrium for a longitudinal motion is near a wave crest; stable one in near a wave trough. The latter equilibrium corresponds to surf-riding. The critical condition for surf-riding in following seas is provided when an unstable manifolds from an unstable equilibrium is connected to a different unstable equilibrium. This condition can be estimated by numerically solving a two-point boundary value problem (Umeda, 1990, Kan, 1990) or by using a perturbation method (Ananiev, 1993). An example is shown in Fig. 7. To escape from surf-riding by gradually reducing the propeller revolution, it is necessary to reduce the revolution up to the necessary condition. As reducing propeller revolution corresponds to reducing rudder force, it is rather danger to reduce propeller revolution during surf-riding. (Umeda, 1990)

If we consider also lateral motions, the wave-induced yaw moment can make the equilibrium near a wave trough unstable. As shown in Figs. 8-9, the maximum of real parts of eigenvalues is positive. This indicates that surf-riding equilibrium near a wave trough is a saddle. (Umeda and Renilson, 1992) If the auto pilot is effective enough, this instability can sometimes be prevented. (Umeda and Renilson, 1993) In the case of these figures even under the maximum rudder angle, -35 degrees, unstable equilibrium does not disappear. As a result, with keeping the maximum opposite rudder angle, the ship's yaw rate increases in an uncontrolled manner. One of the unstable invariant manifolds from the unstable surf-riding equilibrium represents a typical trajectory of this behaviour. This indicates that even the bang-bang control, which can be regarded as the maximum steering effort, cannot prevent the uncontrolled yawing.

135 GT purse seiner
H／λ＝1/15

Surf-Riding conditions

.... necessary cond.

— critical cond.

—· T=0
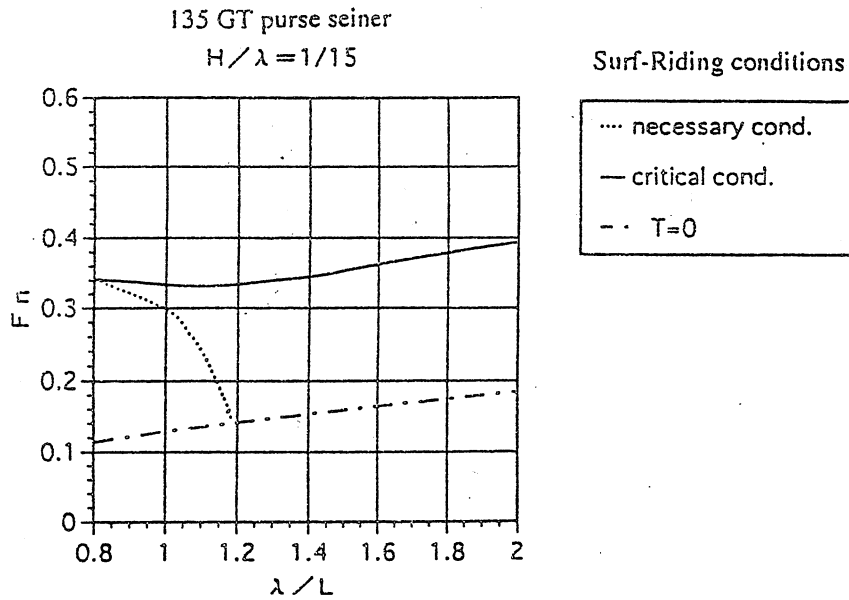
Fig. 7   Critical and necessary   conditions for   Surf-riding of the purse seiner in following seas without lateral motions

H/λ=1/15
λ/L=1.5
Fn=0.4
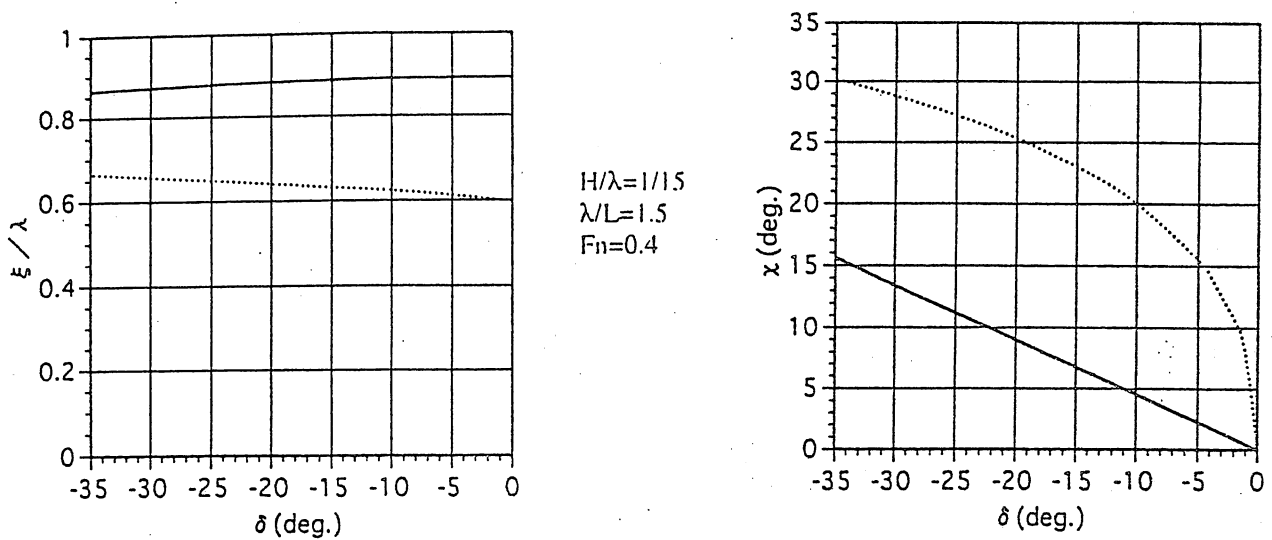
**Fig. 8**   Surf-riding equilibria of the purse seiner in quartering seas
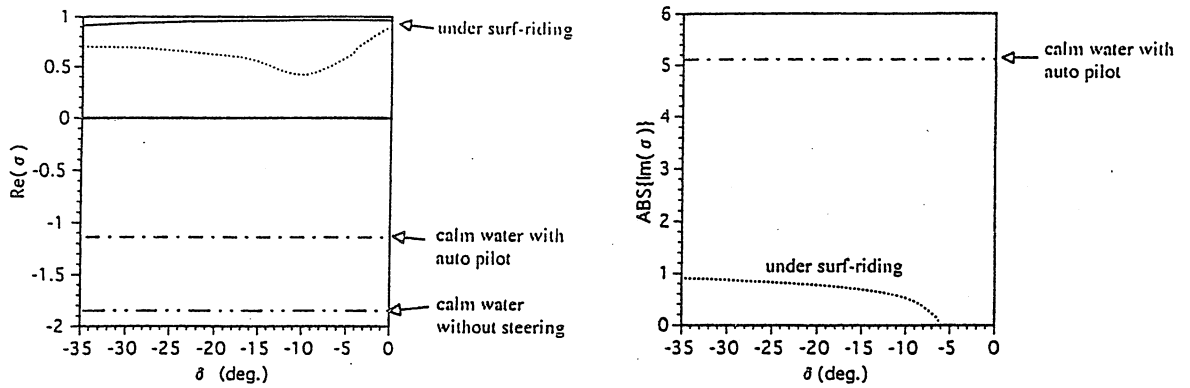
Fig. 9   Maximum of eigenvalues of surf-riding equilibria of the purse
   seiner in quartering seas
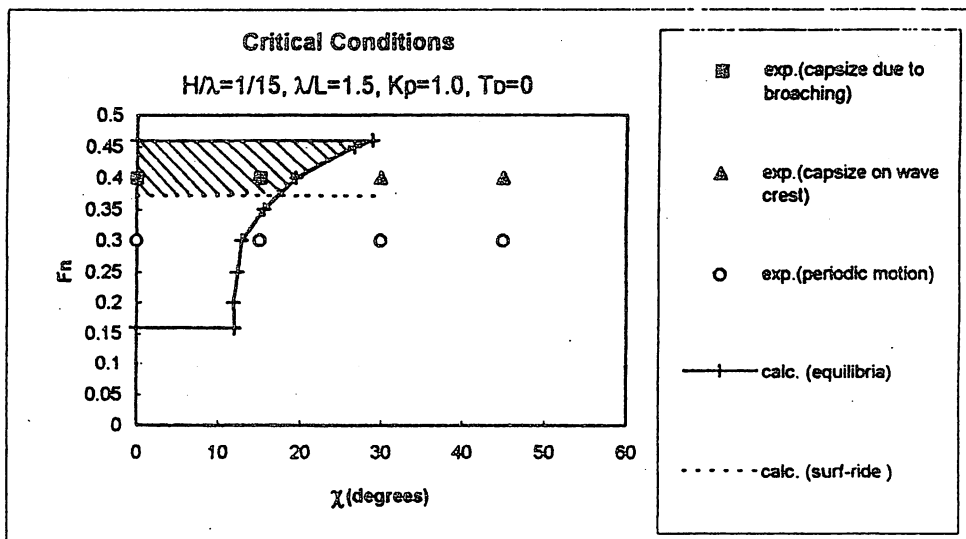
Fig. 10   Dangerous zone for broaching of the purse seiner (shaded zone)

Based on the above knowledge, a scenario toward broaching can be provided as follows. When a ship suffering a periodic motion in following and quartering seas increases her propeller revolution, stability of the periodic motion decreases and surf-riding equilibria potentially emerge. Eventually the ship may leave the periodic motion and be attracted by a surf-riding equilibrium near a wave trough. In other words, the ship is accelerated up to almost the wave celerity. Since this equilibrium is a saddle, the ship is firstly attracted by the equilibrium and then repelled. Even if the maximum opposite rudder angle is commanded immediately after approaching to the equilibrium, the ship's yaw angle may increase at a wave downslope near a wave trough. This series of events can be regarded as broaching. If the yaw rate during broaching is large enough, the ship can capsize. If not, the ship's heading angle becomes too large to maintain surf-riding and eventually she is overtaken by a successive wave crest. In case of a large seakeeping basin, it is often reported that the ship model escaped from broaching suffers broaching again by the successive wave.

2) Critical Condition for broaching

Following the above qualitative description on broaching, the problem how we can quantitatively predict a critical condition for broaching raises. In other words, a method is required to identify initial conditions leading to broaching for a given control parameter set. Although the standard procedure for this problem is the invariant manifolds analysis (Hayashi, 1964), the number of the state variable in the mathematical model is too large to visualise the invariant manifolds.

The second method is a systematic numerical simulation from all combinations of initial value plane. (Thompson, 1990) Since the dimension of the initial value plane is also too large, this method cannot be directly used for broaching. From practical viewpoint, Vassalos (1995) proposed a "reduced degrees-of-freedom" approach in which the degrees-of-freedom are reduced and the range of the initial value plane is limited. A numerical example of this approach is found in Ananiev's work (1994) on capsizing due to broaching from surf-riding and more recently Spyrou (1995-96) reported several numerical examples based on this approach. Although this approach can be practical, its theoretical background is not so strong.

For a ship master, the essential issue is which operational actions lead to broaching from a normal periodic motion. By focusing on this point, the author (1995) proposed the third method. Here we assume that the ship has a steady periodic motion with a certain set of operational parameters and then suddenly changes the operational parameter, namely, propeller revolution or commanded angle for the auto pilot. As a result, the initial

conditions in this case can be determined with an analytical result for a steady periodic motion except for a phase lag between waves and the change of operational parameter. Thus the initial value plane has been limited to 1 dimensional. However, the combinations of change of operational parameters should be considered to be explored numerically.

These above-mentioned methods repeating numerical simulations are still too tedious to be directly adopted as a tool for practical design or operational criteria of ship stability. Although regression analysis with many numerical results by the above methods can be proposed, recent innovative and continuous improvements in ship design cannot accept such conservative ideas. Current life expectancy of a regression analysis is as short as that of a hull form. Therefore, in this paper, the author presents a simple method for a practical use, excluding any numerical simulations. This method defines the dangerous zone for broaching as the zone satisfying both the critical condition for surf-riding without lateral motions in following seas and the existing condition for unstable equilibria with the maximum opposite rudder angle. This idea is based on the following physical background. First a ship runs with a periodic motion in following seas. Then the ship increases her propeller revolution beyond the critical condition for surf-riding. As a result, surf-riding occurs. As soon as the ship's yaw rate appears, the helmsman commands the maximum opposite rudder angle as a bang-bang control. If the ship's yaw motion still increases in spite of this steering action, we can regard this phenomenon as broaching.

A comparison of this dangerous zone and free running model experiments of a fishing vessel by Hamamoto et al. (1996) is shown in Fig. 10. The present simple method well predicts the occurrence of broaching, although physical sequences in the experiments are not always same as the assumed scenario for the present simple method. Further comparisons of this simple method with experiments and numerical simulations are expected.

Conclusions

On the basis of this work the following conclusions can be drawn:

(1) Based on the results of captive model experiments, this study recommends the surge-sway-yaw-roll mathematical model for analysing broaching in even heavy quartering seas.

(2) In the mathematical model, wave forces without lateral motions and linear manoeuvring forces in still water should be taken into account. Some higher order terms require further hydrodynamic and experimental investigations.

(3) In the light of non-linear dynamics, broaching can be qualitatively explained as follows:

When a ship suffering a periodic motion in following and quartering seas increases her propeller revolution, stability of the periodic motion decreases and surf-riding equilibria potentially emerge. Eventually the ship may leave the periodic motion and be attracted by a surf-riding equilibrium near a wave trough. In other words, the ship is accelerated up to almost the wave celerity. Since this equilibrium is a saddle, the ship is firstly attracted by the equilibrium and then repelled. Even if the maximum opposite rudder angle is commanded immediately after approaching to the equilibrium, the ship's yaw angle may increase at a wave downslope near a wave trough.

(4) A simple prediction method of dangerous condition for broaching without repeating numerical simulations is proposed and well compared with an existing free running model experiments.

References

Ananiev, D.(1993): Determination of Vessel's Surf-Riding Regime Domain on the Basis of Stability of Surging Analysis, *Proceedings of the International Workshop on the Problems of Physical and Mathematical Stability Modelling*, Kaliningrad, Vol. 1, paper 12, pp. 1-12.

Ananiev, D. (1994): Vessel's Heeling and Stability in the Regime of manoeuvring and Broaching in Following Seas, *Proceedings of the 5th International Conference on Stability of Ships and Ocean Vehicles*, Melbourne, Vol. 5.

Ananiev, D. (1995): On the Exciting Forces Acting on Ship in Horizontal Plane During her Motion with Drift and Rotation, *Proceedings of the International Symposium on Ship Safety in a Seaway: Stability, Manoeuvrability, Nonlinear Approach*, Kaliningrad, Vol. 1, paper 11, pp. 1-12.

Fujino, M, et al. (1982): On the Stability Derivatives of a Ship Travelling in the Following Waves, *Journal of the Society of Naval Architects of Japan*, No. 152, pp. 167-179, (in Japanese.)

Fuwa, T., et al. (1983): An Experimental Study on Broaching of a Small High Speed Craft, Papers of Ship Research Institute, No. 66, pp. 1-40.

Hamamoto, M. (1971): On the Hydrodynamic Derivatives for the Directional Stability of Ships in Following Seas, *Journal of the Society of Naval Architects of Japan*, No. 130, pp. 83-94, (in Japanese.)

Hamamoto, M. et al. (1996): Model Experiments of Ship Capsize in Astern Seas -Second Report-, *Journal of the Society of Naval Architects of Japan*, No. 179, pp. 77-87.

Hayashi, C. (1964): *Nonlinear Oscillations in Physical Systems*, Princeton University Press, Princeton, pp.238-261.

Kan, M. (1990): A Guideline to Avoid the Dangerous Surf-Riding, *Proceedings of the 4th International Conference on Stability of Ships and Ocean Vehicles*, Naples, pp.90-97.

Matsuda, A., N. Umeda and S. Suzuki (1996): Vertical Motions of a Ship Running in Following and Quartering seas, *Pre-prints of Autumn Meeting of the Kansai Society of Naval Architects*, in press, (in Japanese.)

Renilson, M.R. (1982): An Investigation into the Factors Affecting the Likelihood of Broaching-to in Following Seas, *Proceedings of the 2nd International Conference on Stability of Ships and Offshore Vehicles*, Tokyo, pp. 551-564.

Son, K. and K. Nomoto (1983): On the Coupled Motion of Steering and Rolling of a Ship in Following Seas, *Journal of the Society of Naval Architects of Japan*, No. 152, pp. 180-191, (in Japanese.)

Spyrou, K.J. (1995): Surf-Riding, Yaw Instability and Large Heeling of Ships in Following/Quartering Waves, *Schiffstechnik*, Bd. 42, 103-112.

Spyrou, K.J. and N. Umeda (1995): From Surf-Riding to Loss of Control and Capsize: A Model of Dynamic Behaviour of Ships in Following/Quartering Seas, *Proceedings of the 6th International Symposium on Practical Design of Ships and Mobile Units*, Seoul, Vol. 1, pp.494-505.

Spyrou, K.J. (1995): Surf-Riding and Oscillations of a Ship in Quartering Waves, *Journal of Marine Science and Technology*, No.1, pp.24-36.

Spyrou, K.J. (1996): Dynamic Instability in Quartering Seas: The Behaviour of A Ship During Broaching, *Journal of Ship Research*, to be appeared.

Thompson, J.M.T. (1990): Transient Basin: A New Tool for Designing Ships Against Capsize, *Dynamics of Marine Vehicles and Structures in Waves* (Price, W.G. et al. eds.), Elsevier Science Publishers, pp.325-331.

Umeda, N. (1990): Probabilistic Study on Surf-Riding of a Ship in Irregular Following Seas, *Proceedings of the 4th International Conference on Stability of Ships and Ocean Vehicles*, Naples, pp.336-343.

Umeda, N. and M.R. Renilson (1992): Broaching - A Dynamic Analysis of Yaw Behaviour of a Vessel in a Following Sea, *Manoeuvring and Control of Marine Craft* (Wilson, P.A. eds.), Computational Mechanics Publications (Southampton), pp.553-543.

Umeda, N. and M.R. Renilson (1993): Broaching in Following Seas, *Bulletin of National Research Institute of Fisheries Engineering*, No. 14, pp. 175-186.

Umeda, N. and M.R. Renilson (1994): Broaching of a Fishing Vessel in Following and Quartering Seas, *Proceedings of the 5th International Conference on Stability of Ships and Ocean Vehicles*, Melbourne, Vol. 3, pp.115-132.

Umeda, N. (1995): Application of Nonlinear Dynamical System Approach to Ship Capsize in Regular Following and Quartering Seas, *Workshop: Numerical And Physical Simulation of Ship Capsize in Heavy Seas*, Strathclyde.

Umeda, N., Y. Yamakoshi and S. Suzuki (1995): Experimental Study for Wave Forces on a Ship Running in Quartering Seas with Very Low Encounter Frequency, *Proceedings of the International Symposium on Ship Safety in a Seaway: Stability, Manoeuvrability, Nonlinear Approach*, Kaliningrad, Vol. 1, paper 14, pp. 1-18.

Umeda, N. and D. Vassalos (1996): Non-Linear Periodic Motions of a Ship Running in Following and Quartering Seas, *Journal of the Society of Naval Architects of Japan*, No. 179, pp. 89-101.

Vassalos, D. (1995): A Unified Treatment of Ship Stability: A Heuristic Approach Using Recent Findings in Non-Linear System Approach, *Proceedings of the International Symposium on Ship Safety in a Seaway: Stability, Manoeuvrability, Nonlinear Approach*, Kaliningrad, Vol. 1, paper 3, pp. 1-16.

Nomenclature

Fn	Froude Number	δ	rudder angle
g	gravitational acceleration	λ	wave length
H	wave height		
K_p	rudder gain	ξ_G	distance from a wave crest
L	ship length	χ	heading angle from wave direction
T	propeller thrust		
T_D	time constant for differential control		
		ω_e	encounter frequency
U	forward velocity		

Analysis on Parametric Resonance of Ships in Astern Seas

Masami Hamamoto
James P.Panjaitan
Dept. of Naval Architecture and Ocean Engineering,
Osaka University,
2-1 Yamada-oka, Suita, Osaka 565 Japan

Summary

A study of the ship capsize phenomenon due to parametric resonance is conducted aiming to identify the occurence of a critical condition leading to capsize by considering an analytical solution of an equivalent linearised equation describing the problem in conjunction with results of numerical simulation of the non-linear equation. The main objective of this paper is to formulate the problem in a way that enables an analytical solution to be derived and facilitates an investigation towards identifying the occurence of the critical condition leading to capsize through comparative studies between the analytical solution and the results of numerical simulation.

Finally, a method for judging the possibility of ship capsize due to parametric resonance is proposed based on application of the energy balance method during the critical rolling motion.

1. Introduction

If a ship is running through in astern seas, she will experience periodic variations in her transverse stability, which will affect the roll behaviour of the vessel. The wave-induced stability changes and the resulting parametrically-induced roll motion play an important role in affecting extreme motions and capsizing. In studying large amplitude of rolling motion of ships in astern seas, the wave-induced instability, damping coefficient, natural rolling period and encounter period of ship in waves are pointed out as items relating to capsizing, deriving from the results of experimental analysis[1]. In this respect, it is of particular interest to attempt to develop an analytical approach to relate these items to a critical condition leading to capsize in astern seas corresponding to the Weather Criterion IMO A.562[6] which addresses the beam sea condition. The main problems in following such an approach are considered to be the non-linearity and the time-dependent variation of righting arm curves. Significant variations are caused by the change in the immersed geometry as the ship is overtaken by successive longitudinal waves. In general, for waves with length nearly equal to the ship length, the righting arm curves increase if a wave trough is near amidships and decrease when a crest is near amidships[2],[3]. In this situation, the ship motion can be described by coupled roll, pitch and heave, and hence the righting arm curves should include the effects relevant to these motions[7],[8],[9].

In this situation, the equation of rolling motion can be described in a non-linear form that includes time-dependent terms in a way that is possible to obtain a numerical solution of it from a step-by-step approximation method but it is difficult to obtain an analytical solution leading to a deeper understanding in the study of capsizing.

The main objective of this paper is to obtain such an analytical solution from an equivalent linearised equation of motion and to investigate the occurence of the critical condition leading to capsize by considering the analytical solution in conjunction with the results of numerical simulation of the non-linear equation. The equivalent linearisation is a method which is generally suitable for describing a dynamic system in which large deviations from linear behaviour are not anticipated. A reasonable approximation to the exact behaviour of the real system, therefore, is given by an equivalent linear system having suitably selected coefficients. The principal shortcoming of this method, is that the limits of applicability depend on the degree of approximation which is difficult to estimate.

Finally, a method of judging capsize due to parametric resonance is proposed based on an application of the energy balance method during the critical rolling motion.

2. Equation of Motion and its Equivalent Linearised Equation

An equation of motion including the effect of pitching and heaving of a ship running in following seas may be described in the following form:

$$(I_x + J_x)\ddot{\phi} + D(\dot{\phi}) + W \cdot GZ(\phi, t) = 0 \tag{1}$$

where $I_x + J_x$ are the real and added moments of inertia, respectively, $D(\dot{\phi})$ the damping force, W the ship weight and $GZ(\phi, t)^{4)}$ the righting arm including the wave-induced, time-dependent variation.

Taking into account the equivalent damping coefficient α_e, the natural rolling frequency ω_0, and the metacentric height GM, Eq.(1) can be rewritten as follows

$$\ddot{\phi} + 2\alpha_e\dot{\phi} + \omega_0^2 \frac{GZ(\phi, t)}{GM} = 0 \tag{2}$$

where

$$2\alpha_e\dot{\phi} = \frac{D(\dot{\phi})}{I_x + J_x}, \quad \omega_0^2 = \frac{W \cdot GM}{I_x + J_x} \tag{3}$$

In Eq.(2) the equivalent linear damping coefficient α_e is related to the extinction coefficient a_e, natural rolling period T_ϕ, Bertin coefficient N and the amplitude of rolling angle ϕ_0 as shown by the following expressions

$$\alpha_e = \frac{2a_e}{T_\phi}, \quad a_e = N\phi_0 \tag{4}$$

Next, let us consider the righting arm variation with respect to the relative position of ship in waves $GZ(wave)$ on a longitudinal wave. As indicated earlier, the $GZ(wave)$ increases with the wave trough amidships and decreases with the wave crest amidships in comparison with the righting arm $GZ(still)$ in still water. For example, Fig.1 shows the righting arm curves of a $15000GT$ container vessel referring to the ship on the wave trough $GZ(trough)$, wave crest $GZ(crest)$ and in still water $GZ(still)$.

When the ship is rolling in severe following seas, the rolling angle becomes significantly large. Therefore, the equivalent metacentric height must be determined on the basis of the righting arm curve considered up to an appropriate angle of inclination as follows:

$$GM(still) = \frac{2}{\phi^2} \int_0^\phi GZ(still)d\phi$$

$$GM(trough) = \frac{2}{\phi^2} \int_0^\phi GZ(trough)d\phi \qquad (5)$$

$$GM(crest) = \frac{2}{\phi^2} \int_0^\phi GZ(crest)d\phi$$

Fig.2 shows these equivalent linearised metacentric heights obtained from Eq.(5) which has been applied to the $GZ(still)$, $GZ(trough)$ and $GZ(crest)$ shown in Fig.1, respectively. Since the metacentric heights, as shown in Eq.(5) vary with the appropriate angle of inclination, a further consideration is required to specify this angle on the basis of a reasonable method leading to a really equivalent solution. For this problem, an assumption is made here that the variation of metacentric height $GM(wave)$ is sinusoidal, as shown in Fig. 3, and given by the relation

$$GM(wave) = GM(still) \left[1 + a_0 + a_1 \cos k\xi_G \right] \qquad (6)$$

where a_0 is the average movement of the center of buoyancy predicted as

$$1 + a_0 = \frac{GM(trough) + GM(crest)}{2 \cdot GM(still)} \qquad (7)$$

a_1 the amplitude of wave-induced variation in metacentric height given by

$$a_1 = \frac{GM(trough) - GM(crest)}{2 \cdot GM(still)} \qquad (8)$$

k the wave number and ξ_G the relative position of ship in waves which is defined as shown in Fig.4, and described by using the ship speed U, the phase velocity of wave c and an initial position of the ship at time $t = 0$, in the following form

$$\xi_G = \xi_0 - |c - U|t \qquad (9)$$

According to the method mentioned in Section 1, an equivalent linearised righting arm $GZ(\phi, t)$ could be described as

$$GZ(\phi, t) = GM \left[1 + a_0 + a_1 \cos(k\xi_0 - \omega_e t) \right] \phi \qquad (10)$$

yielding Eq.(2) in the following linearised form

$$\ddot{\phi} + 2\alpha_e \dot{\phi} + \omega_0^2 \left[1 + a_0 + a_1 \cos(k\xi_0 - \omega_e t) \right] \phi = 0 \qquad (11)$$

3. Parametric Resonance in Critical Condition, Stable and Unstable Regions

When a ship is running in following seas, she normally rolls with a frequency nearly equal to the natural frequency ω_0. Accordingly, the rolling angle $\phi(t)$ can be approximated by

$$\phi(t) = A \cos \omega_0 t + B \sin \omega_0 t \qquad (12)$$

Let us now consider what would be the encounter frequency leading to critical parametric resonance. To answer this question, use will be made of the energy balance method. Applying this method to the half cycle of rolling motion in Eq.(11) yields

$$\int_0^{T/2} \ddot{\phi} d\phi + 2\alpha_e \int_0^{T/2} \dot{\phi} d\phi + \omega_0^2(1 + a_0) \int_0^{T/2} \phi d\phi + \omega_0^2 a_1 \int_0^{T/2} \phi \cos(k\xi_0 - \omega_e t) d\phi = 0 \qquad (13)$$

and substituting Eq.(12) and its derivatives into Eq.(13), it follows

$$\alpha_e \omega_0^2 (A^2 + B^2)\frac{T}{2} + a_1\omega_0^3 \int_0^{T/2} \left[AB\cos 2\omega_0 t - \frac{1}{2}(A^2 - B^2)\sin 2\omega_0 t \right] \cos(k\xi_0 - \omega_e t)dt = 0$$

(14)

In Eq.(14), the encounter frequency should be equal to twice the natural rolling frequency, $\omega_e = 2\omega_0$, to keep a critical rolling of constant amplitude. This condition requires the following relationship

$$\alpha_e(A^2 + B^2) + a_1\omega_0\frac{1}{4}\left[2AB\cos k\xi_0 - (A^2 - B^2)\sin k\xi_0 \right] = 0$$

(15)

Here, Eq.(12) can be rewritten as

$$\phi(t) = \phi_0 \cos(\omega_0 t - \epsilon)$$

(16)

where

$$\phi_0 = \sqrt{A^2 + B^2}, \qquad \epsilon = \tan^{-1}\left(\frac{B}{A}\right)$$

(17)

From Eqs.(4),(15) and (16), A and B are determined by

$$A^2 = \frac{\phi_0^2}{2}\left[1 + \left(\frac{4a_e}{\pi a_1}\right)\sin k\xi_0 \pm \sqrt{1 - \left(\frac{4a_e}{\pi a_1}\right)^2}\ \cos k\xi_0 \right]$$

(18)

$$B^2 = \frac{\phi_0^2}{2}\left[1 - \left(\frac{4a_e}{\pi a_1}\right)\sin k\xi_0 \mp \sqrt{1 - \left(\frac{4a_e}{\pi a_1}\right)^2}\ \cos k\xi_0 \right]$$

(19)

Eqs.(18) and (19) describe a critical condition where a constant rolling amplitude is maintained.

Let us consider next the conditions in which the rolling angle grows up to an unstable region and decays to a stable region. It will be possible for this analysis to describe the rolling angle[5] as follows

$$\phi(t) = A(t)\cos\omega_0 t + B(t)\sin\omega_0 t$$

(20)

Here, $A(t)$ and $B(t)$ are functions of time. Therefore, the stable and unstable regions can be specified from the behaviour of $A(t)$ and $B(t)$. In this method, the equation of motion relates to the equation at the critical condition as follows

$$\ddot{\phi} + 2\alpha_e\dot{\phi} + \omega_0^2[1 + a_0 + a_1\cos(k\xi_0 - 2\omega_0 t)]\phi = 0$$

(21)

Substituting Eq.(20) and its derivatives into Eq.(21), yields the following

$$[\ddot{A} + 2\alpha_e\dot{A} + \omega_0^2\left(a_0 + \frac{a_1}{2}\cos k\xi_0\right)A + 2\omega_0\dot{B} + \left(2\alpha_e\omega_0 + \frac{a_1}{2}\omega_0^2\sin k\xi_0\right)B]\cos\omega_0 t$$

$$+ \ [\ddot{B} + 2\alpha_e\dot{B} + \omega_0^2\left(a_0 - \frac{a_1}{2}\cos k\xi_0\right)B - 2\omega_0\dot{A} - \left(2\alpha_e\omega_0 - \frac{a_1}{2}\omega_0^2\sin k\xi_0\right)A]\sin\omega_0 t$$

$$+ \ \frac{a_1}{2}\omega_0^2(A\cos k\xi_0 - B\sin k\xi_0)\cos 3\omega_0 t + \frac{a_1}{2}\omega_0^2(A\sin k\xi_0 + B\cos k\xi_0)\sin 3\omega_0 t = 0$$

(22)

Although there exist two kinds of frequency components in Eq.($\overline{22}$), namely, ω_0 and $3\omega_0$, the main frequency at the parametric resonance is approximately equal to the natural rolling frequency, and the effect of the frequency component $3\omega_0$ to rolling motion will be small enough to neglect.

Accordingly, $A(t)$ and $B(t)$ are determined by an approximate analytical solution to satisfy the reduced Eq.(22), resulting by neglecting the last two terms, thus yielding the following relations

$$\ddot{A} + 2\alpha_e \dot{A} + \omega_0^2 \left(a_0 + \frac{a_1}{2}\cos k\xi_0 \right) A + 2\omega_0 \dot{B} + (2\alpha_e\omega_0 + \frac{a_1}{2}\omega_0^2\sin k\xi_0)B = 0$$

$$\ddot{B} + 2\alpha_e \dot{B} + \omega_0^2 \left(a_0 - \frac{a_1}{2}\cos k\xi_0 \right) B - 2\omega_0 \dot{A} - (2\alpha_e\omega_0 - \frac{a_1}{2}\omega_0^2\sin k\xi_0)A = 0 \quad (23)$$

Eq.(23) is a system of linear differential equations in $A(t)$ and $B(t)$. Applying Laplace transformation to Eq.(23), yields the following equations

$$\left[s^2 + 2\alpha_e s + \omega_0^2(a_0 + \frac{a_1}{2}\cos k\xi_0) \right] \hat{A} + \left[2\omega_0 s + (2\alpha_e\omega_0 + \frac{a_1}{2}\omega_0^2\sin k\xi_0) \right] \hat{B} = 0$$

$$\left[s^2 + 2\alpha_e s + \omega_0^2(a_0 - \frac{a_1}{2}\cos k\xi_0) \right] \hat{B} - \left[2\omega_0 s + (2\alpha_e\omega_0 - \frac{a_1}{2}\omega_0^2\sin k\xi_0) \right] \hat{A} = 0 \quad (24)$$

The determinant which specifies stable and unstable solutions from Eq.(24) as follows

$$(s + \alpha_e)^4 + 2(2\omega_0^2 + a_0\omega_0^2 - \alpha_e^2)(s + \alpha_e)^2 + \omega_0^4 \left(a_0^2 - \frac{a_1^2}{4} \right) - 2a_0\alpha_e^2\omega_0^2 + \alpha_e^4 = 0 \quad (25)$$

In Eq.(25), the rolling motion increases significantly if s is positive ($s > 0$), decays if s is negative ($s < 0$) and is critical if s is equal to zero ($s = 0$). Deriving from the discussion in the foregoing, the condition leading to the capsize of a ship in following seas can be expressed as

$$\frac{a_1\pi}{4a_e} > \sqrt{1 + \left(\frac{a_0\pi}{2a_e} \right)^2} \quad \text{in an unstable region} \quad (26)$$

$$\frac{a_1\pi}{4a_e} < \sqrt{1 + \left(\frac{a_0\pi}{2a_e} \right)^2} \quad \text{in a stable region} \quad (27)$$

$$\frac{a_1\pi}{4a_e} = \sqrt{1 + \left(\frac{a_0\pi}{2a_e} \right)^2} \quad \text{at the critical condition} \quad (28)$$

Fig.5 shows the stable and unstable regions derived from Eqs.(26), (27) and (28). Fig.6 indicates the typical time histories of rolling in the stable and unstable regions and for the critical condition taken at points A, B and C, respectively. In this figure, the circles indicate the solutions obtained from the non-linear Eq.(2), whilst the solid line represent the solution of the equivalent linearised Eq.(11). It is shown that both solutions tend to be consistently close at the appropriate angle of inclination of 34 degrees of $GZ(still)$, determined as shown in Fig.2.

4. Rolling Amplitude at the Critical Condition

Let us next consider the rolling amplitude of Eq.(21) at the critical condition to satisfy Eq.(28). Substituting Eq.(28) then into Eqs.(18) and (19), A and B may be rewritten in the following form

$$A^2 = \frac{\phi_0^2}{2} \left[1 + \sqrt{1 - \left(\frac{2a_0}{a_1}\right)^2} \sin k\xi_0 \pm \left(\frac{2a_0}{a_1}\right) \cos k\xi_0 \right] \tag{29}$$

$$B^2 = \frac{\phi_0^2}{2} \left[1 - \sqrt{1 - \left(\frac{2a_0}{a_1}\right)^2} \sin k\xi_0 \mp \left(\frac{2a_0}{a_1}\right) \cos k\xi_0 \right] \tag{30}$$

Eqs.(29) and (30) are derived from the energy balance Eq.(15). In order to specify A and B, the value of ϕ_0 in Eqs.(29) and (30) has to be obtained from numerical solution of Eq.(21) at the critical condition. In Eq.(21), the rolling angle $\phi(t)$ vary with respect to the initial position ξ_0 at t=0 when the ship inclined at 10deg. as shown in Fig.7.

Fig.8 shows the constant rolling amplitude ϕ_0 at the critical condition as a function of the initial position ξ_0. The constant rolling amplitude will take the maximum when the ship inclined at the initial position ξ_0/λ=0.25 generally and take a minimum when the ship inclined at the initial position ξ_0/λ=0.825.

It is furthermore possible to determine A and B in Eq.(12) at the critical condition by make use of Eqs.(29) and (30). Fig.9 indicates the variations of A and B with respect to the initial position when the ship inclined at 10deg.

5. Energy Balance of GZ curves during Critical Rolling Motion

Following from the discussion in the previous section, the relationship between the critical rolling $\phi(t)$ and the variation of metacentric height $GM(t)$ can be described in a form that includes the effects of average movement of the center of buoyancy a_0, the amplitude of wave-induced metacentric height a_1, Bertin coefficient N, the natural rolling frequency ω_0 and the initial position of the ship relative to wave, ξ_0 at time $t = 0$, which are

$$\phi(t) = \frac{\pi a_1}{4N} \sqrt{1 - \left(\frac{2a_0}{a_1}\right)^2} \cos(\omega_0 t - \epsilon) \tag{31}$$

$$\epsilon = \tan^{-1} \left[\frac{1 - \sqrt{1 - (2a_0/a_1)^2} \sin k\xi_0 \mp (2a_0/a_1) \cos k\xi_0}{1 + \sqrt{1 - (2a_0/a_1)^2} \sin k\xi_0 \pm (2a_0/a_1) \cos k\xi_0} \right]^{1/2} \tag{32}$$

$$GM(t) = GM[1 + a_0 + a_1 \cos(2\omega_0 t - k\xi_0)] \tag{33}$$

Fig.10 shows the relationship between the variation of metacentric height and the critical rolling of constant amplitude ϕ_0 in the time domain. In this figure, the roll angle increases to the maximum at $GM(1 + a_0)$ which is nearly equal to $GM(still)$. It then decreases from maximum to the upright condition when the metacentric height $GM(t)$ is smaller than $GM(still)$ and again increases from the upright condition to the maximum on the reverse direction when the metacentric height $GM(t)$ is bigger than $GM(still)$. The above process is necessary in order to keep a constant amplitude during the critical rolling. In this case, the wave-induced variation in metacentric height controls the rolling angle in a

4. Rolling Amplitude at the Critical Condition

Let us next consider the rolling amplitude of Eq.(21) at the critical condition to satisfy Eq.(28). Substituting Eq.(28) then into Eqs.(18) and (19), A and B may be rewritten in the following form

$$A^2 = \frac{\phi_0^2}{2} \left[1 + \sqrt{1 - \left(\frac{2a_0}{a_1}\right)^2} \sin k\xi_0 \pm \left(\frac{2a_0}{a_1}\right) \cos k\xi_0 \right] \tag{29}$$

$$B^2 = \frac{\phi_0^2}{2} \left[1 - \sqrt{1 - \left(\frac{2a_0}{a_1}\right)^2} \sin k\xi_0 \mp \left(\frac{2a_0}{a_1}\right) \cos k\xi_0 \right] \tag{30}$$

Eqs.(29) and (30) are derived from the energy balance Eq.(15). In order to specify A and B, the value of ϕ_0 in Eqs.(29) and (30) has to be obtained from numerical solution of Eq.(21) at the critical condition. In Eq.(21), the rolling angle $\phi(t)$ vary with respect to the initial position ξ_0 at t=0 when the ship inclined at 10deg. as shown in Fig.7.

Fig.8 shows the constant rolling amplitude ϕ_0 at the critical condition as a function of the initial position ξ_0. The constant rolling amplitude will take the maximum when the ship inclined at the initial position $\xi_0/\lambda=0.25$ generally and take a minimum when the ship inclined at the initial position $\xi_0/\lambda=0.825$.

It is furthermore possible to determine A and B in Eq.(12) at the critical condition by make use of Eqs.(29) and (30). Fig.9 indicates the variations of A and B with respect to the initial position when the ship inclined at 10deg. Thus, it would be important to predict the critical rolling angle at the initial position $\xi_0/\lambda=0.25$ where ship inclining at appropriate angle.

5. Energy Balance of GZ curves during Critical Rolling Motion

Following from the discussion in the previous section, the relationship between the critical rolling $\phi(t)$ and the variation of metacentric height $GM(t)$ can be described in a form that includes the effects of average movement of the center of buoyancy a_0, the amplitude of wave-induced metacentric height a_1, Bertin coefficient N, the natural rolling frequency ω_0 and the initial position of the ship relative to wave, ξ_0 at time $t = 0$, which are

$$\phi(t) = \frac{\pi a_1}{4N} \sqrt{1 - \left(\frac{2a_0}{a_1}\right)^2} \cos(\omega_0 t - \epsilon) \tag{31}$$

$$\epsilon = \tan^{-1} \left[\frac{1 - \sqrt{1 - (2a_0/a_1)^2} \sin k\xi_0 \mp (2a_0/a_1) \cos k\xi_0}{1 + \sqrt{1 - (2a_0/a_1)^2} \sin k\xi_0 \pm (2a_0/a_1) \cos k\xi_0} \right]^{1/2} \tag{32}$$

$$GM(t) = GM[1 + a_0 + a_1 \cos(2\omega_0 t - k\xi_0)] \tag{33}$$

Fig.10 shows the relationship between the variation of metacentric height and the critical rolling of constant amplitude ϕ_0 in the time domain. In this figure, the roll angle increases to the maximum at $GM(1 + a_0)$ which is nearly equal to $GM(still)$. It then decreases from maximum to the upright condition when the metacentric height $GM(t)$ is smaller than $GM(still)$ and again increases from the upright condition to the maximum on the reverse direction when the metacentric height $GM(t)$ is bigger than $GM(still)$. The above

process is necessary in order to keep a constant amplitude during the critical rolling. In this case, the wave-induced variation in metacentric height controls the rolling angle in a way that it does not develop further at the critical condition. Therefore, the wave-induced metacentric height variation acts as an external wave force correspondingly similar to that of the beam sea condition, as

$$\ddot{\phi} + 2\alpha_e\dot{\phi} + \omega_0^2(1 + a_0)\phi = -\omega_0^2 a_1\phi\cos(2\omega_0 t - k\xi_0) \tag{34}$$

On the basis of the above consideration, it will be possible to make use of the energy balance method. In this method, the area under $GZ(still)$ up to the vanishing angle ϕ_r must be larger than the area up to the critical rolling angle ϕ_0, as shown in Fig.14. Furthermore, for judging ship capsize in following seas, the condition which derives from the same concept as that in beam sea condition may in this case be expressed as

$$\phi_r > \phi_0 \tag{35}$$

where ϕ_0 is calculated from Eq.(21) and ϕ_r obtained from GZ curve in still water.
The energy balance shown in Fig.14 is for the critical rolling at point B shown in Fig.5.

Experiment Verification of Roll Motion Occurence in Critical, Stable and Unstable regions

Free running model experiments were carried out in the towing tank of Osaka University aiming to identify the occurence of critical, stable and unstable rolling motion for a 15000GT container carrier as shown in Fig.11. Regular waves of wave to ship length ratio $\lambda/L = 1.2$ and wave height to length ratio $H/\lambda = 1/25$ for unstable motion and $H/\lambda = 1/30$ for critical and stable motion as shown in Fig.12 were used for the model experiments. It has to be noted that in such an experiment, it is not easy to keep the model running at the straight course without steering. Therefore, the examples shown in Fig.13 represent a few cases when the model was running in direction which could be in approximately described as following seas condition.

The first case shows pitching, rolling and yawing angles measured by the optical Gyro during the critical rolling motion, whilst the second and third indicate the same motions during the stable and unstable rolling motion, respectively. These three cases represent results obtained from experiments in the same regular waves but in different wave heights.

Finally, Fig.14 shows the energy balance of critical rolling motion in following sea condition compared with that in beam sea condition obtained from IMO A.562. The rolling angle for the same waves in following sea condition is larger than that in beam sea condition. This will be an interesting problem to be considered next.

6. Concluding Remarks

An analytical study of the ship capsize phenomenon due to parametric resonance is conducted to investigate the occurence of the critical condition leading to capsize by considering the analytical solution of an equivalent linearised equation of motion in conjunction with the results of numerical simulation of the non-linear equation. The main conclusions are summarized as follows

(1) An analytical solution is derived for specifying the stable, unstable regions of rolling motion and the critical condition where a constant rolling amplitude is maintained.

(2) The constant rolling amplitude can be predicted by using the Bertin coefficient N, the equivalent linearised metacentric height and the equivalent metacentric heights evaluated from the righting arm curves with the wave trough and crest amidships, and in still water.

(3) It is finally concluded that a method for judging ship capsize due to parametric resonance is possible by considering an application of the energy balance method during the critical rolling motion.

This study was carried out under the auspices of RR 71 research panel of Shipbuilding Research Association of Japan. The authors wish to express their gratitude to the members of the RR 71, chaired by Prof. M. Fujino for their constructive discussion. The authors would also like to thank Prof. D. Vassalos of Strathclyde University, U.K, a visiting Professor in Osaka University, for fruitful discussion and for kindly reading through this paper.

References

1) Grim,O. : Rollschwingungen, *Stabilität* und Sicherheit im Seegang, Schiffstechnik, Vol.1, (1952), pp.10–21.

2) Kerwin, J.E. : Notes on Rolling in Longitudinal Waves, International Shipbuilding Progress, Vol.2, No.16, (1955), pp.597–614.

3) Paulling, J.R. : The Transverse Stability of a Ship in a Longitudinal Seaway, Journal of Ship Research, SNAME, Vol.4, No.4, (1961), pp.37–49.

4) Hamamoto, M., Nomoto, K., : Transverse Stability of Ships in a Following Sea, STABILITY'82, (1982).

5) Hamamoto, M., Fujino, M., : Capsizes of Ship in Following Seas, Third Symposium on Marine Dynamics, The Society of Naval Architect of Japan, (1986), pp.125-157.

6) IMO, : The IMO Intact Stability Criteria, Resolution A.562, (1985).

7) Hamamoto, M., Sera, W., Panjaitan, J.P,: Analyses on Low Cycle Resonance of Ship in Irregular Astern Seas, Journal of the Society of Naval Architects of Japan, Vol.178, (1995), pp.137-145.

8) Umeda N., Hamamoto, M., Takaishi Y., Chiba Y., Matsuda A., Sera, W., Suzuki S., Spyrou K., Watanabe K., : Model Experiment of Ship Capsize in Astern Seas, Journal of the Society of Naval Architect of Japan, (1995), Vol.177, pp.207-217

9) Hamamoto, M., Enomoto, T., Sera, W., Panjaitan, J.P., Ito, H., Takaishi, Y., Kan, M., Haraguchi, T., Fujiwara, T., : Model Experiment of Ship Capsize in Astern Seas (Second Report), Journal of the Society of Naval Architect of Japan, (1996), Vol.179, pp.77-87.
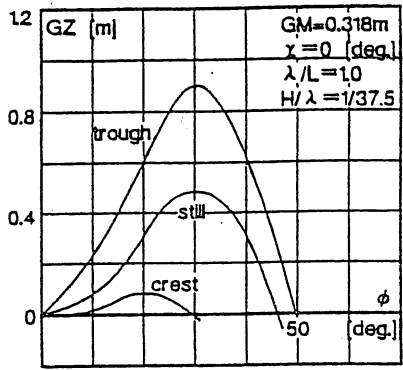
Fig.1 The righting arm GZ curves of container vessel
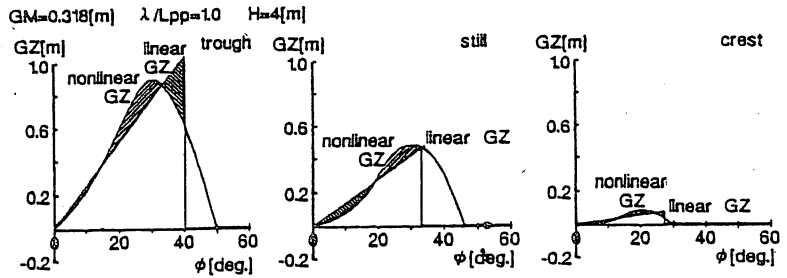
Fig.2 The equivalent linearised metacentric height GM of container vessel
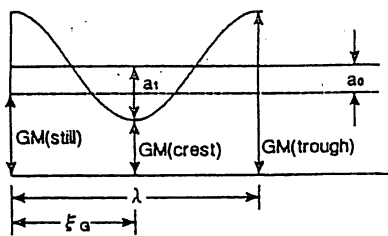
Fig.3 The variation of metacentric height $GM(wave)$
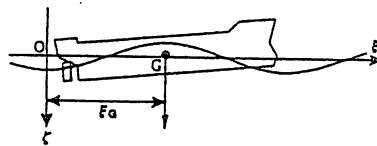
Fig.4 The relative position of ship to waves
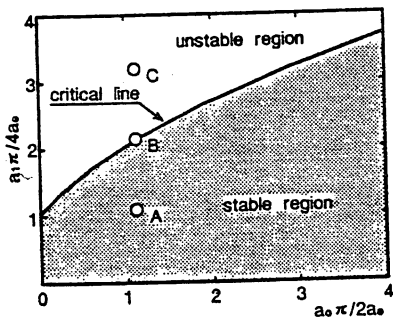
Fig.5 Stable and unstable region
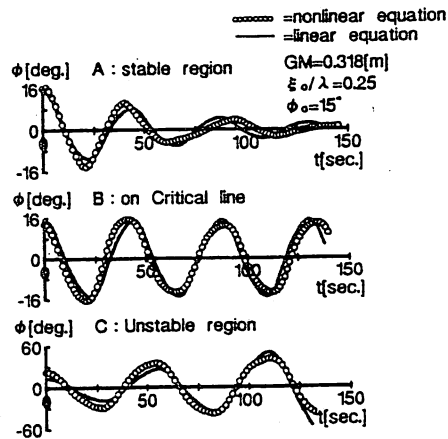
Fig.6 Typical time histories of rolling in stable, unstable region, and for the critical line
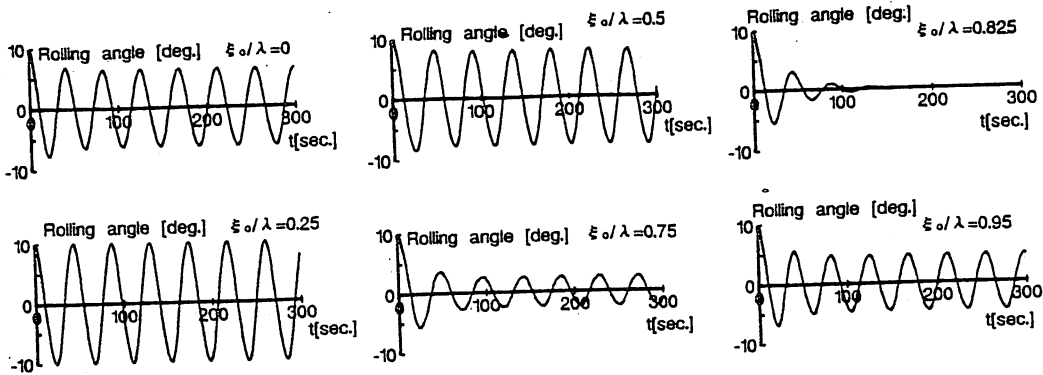
Fig.7 Time histories of constant rolling amplitude
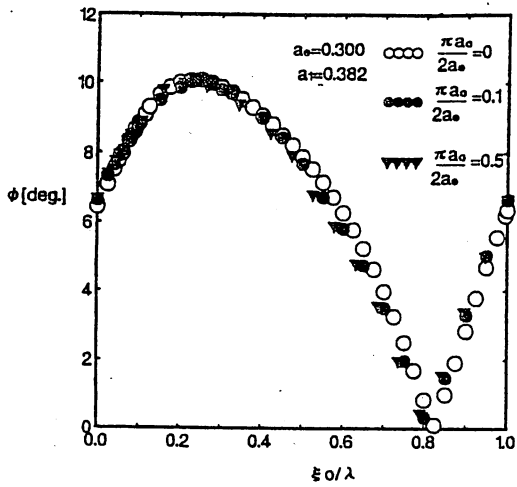
Fig.8 Constant rolling amplitude with respect to relative initial position of ship in a wave (ξo/λ)
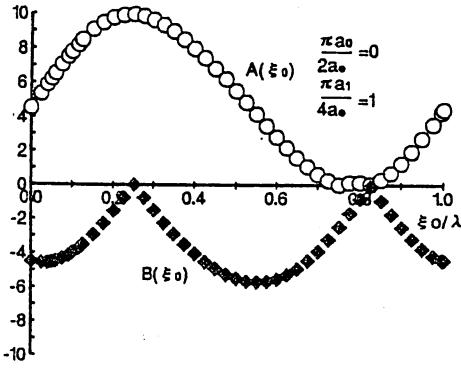
Fig.9 Variations of A and B with respect to relative intial position of ship in a wave (ξo/λ)
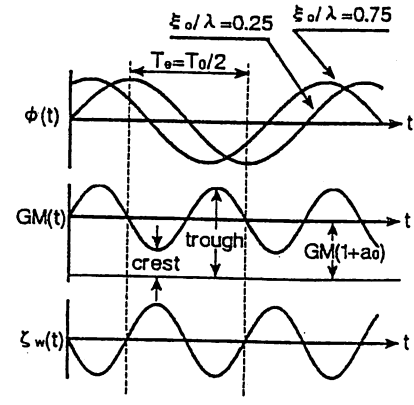
Fig. 10 Variation of GM at maximum and minimum rolling amplitude

Items		Ship	Model
Length	L(m)	150.0	2.5
Breadth	B(m)	27.2	0.453
Depth	D(m)	13.5	0.225
Draft	d_f(m)	8.50	0.142
	d_a(m)	8.50	0.142
Block Coef.	C_b	0.667	0.667
Metacentric height	GM(m)	0.318	0.0053
Natural Period	T(sec.)	38.73	5.0
Model Scale	—	—	1/60
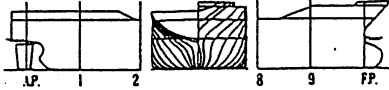
Fig.11 Principal Dimension of Container Carrier

Exp. No.16 λ/L=1.2 H/λ=1/25 Tw=1.38[sec.]

wave profile for unstable motion

Exp. No.18 λ/L=1.2 H/λ=1/30 Tw=1.38[sec.]

wave profile for critical and stable motions
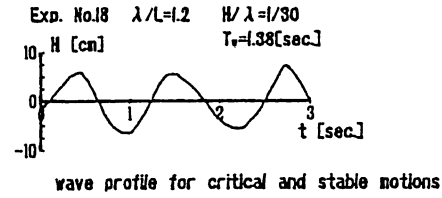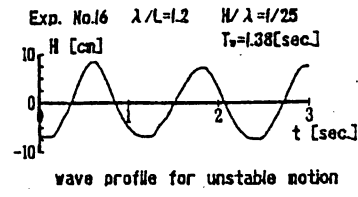
Fig.12 Wave profile used for experiments

Exp. No. 18 critical motions
λ/L=1.2 H/λ=1/30

Exp. No. 17 stable motions
λ/L=1.2 H/λ=1/30

Ex. No. 16 unstable motion
λ/L=1.2 H/λ=1/25
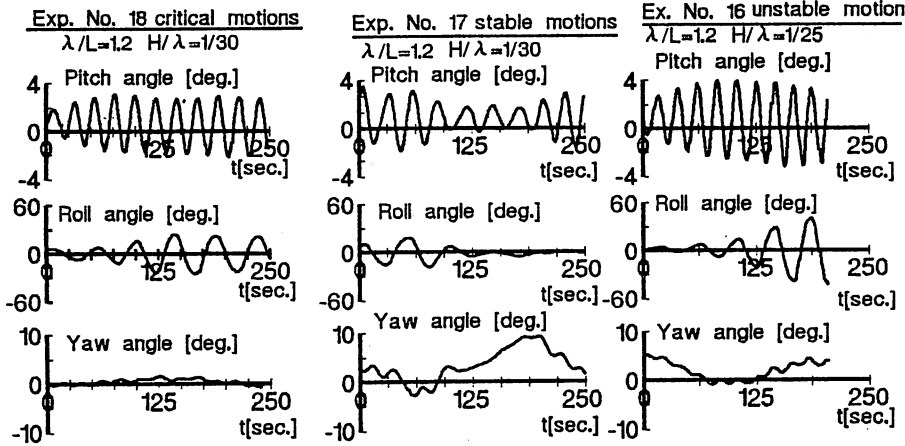
Fig.13 Time histories in critical, stable and unstable motion

Exp. No. 18 critical motions
λ/L=1.2 H/λ=1/30 ar=0.662
Fn=0.20 N=0.017

········ =simulation
——— =experiment
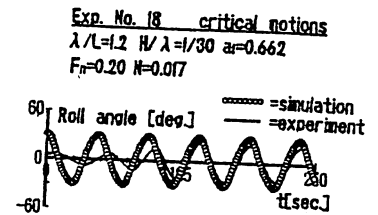
harmonic resonance in beam seas condition

GM=0.318m
χ=90 [deg.]
λ/L=1.2
H/λ=1/30
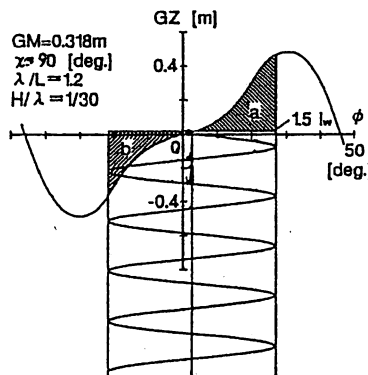
parametric resonance in following seas condition

GM=0.318m
χ=0 [deg.]
λ/L=1.2
H/λ=1/30
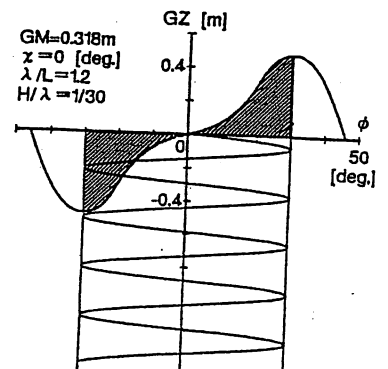
Fig.14 Energy balance diagram for beam and following seas condition

PROBABILITY TO ENCOUNTER HIGH RUN OF WAVES IN THE DANGEROUS ZONE SHOWN ON THE OPERATIONAL GUIDANCE/IMO FOR FOLLOWING/QUARTERING SEA

Yoshifumi Takaishi

College of Science and Technology, Nihon University

7-24-1 Narashinodai, Funabashi, Chiba 274, Japan

SUMMARY

The time history of encounter waves differs from the wave record at a fixed point, i.e. the groupiness of encounter waves varies according to ship course and speed. The groupiness of ocean waves itself had been estimated statistically by using characteristic values of wave spectrum. This method has been applied to the encounter waves, and the variation of the groupiness has been determined as a function of V/T, i.e. ship speed/wave period, in following and quartering seas. The probability to encounter high run is shown as functions of V/T and number of runs. It is concluded that the groupiness or probability to encounter high run becomes higher in a range of V/T between 1.0 and 2.0 (kt/sec).

INTRODUCTION

One of the dangerous situations for ships navigating in following and quartering seas is to encounter occasionally a group of high waves, i.e. high run. The present author had been explained this phenomena by introducing a concept of the wave energy concentration ratio which is determined on the encounter wave spectrum, and he has proposed the dangerous zone to encounter high run on the V/T-Diagram[1]. This idea is now included in the "Guidance to the Master for Avoiding Dangerous Situations in Following and Quartering Seas", which recently has been adopted as the MSC/IMO Circular[2].

However, this V/T-diagram gives no quantitative information on the degree of encountering

high run. Then, the author has tried to derive the statistical properties of this encounter wave grouping phenomena in following and quarteringseas to quantify the probability of occurrence of high runs in wave group, applying the Longuet-Higgins' method[3] that the groupiness of ocean wave itselfdepends on the characteristic values of energy spectrum. A band-width parameter,which is calculated for the encounter wave spectrum transformed from the ocean wave spectrum, is used to estimate the probability of wave group length or high run to be appeared in encounter waves of a ship.

The results have been confirmed by the statistical analysis of simulated time series of encounter waves that the probability of occurrence of high runs in following sea becomes higher in the range of $V / T = 1.0 \sim 2.0$ with the highest value at $V / T \cong 1.45$. The influences of directional distribution of wave energy, i.e. the effects of short-crestedness of ocean waves have been also investigated and it has been shown that the increment of encounter wave groupiness is less, as the directional distribution of wave energy becomes wider.

STATISTICAL ANALYSIS OF WAVE GROUP

Longuet-Higgins' Method

The run is the number of successive wave train in a group, all of which exceed a level ρ, as shown in Fig.1. According to Longuet-Higgins, the mean length of wave group, $\bar{l}$, the mean values of wave number and run in a group, $\bar{G}$ and $\bar{H}$, are represented by the following formulae as the functions of the band-width parameter, v, of the wave spectrum.

$$\bar{l} = \left\{ \mu_2 / (2\pi) \right\}^{-1/2} (\mu_0 / \rho) e^{\rho^2 / (2\mu_0)} \tag{1}$$

$$\bar{G} = (2\pi)^{-1/2} [(1+v^2)^{1/2} / v](\mu_0^{1/2} / \rho) e^{\rho^2 / (2\mu_0)} \tag{2}$$

$$\bar{H} = (2\pi)^{-1/2} [(1+v^2)^{1/2} / v]\mu_0^{1/2} / \rho \tag{3}$$

where v is derived from the n-th moment of the spectrum, as follows,

$$v = \sqrt{m_0 m_2 - m_1^2} / m_1 \tag{4}$$

$$\mu_0 = m_0 , \quad \mu_1 = 0 , \quad \mu_2 = m_2 - m_1^2 / m_0 \tag{5}$$

provided that the components of the spectrum in higher frequency range than $1.5 f_p$ as well as the lower frequency range than $0.5 f_p$ are ignored, where f_p is peak frequency of the spectrum.

The probability density functions of l, G and H are represented by an exponential function, respectively, as follows.

$$p(l) = \bar{l}^{-1} e^{-l/\bar{l}} \qquad (6)$$

$$p(G) = \bar{G}^{-1} e^{-G/\bar{G}} \qquad (7)$$

$$p(H) = \bar{H}^{-1} e^{-H/\bar{H}} \qquad (8)$$

The probability that the run exceeds H is calculated by equation (9).

$$P(H) = \int_H^\infty p(H)dH = e^{-H/\bar{H}} \qquad (9)$$

Application to Encounter Wave

The encounter wave spectrum is obtained by transformation of wave spectrum in wave frequency domain ω into encounter wave frequency domain ω_e, i.e.

$$S(\omega_e, \chi) = S(\omega)/|1 - 2\omega V \cos \chi / g| \qquad (10)$$

where V is ship speed, χ is encounter angle, and

$$\omega_e = \omega - \omega^2 V \cos \chi / g \qquad (11)$$

The Longuet-Higgins' method is applied to the encounter wave spectrum. The spectrum of Pierson-Moskowitz type is used for calculation of long-crested sea, as shown by the non-dimensional equation (12) and Fig. 2.

$$S'(\omega') = \frac{2\pi S(\omega)}{T_{01} H_{1/3}^2} = 0.11 \omega'^{-5} \exp\left\{-0.44 \omega'^{-4}\right\} \qquad (12)$$

where $\omega' = \omega / \omega_0$, $\omega_0 = 2\pi / T_{01}$, T_{01} mean wave period, $H_{1/3}$ the significant wave height.

The short-crested wave spectrum is shown by equation (13),

$$S(\omega, \theta_j) = S(\omega) \cdot D(\omega, \theta_j) \qquad (13)$$

with the energy distribution function $D(\omega, \theta)$, as equation (14).

$$D(\theta) = \frac{1}{\sqrt{\pi}} \frac{\Gamma(1+n/2)}{\Gamma(1/2+n/2)} \cos^n \theta \qquad (14)$$

The encounter wave spectrum in short-crested waves is represented by summing the component wave spectrum in various directions, as equation (15),

$$S(\omega_e, \chi) = \sum_{j=1}^{J} S(\omega_{ej}, \chi) = \sum_{j=1}^{J} \frac{S(\omega, \theta_j) \Delta \theta_j}{\left| 1 - 2\omega V \cos(\chi - \theta_j)/g \right|} \tag{15}$$

where

$$\omega_{ej} = \omega - \omega^2 V \cos(\chi - \theta_j)/g \tag{16}$$

The band-width parameters of encounter wave spectra have been calculated for navigation conditions as shown in Fig. 3, where V/T (kt/sec) is taken as the unique factor to govern the encounter wave grouping. Figures 4, 5 and 6 show the encounter spectra of following sea for various exponents of directional distribution function, $n = \infty$, 10 and 4, respectively. Figures 7(a),(b) and (c) show the band-width parameter versus V/T.

Then, the characteristic values of encounter wave groupiness such as $\bar{l}$, $\bar{G}$, and $\bar{H}$ are derived by using equations (1), (2) and (3) for the significant wave height, i.e. $\rho/m_0^{1/2} = 2$ or $\rho = H_{1/3}/2$, as shown in Figures 8 and 9. From these figures it is clearly recognized that the encounter wave groupiness increases remarkably in the range of $V/T = 1.0 \sim 2.0$ and it becomes highest at $V/T = 1.45$.

Statistical Analysis of Encounter Waves Obtained by Simulation

The time series of encounter wave in short-crested sea can be obtained by time-domain simulation as double summation of elemental waves as equation (17),

$$\eta(\mathbf{x}, t) = \sum_{i=1}^{I} \sum_{j=1}^{J} a_{ij} \cos(\omega_i t - \mathbf{k}_{ij} \cdot \mathbf{x} + \varepsilon_{ij}) \tag{17}$$

where

$$a_{ij} = \sqrt{2S(\omega_i, \theta_j) \Delta \omega_i \Delta \theta_j}$$

$$\mathbf{k}_{ij} \cdot \mathbf{x} = k_i \left(x(t) \cos \theta_j + y(t) \sin \theta_j \right) \tag{18}$$

$$(x(t), y(t)) = (x_0 + V \cos \chi \cdot t, y_0 + V \sin \chi \cdot t)$$

The time series of encounter waves in long-crested sea are shown in Fig. 10 for various V/T values. The envelopes of wave amplitudes are drawn on the figure.

STASISTICAL PROPERTIES OF ENCOUNTER WAVE GROUP
AND EFFECTS OF PARAMETERS

The envelopes of time series of encounter waves have been analysed by statistical manner and the probability that number of run exceeds H has been obtained as shown in Figures 11, 12 as well as Table 1.

Table 1 Probability of runs greater than H obtained by simulation

Cond.	A		B		C		D		E		F		G	
H	N'=1557	P(H)	N'=1089	P(H)	N'=630	P(H)	N'=421	P(H)	N'=387	P(H)	N'=409	P(H)	N'=473	P(H)
1	N=1267	0.81374	N=945	0.86777	N=580	0.92064	N=378	0.89786	N=340	0.87855	N=344	0.84108	N=386	0.81607
2	385	0.24727	365	0.33517	331	0.52540	233	0.55344	174	0.44961	161	0.39364	139	0.29387
3	68	0.04367	57	0.05234	142	0.22540	154	0.36580	101	0.26098	77	0.18826	55	0.11628
4	17	0.01092	10	0.00918	48	0.07619	81	0.19240	63	0.16279	36	0.08802	16	0.03383
5	2	0.00129	1	0.00092	15	0.02381	42	0.09976	47	0.12145	22	0.05379	6	0.01269
6	1	0.00064	0	0.00000	8	0.01270	21	0.04988	32	0.08269	14	0.03423	3	0.00634
7	1	0.00064	0	0.00000	3	0.00476	7	0.01663	23	0.05943	11	0.02690	1	0.00211
8	0	0.00000	0	0.00000	2	0.00318	5	0.01188	14	0.03618	9	0.02201	0	0.00000
9	0	0.00000	0	0.00000	0	0.00000	2	0.00475	8	0.02067	9	0.02201	0	0.00000
10	0	0.00000	0	0.00000	0	0.00000	1	0.00238	6	0.01550	5	0.01223	0	0.00000
M_0 [m²SEC]	0.0010929		0.0014062		0.0013826		0.00143098		0.0013334		0.0011938		0.00113237	
$H_{1/3}/2$ [m]	0.064083		0.073212		0.073196		0.0746493		0.072582		0.068045		0.065601	
ν	0.18299		0.16334		0.11256		0.0859457		0.10074		0.11791		0.15733	

The influence of directional distribution of wave spectrum is also shown by chain or broken lines in the figures.

From these results the qualitative features of encounter wave grouping are concluded as follows.

(1) Theoretical calculation and numerical simulation give almost the same tendency that the encounter wave groupiness increases remarkably in the speed range of V / T between 1.0 and 2.0, see Fig. 11.

(2) The probability of exceedance, $P(H)$, that the number of waves in a run is greater than H can be represented by a straight line on Fig. 12. Therefore, by using Fig. 11 and 12, we can estimate $P(H)$ for any conditions of V / T and H.

(3) The increase rate of encounter wave groupiness in the range of $V / T = 1.0 \sim 2.0$ will become greater, as the value of H increases.

(4) The increment of encounter wave groupiness in the above-mentioned range of V / T is less, as the directional distribution of wave energy becomes wider.

CONCLUSIONS

By statistical analyses of encounter waves both in frequency and time domain, the remarkable increase of groupiness in following/quartering seas has been shown qualitatively as the function of V/T and number of waves in a high run. The degree of danger to encounter high run can be classified in the dangerous zone indicated in the operational guidance, and this result will be useful to evaluate ship stability against capsizing by probabilistic approach.

ACKNOWLEDGEMENT

REFERENCES

[1] Takaishi, Y.; Dangerous encounter wave conditions for ships navigating in following and quartering seas, Proc. of 5th STAB, Florida, (1994)

[2] MSC Circular/IMO; Guidance to the master for avoiding dangerous situations in following and quartering seas, (1995)

[3] Longuet-Higgins, M.S.; Statistical properties of wave groups in a random sea state, Phil.Trans.R.Soc. London, A 312, (1984), pp.219-250

[4] Takaishi, Y., Watanabe, K. and Masuda, K.; Statistical properties of encounter wave grouping phenomena in following and quartering seas, J.Society of Naval Architects of Japan, Vol.181, (1996), to be published.

N' : Number of up-cross of a given level per unit time by the wave envelope
N_{max} : Number of maxima of wave elevation
$\bar{I}$: Mean length of wave groups $(=1/N')$
$\bar{G}$: Mean number of waves in a group $(=\bar{I}\cdot N_{max})$
$\bar{H}$: Mean number of waves in a high run

$$\beta = \frac{\sigma_c^2}{\sigma^2} = \frac{\int_{\omega_l}^{\omega_u} S(\omega)d\omega}{\int_0^\infty S(\omega)d\omega}$$

$$= \frac{\int_{\omega_{ec}-\delta\omega_e}^{\omega_{ec}} S(\omega_e)d\omega_e}{\int_0^\infty S(\omega)d\omega}$$
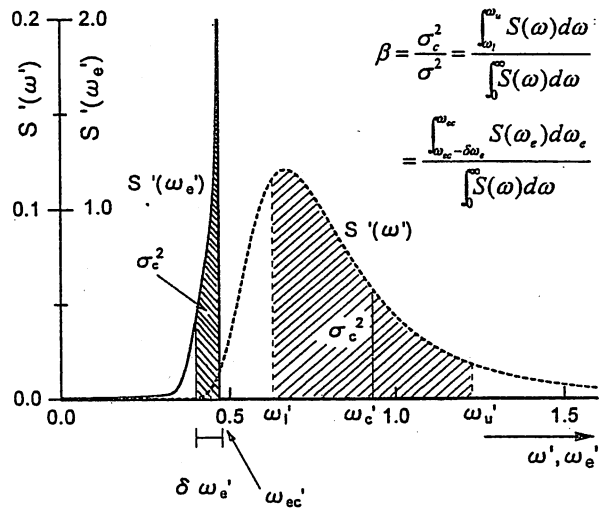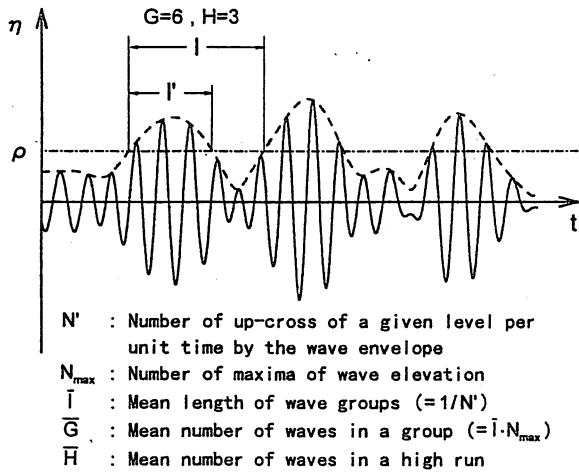
Fig.1 Definition of wave group and high run

Fig.2 Wave spectrum (P-M type), encounter wave supectrum and definition of wave energy concentration ratio, β
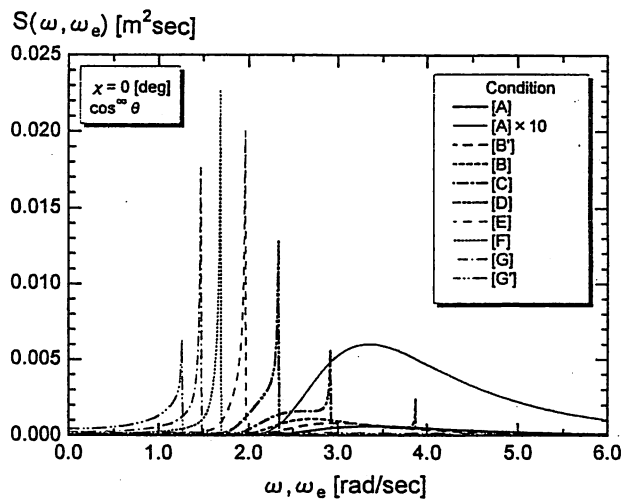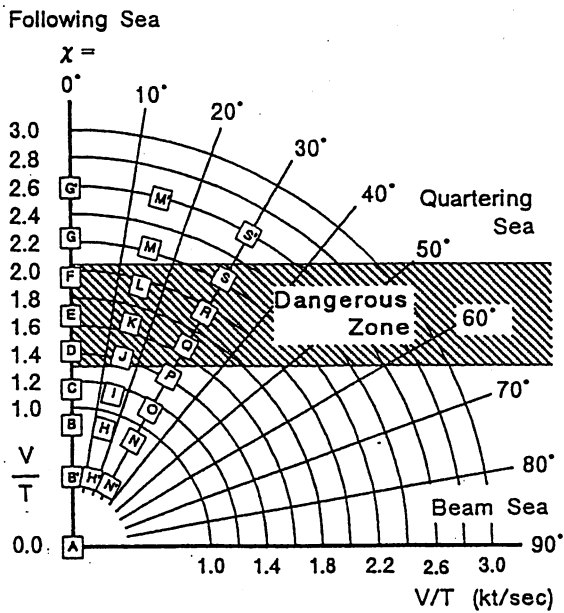
Fig.3 Encounter conditions on V/T-Diagram

Fig.4 Transformation of wave spectra of long-crested waves $S(\omega)$ into spectra of ncounter wave $S(\omega_e)$ in following seas, $\cos^\infty \theta$, $\chi = 0$ [deg]
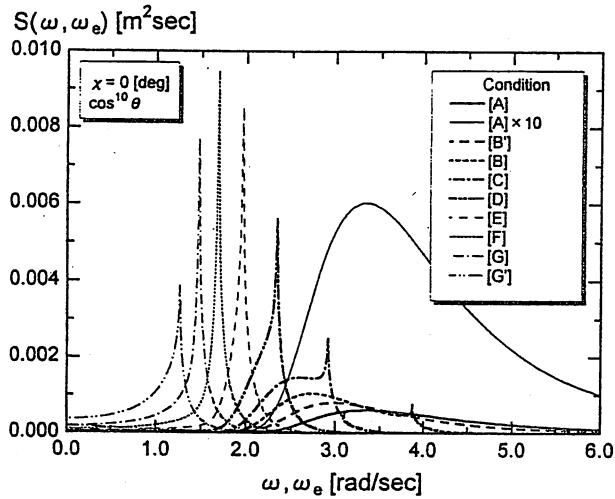
Fig.5 Transformation of wave spectra of short-crested waves $S(\omega,\theta)$ into spectra of encounter wave $S(\omega_e)$ in following seas, $\cos^{10}\theta$, $\chi = 0$ [deg]
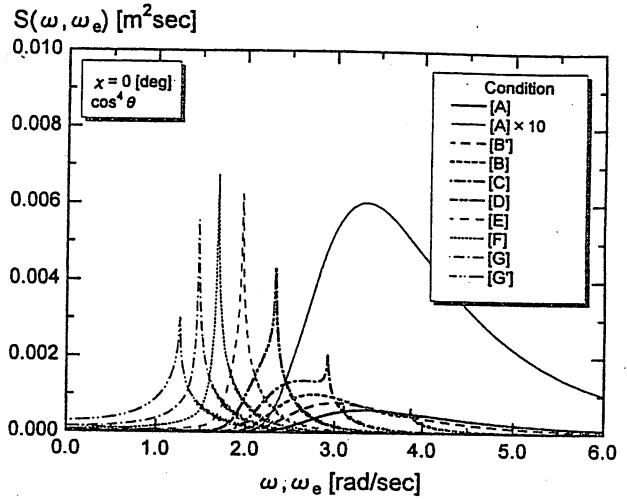
Fig.6 Transformation of wave spectra of short-crested waves $S(\omega,\theta)$ into spectra of encounter wave $S(\omega_e)$ in following seas, $\cos^4\theta$, $\chi = 0$ [deg]
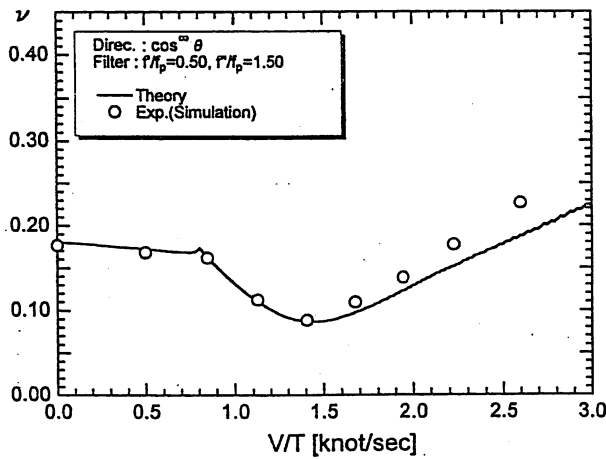
(a) Long-crested wave, $n = \infty$
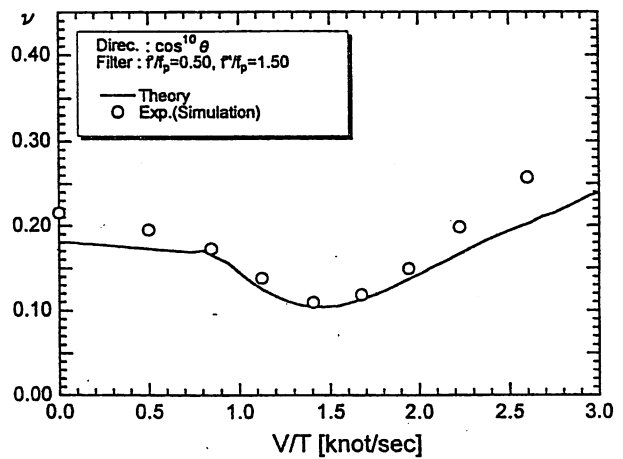
(b) Short-crested wave, $n = 10$

Fig.7 Band width parameter ν vs. V/T in following sea
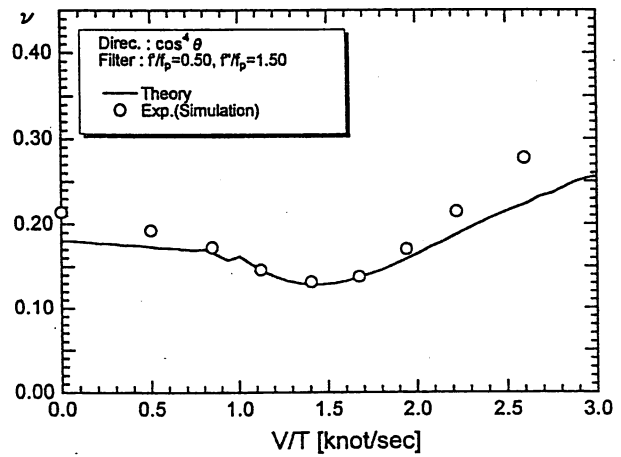
(c) Short-crested wave, $n = 4$
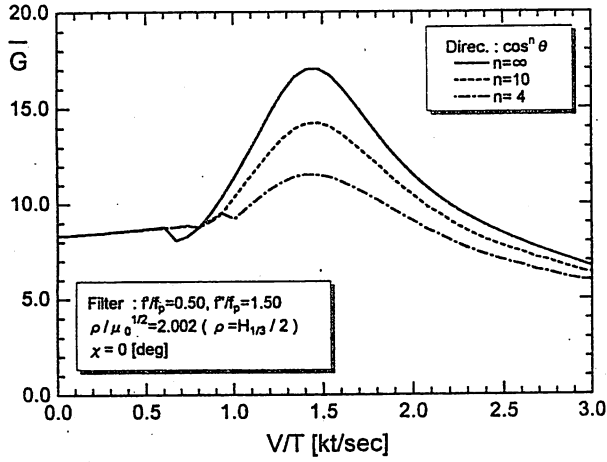
Fig.8   Mean number of waves in a group vs. V / T for the significant wave height
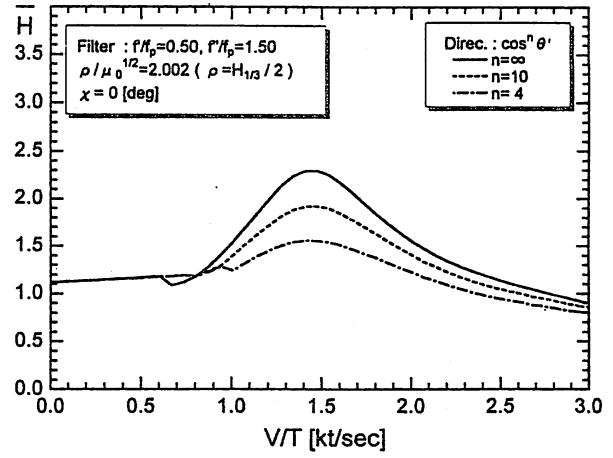
Fig.9   Mean number of waves in a high run exceeding the significant wave height vs. V / T
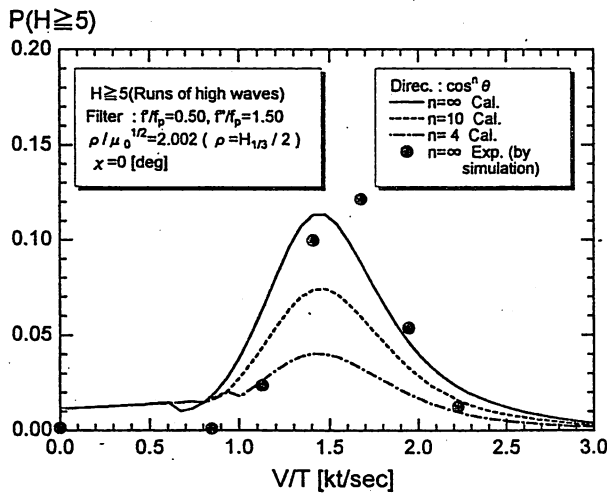
Fig.11   Probability of Runs greater than 5

Fig.12   Probability of runs greater than H

Condition : [A] ($\chi=0°$,V/T=0.000)

[Filter : $f'/f_p=0.5, f''/f_p=1.5$, Direc. : $\cos^{\infty}\theta$]

Condition : [B'] ($\chi=0°$,V/T=0.500)

Condition : [B] ($\chi=0°$,V/T=0.849)

Condition : [C] ($\chi=0°$,V/T=1.126)

Condition : [D] ($\chi=0°$,V/T=1.408)

Condition : [E] ($\chi=0°$,V/T=1.676)

Condition : [F] ($\chi=0°$,V/T=1.944)

Condition : [G] ($\chi=0°$,V/T=2.225)

Condition : [G'] ($\chi=0°$,V/T=2.600)

Amplitude of Envelope (m)

Time (sec)
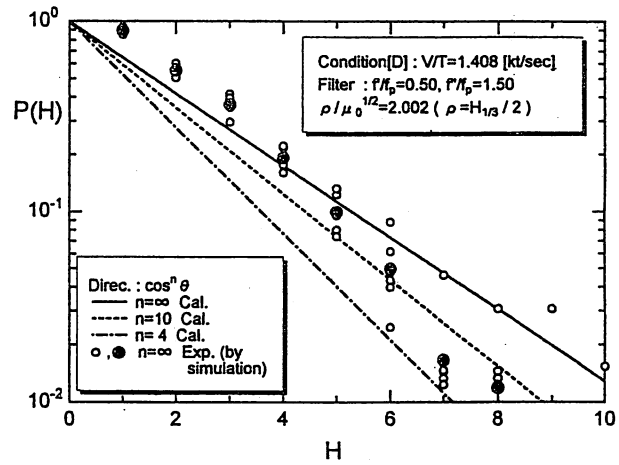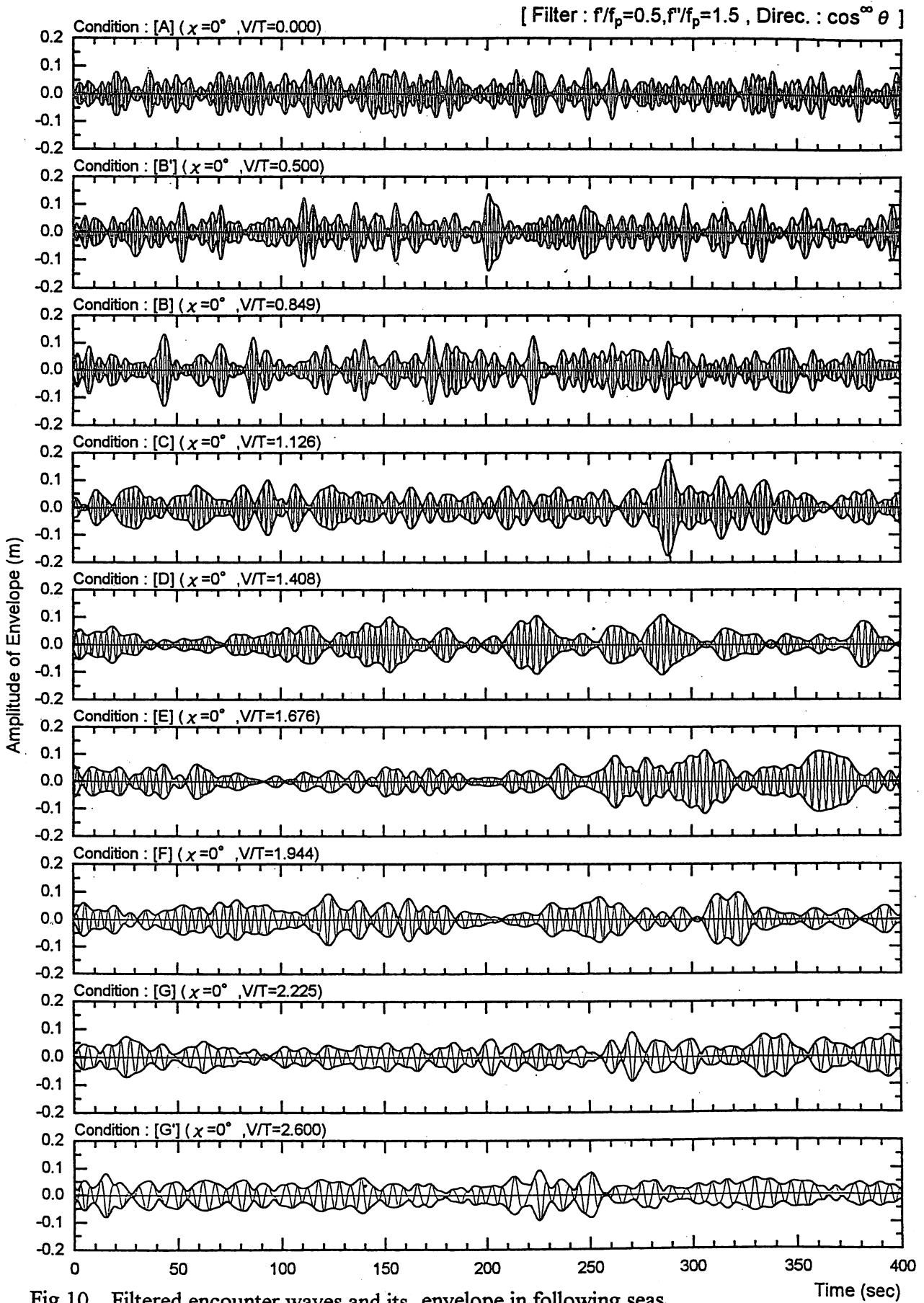
Fig. 10   Filtered encounter waves and its envelope in following seas

STUDY ON THE TRANSVERSE INSTABILITY
OF A HIGH-SPEED CRAFT

Katsuro Kijima, Kyushu University, Japan
Hiroshi Ibaragi, Kyushu University, Japan
Yushu Washio, MHI, Shimonoseki Shipyard, Japan

Summary

Generally, a mono hull type high-speed craft has some advantages such as simple structure and availability for using existing port facilities, then mono hull type is used mainly in high-speed crafts. However, it has been known that a mono hull type craft occasionally lose the transverse stability with increasing her ahead speed, even though she possesses adequate stability at rest condition. Despite the relative severity of the phenomenon, the fundamental characteristics is not known sufficiently. Though, there are some studies concern with instability phenomenon based on experimental method, the mechanism of transverse instability phenomenon is still not clear.
In this paper, in order to make the phenomenon clear, we carried out the numerical calculations on the transverse instability for dynamic pressures, rolling and yawing moment acting on a high speed craft, by applying Maruo's slender ship theory. This paper deals with a phenomenon on the assumption that the craft has constant speed, heave, trim and heel angle, and attempts to know the mechanism of the transverse instability.

1. INTRODUCTION

Generally, a mono hull type high-speed craft has some advantages such as simple structure and availability for using existing port facilities, then mono hull type is used mainly in high-speed crafts. However, it has been known that a mono hull type craft occasionally lose the transverse stability with increasing her ahead speed, even though she possesses adequate stability at rest condition [1],[2]. Eventually, it will be dangerous at high-speed, because progressive heeling and sudden combined roll-yaw motion which is promoted with centrifugal force may cause capsizing.

There are something to be considered for the rules of transverse stability of high-speed crafts, so that the international rules are highly needed. The high-speed crafts are demanded to design faster and larger in recent years, therefore, avoiding transverse instability phenomenon takes on greater importance by considering their stability characteristics at design stage. As for transverse instability of high-speed craft, some experimental studies have been performed, and they clarified that the transverse instability arise easily as craft run faster. However, the mechanism of arising this phenomenon has many unknown factors, and there are a lot of things to be considered for studying the relation with the hull forms. Hence, we notice the dynamic pressure acting on hull surface and attempt to explain the transverse instability of a semi-planing high-speed craft by

numerical calculations.

However it will be impossible to apply the theory that is applied to planing craft or thin ship theory to semi-planing craft, that is now on object in this study. Then to approach this problem, we apply Maruo's slender ship theory [3],[4] , which assumes that the ship is very slender and the breadth and draft are relatively small to length, and which is based on the asymptotic expansion of the Kelvin-source. The advantage of this theory is that when solving unknown quantity, this method doesn't have to consider the effect behind the calculating section.

The transverse instability phenomenon arise heeling and turning motion, while craft's attitude, such as pitch and heave, vary every moment according to her speed increasing. However it is quite impossible to consider all of them by numerical calculation , then we replaced the problem in the state of constant speed, heave, trim angle and heeling angle. In this paper, we examine the hydrodynamic forces according to the increasing of craft's speed and heeling angle, and attempt to clarify the mechanism of the transverse instability.

2. THEORY AND NUMERICAL CALCULATION METHOD

Fig.1 Coordinate system

We consider a uniform flow of inviscid and incompressive fluid with velocity U in the positive direction of x axis with the origin on the undisturbed free surface and take the y axis in the horizontal plane and the z axis vertically downwards, as shown in Fig.1. Assuming a Kelvin-source at point $x = x'$, $y = y'$, $z = z' > 0$, it is expressed by the formula
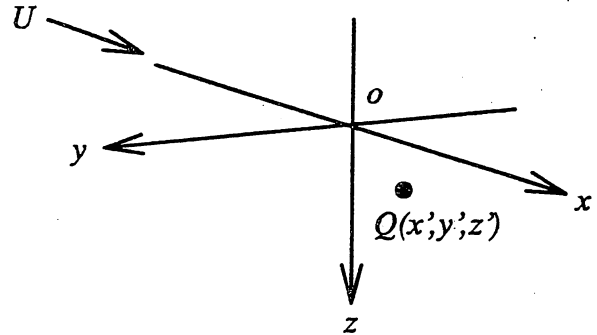
$$G = -\frac{1}{r} + \frac{1}{r'} + \frac{K_0}{\pi} \int \int_{-\infty}^{\infty} \frac{\exp(-\sqrt{\alpha^2 + \beta^2}\,\bar{z} + i\alpha\bar{x} + i\beta\bar{y})}{\alpha^2 - K_0\sqrt{\alpha^2 + \beta^2}} d\alpha d\beta \tag{1}$$

where

$$r = \sqrt{(x - x')^2 + (y - y')^2 + (z - z')^2} \,, \quad r' = \sqrt{(x - x')^2 + (y - y')^2 + (z + z')^2}$$

$$K_0 = g/U^2 \,, \quad \bar{x} = x - x' \,, \quad \bar{y} = y - y' \,, \quad \bar{z} = z + z'$$

The first term in equation (1) is the Rankine source and the second term is its image with respect to the free surface. Then we consider a slender ship fixed in the uniform stream of velocity U. The coordinate system is taken as shown in Fig.2.
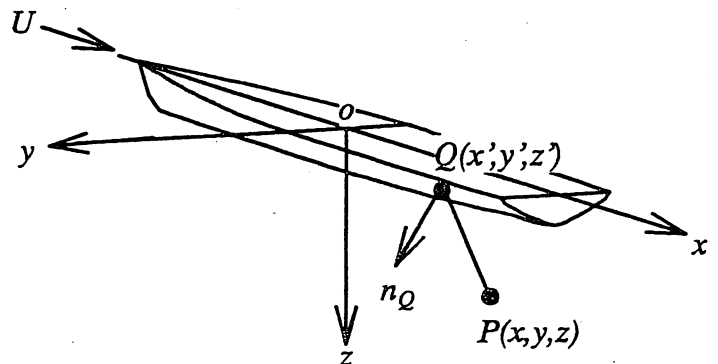

Fig.2 Coordinate system

In order to express the velocity potential of the fluid motion around the hull, we assume a Green function $G(x,y,z;x',y',z')$ and apply Green's theorem in the x',y',z' space bounded by the hull surface below the still water line. Accordingly, the velocity potential due to a source density distribution σ on the hull is as follows.

$$\phi = \int\int_s \sigma(x',y',z')G(x,y,z;x',y',z')dS(x',y',z') \tag{2}$$

Now we consider a portion of the velocity potential defined by $(-1/r+1/r')$. On account of the assumption of slender body, the expression for the velocity potential near the hull surface can be simplified. Omitting higher order terms, one can write the near field expression for ϕ_1 as

$$\phi_1 \approx \int_{C(x)} \sigma(x,y',z') \ln \frac{(y-y')^2+(z-z')^2}{(y-y')^2+(z+z')^2} ds \tag{3}$$

where $C(x)$ is the contour of the hull surface on each transverse section at $x = x'$. The potential ϕ_2 is obtained by subtracting the equation (3) from equation (2).

$$\phi_2 = \int dx' \int_{C(x')} \sigma(x',y',z')G'(x,y,z;x',y',z')ds \tag{4}$$

There are the asymptotic expression for the function G', which is given by

$$G'(x,y,z;x',y',z') \approx \pi K_0 H_1(K_0|x-x'|)$$

$$+ \left\{ \pi K_0 Y_1(K_0|x-x'|) + \frac{2}{|x-x'|} \right\} \{1+2sgn(x-x')\} - 2K_0$$

$$-4\sqrt{K_0}E(x-x',y-y',z+z')\{1+2sgn(x-x')\} \tag{5}$$

$$E(\bar{x},\bar{y},\bar{z}) = \int_0^\infty \exp(-u^2\bar{z})\cos(u^2\bar{y})\sin(u\sqrt{K_0}\bar{x})du \tag{6}$$

where H_1 is the Struve function and Y_1 is the Bessel function of the second kind. Then the velocity potential by the slender body expression is written as the sum of the equation (3) and the equation (4) in the form like

$$\phi = \phi_1 + \phi_2 \tag{7}$$

The boundary condition on the hull surface is

$$\frac{\partial\phi}{\partial n} = -Un_x \tag{8}$$

where n is the outward normal on the hull surface and ν is the outward normal to the contour of the hull surface in the transverse plane. Replacing n with ν, and considering equation (7) and equation (8), the boundary condition is written as follows.

$$\frac{\partial\phi}{\partial n} \approx \frac{\partial\phi}{\partial\nu} = \frac{\partial\phi_1}{\partial\nu} + \frac{\partial\phi_2}{\partial\nu} \tag{9}$$

The derivatives of the velocity potential shown in the equation (3) and the equation (4) are

$$\frac{\partial\phi_1}{\partial\nu} = 2\pi\sigma + \int_{C(x)} \frac{\partial}{\partial\nu} \left\{ \ln \frac{(y-y')^2+(z-z')^2}{(y-y')^2+(z+z')^2} \right\} \sigma(x,y',z')ds \tag{10}$$

$$\frac{\partial \phi_2}{\partial \nu} = -8\sqrt{K_0} \int dx' \int_{C(x')} E_\nu(\bar{x}, \bar{y}, \bar{z}) \sigma(x', y', z') ds \qquad (11)$$

A unit source distribution σ_1 is determined from the following normal-derivative boundary condition.

$$\frac{\partial \phi}{\partial \nu} = -\nu_x \qquad (12)$$

where

$$\sigma = U\sigma_1 \qquad (13)$$

The boundary condition on the hull surface given by the equation (12) is written as follows.

$$\frac{\partial \phi_1}{\partial \nu} = -\nu_x - \frac{\partial \phi_2}{\partial \nu} \qquad (14)$$

The solution is obtained by a marching procedure of step by step integration starting from the bow end. Once the velocity potential is obtained, velocities on the hull surface are determined immediately by differentiating the velocity potential. Then the pressure distribution is obtained by Bernoulli's theorem.

$$P = p - p_0 = \rho \left[-U\frac{\partial \phi}{\partial x} - \frac{1}{2} \left\{ \left(\frac{\partial \phi}{\partial y}\right)^2 + \left(\frac{\partial \phi}{\partial z}\right)^2 \right\} + gz \right] \qquad (15)$$

The hydrodynamic forces and moments of the ship are determined from the integration of the pressure over the hull surface.

$$R_x \simeq -\int\int_S P\nu_x dS \ , \ R_y \simeq -\int\int_S P\nu_y dS \ , \ R_z \simeq -\int\int_S P\nu_z dS \qquad (16)$$

$$M_x \simeq \int\int_S P(\nu_y z - \nu_z y) dS \ , \ M_z \simeq \int\int_S P(\nu_x y - \nu_y x) dS \qquad (17)$$

3. EXAMPLES OF COMPUTER SIMULATION

From the foregoing formulas, the hydrodynamic forces are calculated under the condition that craft's speed, heave, trim angle and heeling angle keeps some constant value. In case of the experimental data are obtained for heave and trim angle according to speed increasing, we use them as its attitude. As to the calculation of hydrodynamic forces, in the first place, we determine the pressure distribution under the still water. Then, we replace the pressure value with zero which position appears above the ship wave surface. However, we neglect the effect of wetted surface that is above still water surface, spray and the equilibrium between dynamic forces and static forces.

The principal of high-speed craft and the body plan are shown in Table 1 and Fig.3. The coordinate system and the positive direction of each force and moment is shown in Fig.4. We carried out the numerical calculations under the similar condition for the tank test performed by one of the authors [1]. And the effect of dynamic pressure acting on craft's hull is considered by comparing the calculated hydrodynamic forces with the measured hydrodynamic forces, provided that the $\overline{\text{GM}}$ value is taken when the transverse instability was remarkable by the model

test. As an example, the measured heeling angle is shown in Fig.5. In this test, only sway and yaw motion of the model was fixed, and $\Delta \Phi$ is the ultimately settled heeling angle according to each speed. Fig.5 confirms that the transverse instability tends to arise in proportion to speed.

In order to make the transverse instability occur easily in non-disturbance condition and to grasp the tendency, the $\overline{GM}$ value is quite smaller than that of normal operation. Numerical calculations are carried out by using 120 × 40 panels for the hull surface.

Table 1   Principal particulars of model
           ship and $\overline{GM}$

Hull-type	Hard-chine
Length	3.80 (m)
Breadth	0.63 (m)
Draft	0.14 (m)
Scale	1/12.3
$\overline{GM}$	0.06 (m)
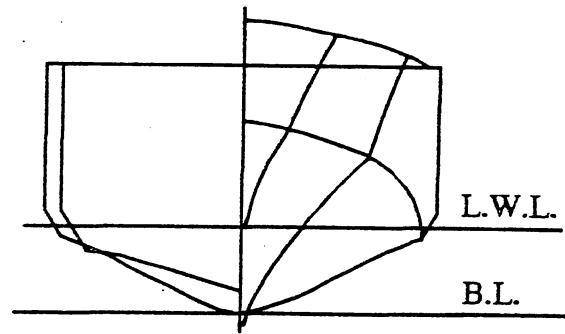
Fig.3 Hard-chine type hull form
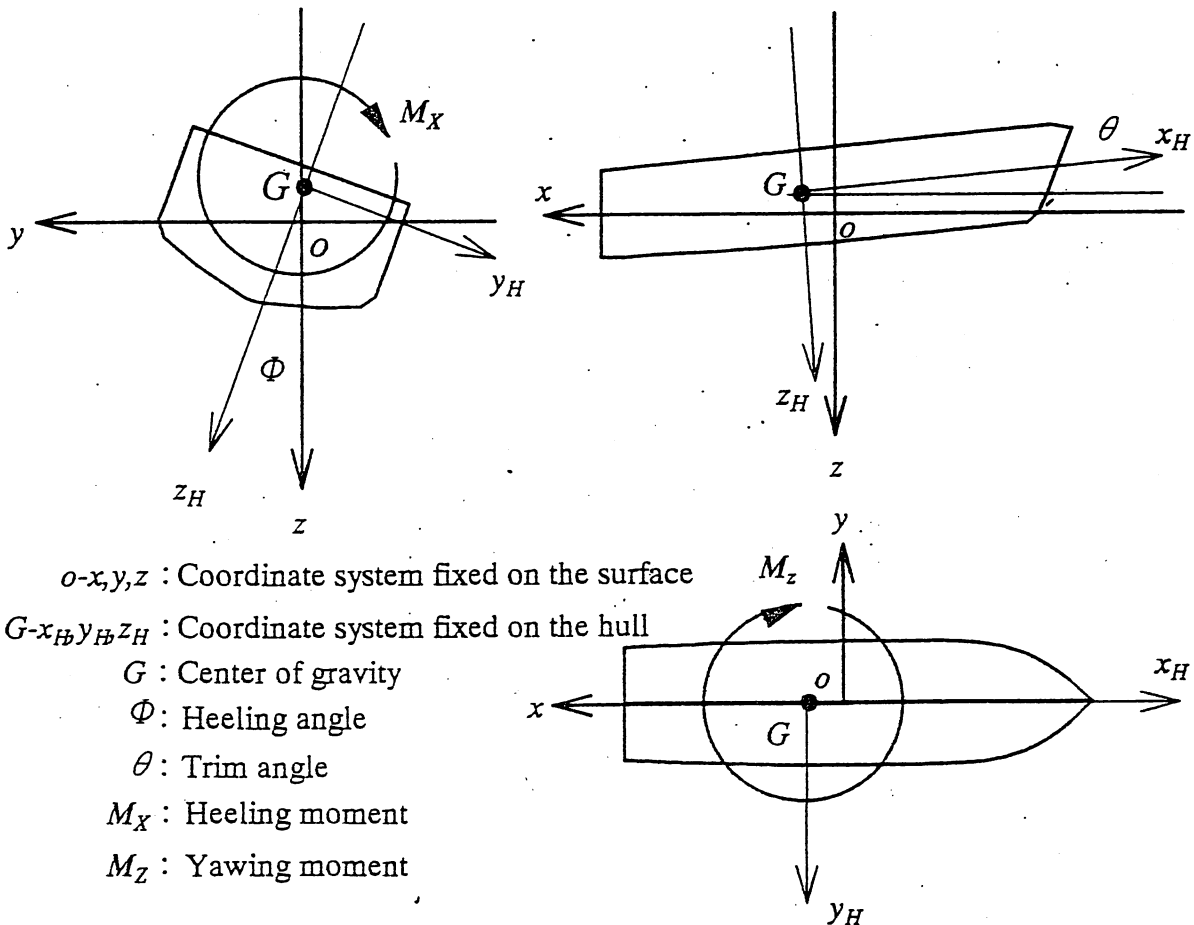
$o\text{-}x,y,z$: Coordinate system fixed on the surface

$G\text{-}x_H,y_H,z_H$: Coordinate system fixed on the hull

  G : Center of gravity

  Φ : Heeling angle

  θ : Trim angle

  M_X : Heeling moment

  M_Z : Yawing moment

Fig.4 Coordinate systems and symbols
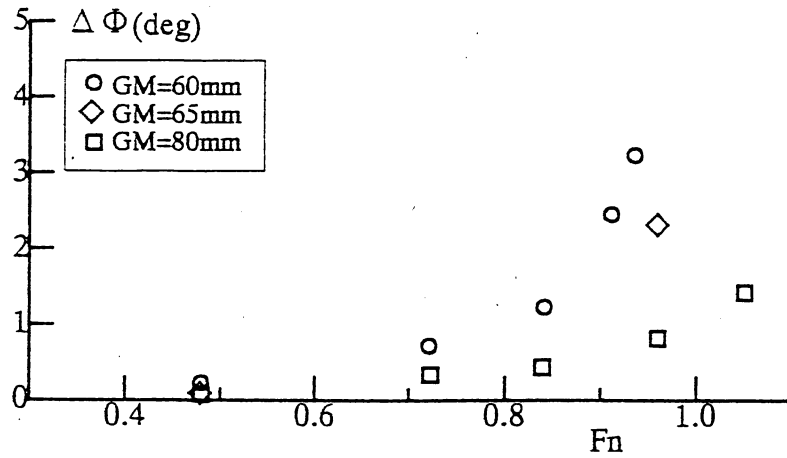
Fig.5 Measured heel angle (sway and yaw fixed)
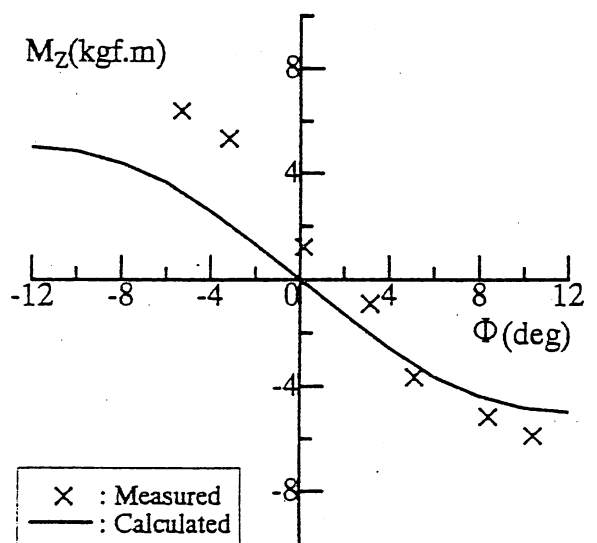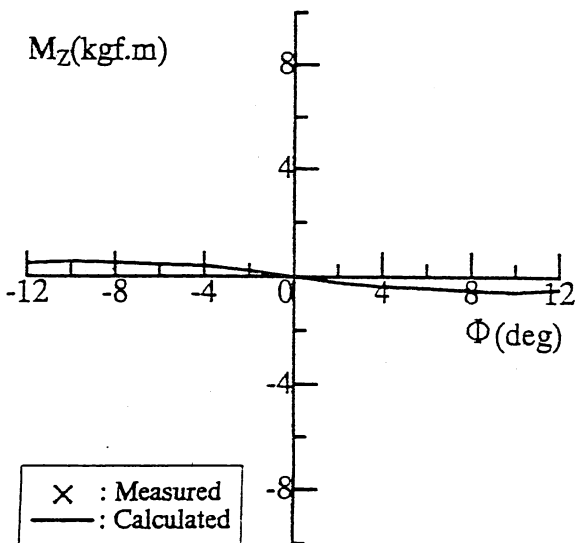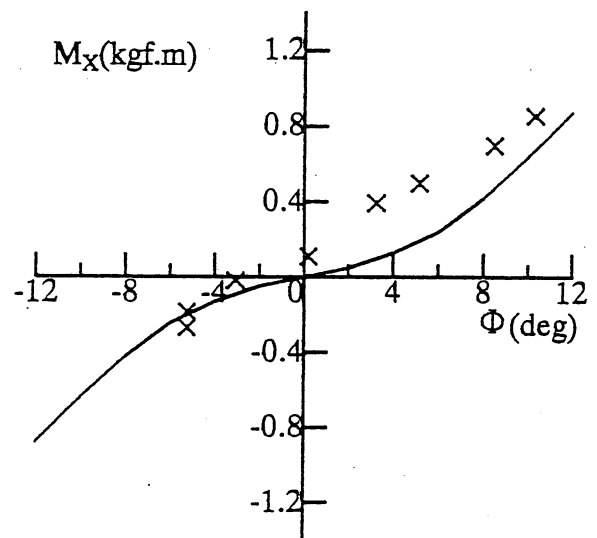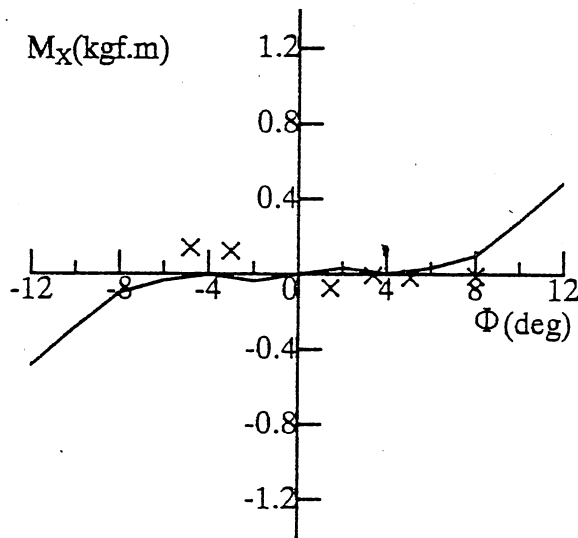
Fig.6 Heeling moment and yawing moment
at Fn=0.72 (z_H/d=-0.03, θ =1.9°)

Fig.7 Heeling moment and yawing moment
at Fn=0.96 (z_H/d=-0.10, θ =2.0°)

3.1. COMPARISON OF MEASURED AND CALCULATED MOMENT

The measured and the calculated heeling moment M_X and yawing moment M_Z are shown in Fig.6 and Fig.7, respectively at Froude number $Fn = 0.72$ and $Fn = 0.96$, under the condition that the motion of the craft is fully fixed.

In Fig.6, the measured heeling moment M_X against heeling angle Φ is nearly zero in the range of 0 degree to 8 degree. This means that the craft has little stability when some disturbance make her heel. The calculated result shows similar tendency compared with the measured result, however, calculated M_X takes larger value at the heeling angle is larger than 8 degree. In Fig.7 the measured M_X against Φ has positive incline. Then this means when some disturbance make the craft heel, Φ takes larger value gradually, and finally, capsizing may occur. The calculated result takes smaller value compared with the measured result as a whole, however, both results show similar tendency.

And in Fig.6, the calculated yawing moment M_Z against the heeling angle Φ takes small value relatively at least 0.5kgf.m. However the measured yawing moment at $Fn = 0.72$ doesn't be obtained. In Fig.7, the measured M_Z against Φ has negative incline. Then this means when the craft heels to starboard side ($\Phi > 0$), the hydrodynamic force acts to turn to the port side. As Φ takes larger value, M_Z becomes large, then the turning radius becomes small. Consequently, the centrifugal force will make the heeling angle become larger. On the other hand, the calculated result takes small incline compared with the measured result, however, it shows similar tendency.

3.2 DYNAMIC PRESSURE DISTRIBUTION

Fig.8 shows the dynamic pressure distribution on the hull at $Fn = 0.4$ and $Fn = 1.0$, and $z_H/d = 0.0$, $\theta = 0.0°$, $\Phi = 3.0°$. In this figure, the normal component of the dynamic pressure projected on the $x - y$ plane at the square station 1, 3, 5, 7 and 9 are indicated. The dynamic pressure near the keel is indicated by a broken line. The pressure coefficient C_p is written as follows.

$$C_p = \frac{P}{1/2\rho U^2} \qquad (18)$$

When Fn is equal to 0.4, the broken line shows that the dynamic pressure contains positive and negative value relatively even as a whole along the longitudinal direction. For the positive and negative pressure distribution cancels mutually, the heeling moment isn't thought to act strongly as a whole. And at low speed, the fluiddynamic force doesn't have a large effect.
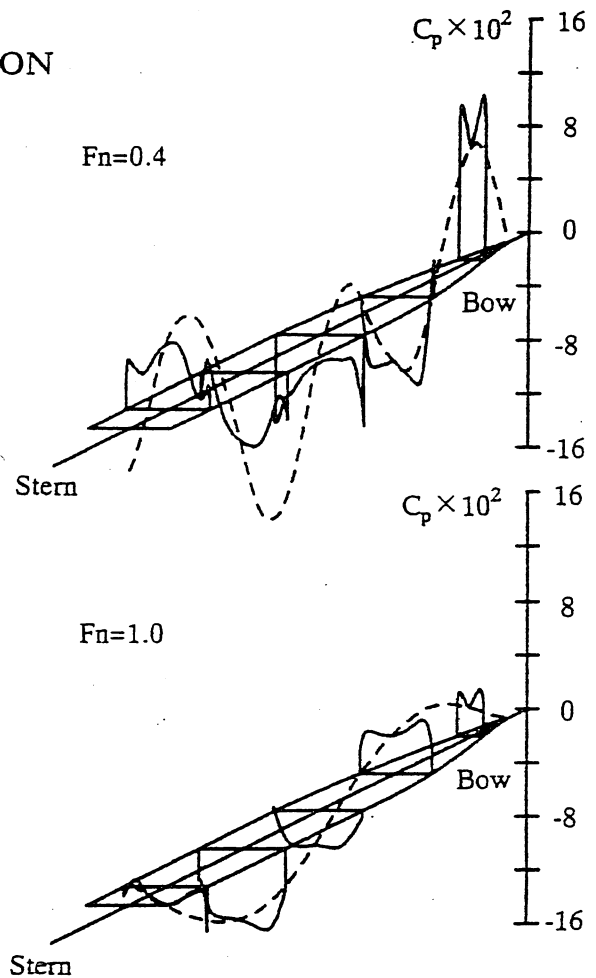

Fig.8 Pressure distribution in x-y plane

When Fn is equal to 1.0, the broken line shows that the positive dynamic pressure distributes on the fore hull and the negative pressure distributes on the aft hull. And it shows that the positive pressure has uneven distribution to starboard side for fore hull, and the negative pressure distribution to port side for aft hull. Moreover at high-speed, the fluid dynamic force has a large effect.

Secondly, in order to see the effect of heeling angle, Fig.9 shows the dynamic pressure distribution on the hull at heeling angle $\Phi = 0°$ and $\Phi = 12°$, and $Fn = 0.96$, $z_H/d = -0.10$, $\theta = 2.0°$. In comparison of these two results, at $\Phi = 12°$ we can see that the positive dynamic pressure acts unevenly to the starboard side on fore hull and the negative dynamic pressure acts unevenly to the port side on aft hull. Then taking into consideration that a high-speed craft has a large deadrise angle for fore hull and a small deadrise angle for aft hull, such uneven pressure distribution is thought to make a craft heel easily as the $\overline{KG}$ is large. Like this, the increase of the heeling angle have the unevenness of the dynamic pressure distribution become large, then we consider this leads to the increase of the heeling moment.

Fig.9 Pressure distribution in x-y plane

From the above, in case of high-speed craft, we consider that the one reason for the transverse instability is the unevenness of dynamic pressure distribution in fore and aft hull at high-speed and the unevenness of dynamic pressure distribution in port side and starboard side to increase the heeling angle that is promoted by the difference of the deadrise angle between fore and aft hull.

3.3 EFFECT OF AFT HULL WARP

The deadrise angle of the model shown in Fig.3 changes gradually smaller from midship to stern. However according to the reference [2], it mentioned that such change of deadrise angle tends to make the transverse stability smaller. Then in order to examine the effect of aft hull shape on the transverse instability, we compare the two models, the model whose midship is extended to stern as shown in Fig.10 and the original model. Fig.11 shows the heeling moment M_X and the yawing moment M_Z at $Fn = 0.96$. In comparison of these two results, we confirmed that the hull that has no warp at aft hull shows a tendency to be stable as the reference [2].
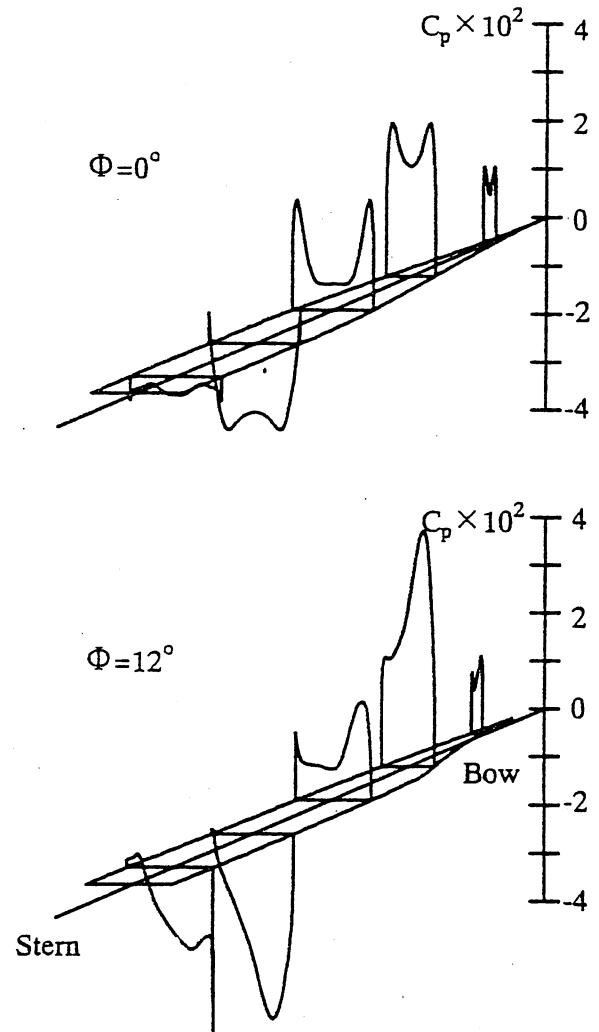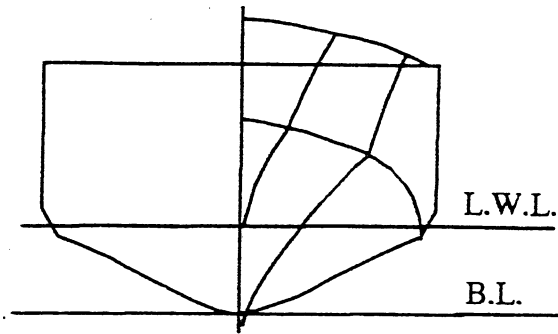
Fig.10 Hull form (no warp at aft hull)

L.W.L.

B.L.
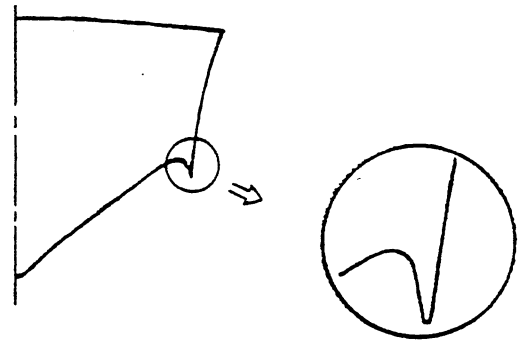
Fig.12 Section of Flap Chine

M_X(kgf.m)

Φ(deg)

M_X(kgf.m)

Φ(deg)

M_Z(kg.m)

Φ(deg)

——— : No warp
　　　at aft hull
——— : Original

M_Z(kgf.m)

Φ(deg)

×　 : Measured
——— : Calculated
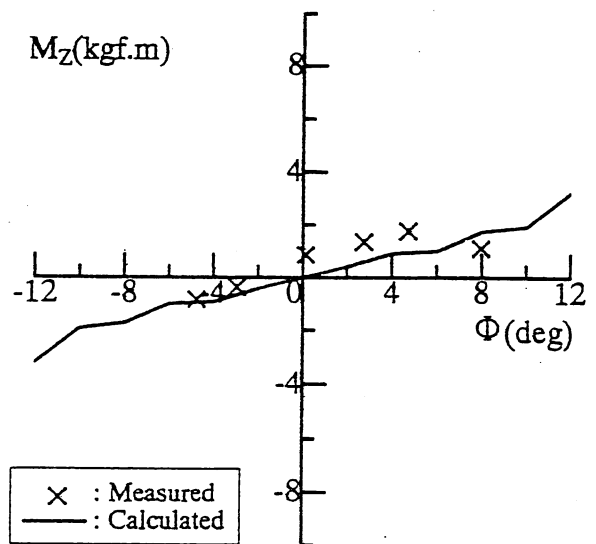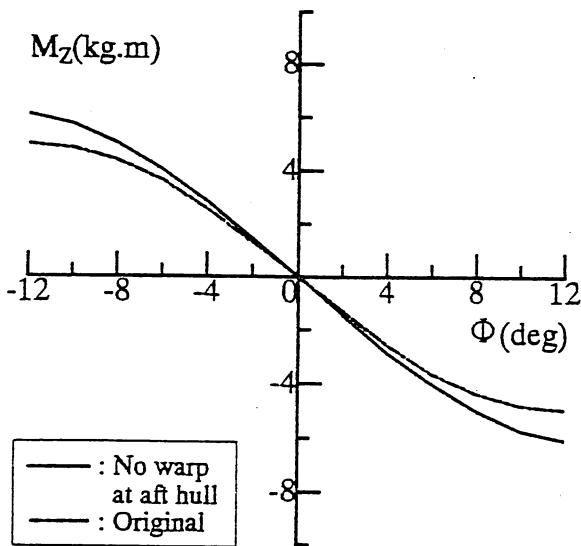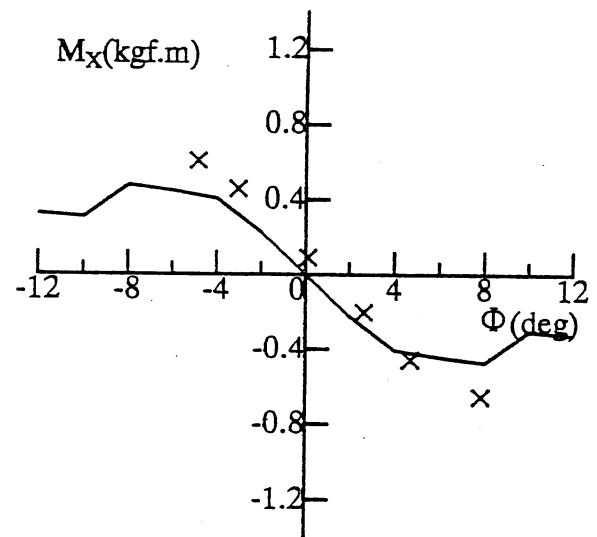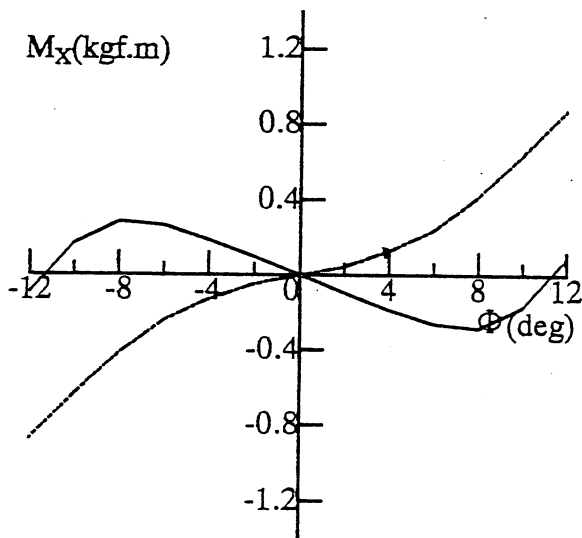
Fig.11 Heeling moment and yawing moment
　　　at Fn=0.96 (z_H/d=-0.10, θ =2.0°),
　　　with no warp at aft hull

Fig.13 Heeling moment and yawing moment
　　　at Fn=0.96 (z_H/d=-0.10, θ =2.0°),
　　　with Flap Chine

3.4   EFFECT OF FLAP CHINE

One of the authors confirmed that the Flap Chine has a good effect on transverse stability by the tank test as shown in Fig.12 [1]. It is equipped along the chine over the still water. Then, in order to take an effect of the Flap Chine on the transverse instability, we assumed that the force acting on the Flap Chine is expressed by the dynamic pressure at $z = 0$ and the incline of the hull surface. The measured and the calculated heeling moments M_X and yawing moments M_Z are shown in Fig.13 at $Fn = 0.96$. The measured M_X against Φ has negative incline, then, this means even if some disturbance make the craft heel, the craft recovers the heeling angle. The calculated result takes insufficient agreement at $\Phi > 8°$ with measured result, however, it shows a similar tendency.

4.   CONCLUSIONS

In this paper, we estimated the hydrodynamic forces by noticing the dynamic pressure acting on the hull surface. This calculation method still leaves the problem to be solved and the calculated results have insufficient agreement with the measured results. However, we confirmed that they show a similar tendency and see it was understood that the dynamic pressure has not a few influence on the transverse instability on the high-speed craft. The following are the results.

1. One reason for the transverse instability at high-speed is the unevenness of dynamic pressure distribution in fore and aft and the unevenness of dynamic pressure distribution in port side and starboard side to increase the heeling angle that is promoted by the difference of the deadrise angle between fore and aft hull.

2. The heeling moment tends to become larger as the deadrise angle becomes smaller from midship to stern.

3. The calculated results of the effect of the Flap Chine on the transverse instability have a similar tendency with the measured results and the Flap Chine will be useful to improve the transverse instability.

REFFERENCES

[1] Washio, Y., Nagamatsu, T. and Kijima, K. :On the Improvement of Transverse Stability for High-Speed Craft, *Transactions of the West-Japan Society of Naval Architects*, No.86, (1993), pp.77-85

[2] Werenskiold, P. :Methods for Regulatory and Design Assessment of Planing Craft Dynamic Stability, *Fast'93*, (1994), pp.883-894

[3] Maruo, H. :New Approach to the Theory of Slender Ships with Forward Velocity, *Bulletin of the Faculty of Engineering, Yokohama National Univ.*, Vol.31, (1982), pp.85-100

[4] Song, W., Ikehata, M. and Suzuki, K. :Computation of Wave Resistance and Ship Wave Pattern by the Slender Body Approximation, *Journal of the Kansai Society of Naval Architects, Japan* , Vol.209, (1988), pp.25-36

Sensitivity of Capsize to a Symmetry Breaking Bias

by
B. Cotton,
S.R. Bishop
and
J.M.T. Thompson
University College London

NONLINEAR ROLL MOTION OF A SHIP WITH WATER-ON-DECK IN REGULAR WAVES

Sunao Murashige*, Kazuyuki Aihara†, and Taiji Yamada‡

* Ship Research Institute, Ministry of Transport, Japan
† Department of Mathematical Engineering, The University of Tokyo, Japan
‡ AIHARA Electrical Engineering Co., Ltd., Japan

SUMMARY

This paper describes nonlinear motion of a Ro-Ro type ship with water-on-deck in regular beam seas. Experiments using a Ro-Ro model demonstrate that different modes of roll motion coexist and that some of them can exhibit large amplitude motion even for incident waves of moderate amplitude. Observations of the experiments suggested that nonlinear coupling of a ship and water-on-deck dominates this phenomenon. We derive model equations of the nonlinearly coupled motion. Numerical simulations of them also show coexistence of some modes similar to the experimental results. It should be emphasized that dynamic effects of water-on-deck on a ship in waves cause this nonlinear motion.

INTRODUCTION

There have been a good deal of works on nonlinear roll motion of a ship in waves because it is deeply related to safety of it, for example capsizing problem [1−4]. Since it is dynamic motion with large amplitude, neither assumption of linear motion with small amplitude nor that of static motion is valid. Thus most of the past studies investigate a basic equation of roll motion in the time domain. Nonlinearities of a restoring and a damping force terms in the equation of motion become dominant with increase of amplitude of motion. Coupled motion with the other modes, heave and pitch, makes the roll response further compliclated. Nonlinear dynamics approach may be one of promising methods to elucidate this challenging problem [5−11].

It is well known that fluid with a free surface, 'free water', inside a ship has some influences on the ship motion [12,13]. The static effect decreases the metacentric height $\overline{GM}$ by $\dfrac{\rho'}{\rho} \cdot \dfrac{i}{V}$ where ρ and ρ' denote the densities of sea water and fluid in a ship, i the moment of inertia of a free surface of fluid in a ship about the center of the free surface, and V the displaced volume of a ship, respectively. The anti-rolling tank utilizes the dynamic effects to stabilize the roll motion in waves [14]. On the other hand, nonlinear features of dynamic effects have not been investigated in so much detail. It may be crucial, for example in the case of a flooded ship in waves.

This paper describes nonlinearly coupled motion of a ship and water-on-deck in regular waves. In particular, we consider coexistence of different modes of roll motion found in experiments and discuss it using model equations.

EXPERIMENTS

Model and experimental method

Experiments were performed using a Ro-Ro model in the wave tank 8m wide, 50m long, and 4.5m deep at Ship Research Institute. The overview and principal particulars of the model are given in fig.1 and table 1. The model was placed at a position 18.75m away from a wave maker of the wave tank so that incident waves came from starboard to port. A closed vessel (the shaded area in fig.1) was fixed in the model and imitates a vehicle deck. We put a prescribed amount of water on the vehicle deck and measured motion of the model in regular beam seas. We also observed behavior of water-on-deck using a video camera attached in the vehicle deck.
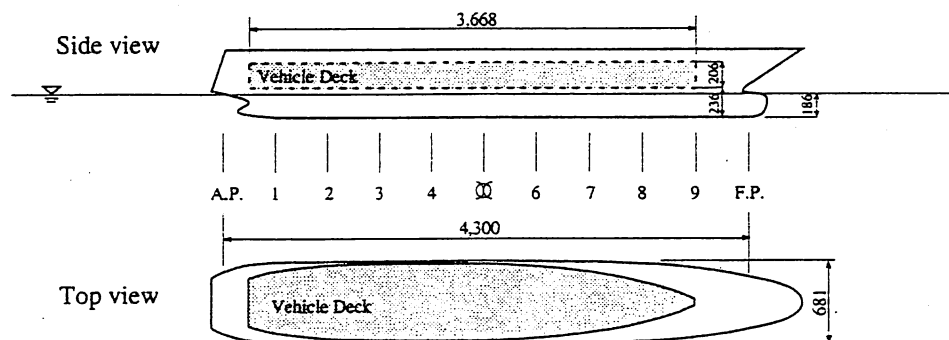

Fig.1 Ro-Ro model
(unit:mm. The shaded area represents the vehicle deck.)

Table 1. Principal particulars of the Ro-Ro model
(scale ratio:1/23.5, without water-on-deck)

Length L_{pp}	4.3 m	Vehicle deck height h	0.206 m
Breadth B	0.681 m	Displacement W	272.69 kg
Depth D	0.236 m	Height of center of gravity $\overline{KG}$	0.25 m
Draft d	0.186 m	Metacentric height $\overline{GM}$	0.069 m
Freeboard f	0.050 m	Natural period of roll motion T_r	1.94 sec.

Experimental results

The experiments were started after the model was placed at the statically balanced positions in still water. There are two static equilibrium points of the model with water-on-deck in the lee and the weather sides. Figs.2.(a) and (b) show examples of the time history of the measured roll angle $\phi(t)$ when the amount of water-on-deck w was 20% of the displacement of the model W and the height H_i and the period T_i of incident waves were 13.0cm and 1.44sec., respectively. In this case, the static equilibrium angle is ±19.0deg.. The roll angle $\phi(t)$ is defined to be positive when the model heels to the lee side.

(a) $\phi(t = 0) = -19.0$deg.(weather side)   (b) $\phi(t = 0) = +19.0$deg.(lee side)
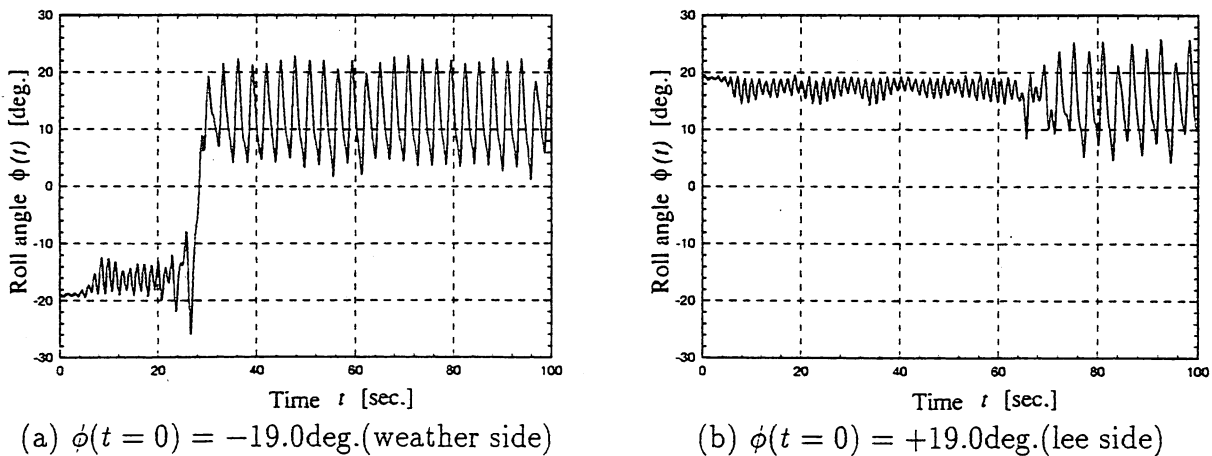
Fig.2 Time history of the measured roll angle $\phi(t)$
(The height of incident waves H_i=13.0cm, the period of incident waves T_i=1.44sec., and the ratio of the amount of water-on-deck w to the displacement of the model W is w/W=0.2. In the case (b), the model was lightly impinged by a stick at $t \simeq 65$sec..)

From these figures, we can see the followings:

• Case (a)

    − At t=0, the model is balanced in the weather side, $\phi(t$=0)=−19.0deg..

- For t <20sec., the model rolls in the weather side with the average amplitude of about 2 deg. and the same period as that of the incident waves.

- At t ≃25sec., the roll motion is changed from the weather side to the lee side.

- For t >30sec., the model rolls in the lee side with the average amplitude of about 9deg. and the average period nearly equal to twice that of the incident waves.

● Case (b)

- At t=0, the model is balanced in the lee side, $\phi(t=0)=+19.0$deg..

- For t <65sec, the model rolls with the average amplitude of about 2 deg. and the same period as that of the incident waves.

- After the model is lightly impinged by a stick at t ≃65sec., the roll motion is changed to the other mode of large amplitude.

These results indicate that some different modes of roll motion coexist for regular incident waves of constant period and amplitude. This is a typical example of nonlinear oscillations.

MODEL EQUATIONS

Modelling the coupled motion of a ship and water-on-deck

Observations of the experiments suggested that the measured nonlinear motion is dominated by the coupling of a ship and water-on-deck. This section derives model equations for the coupled motion. For simplicity, we consider the two-dimensional motion of a box-shaped floating body as shown in fig.3.
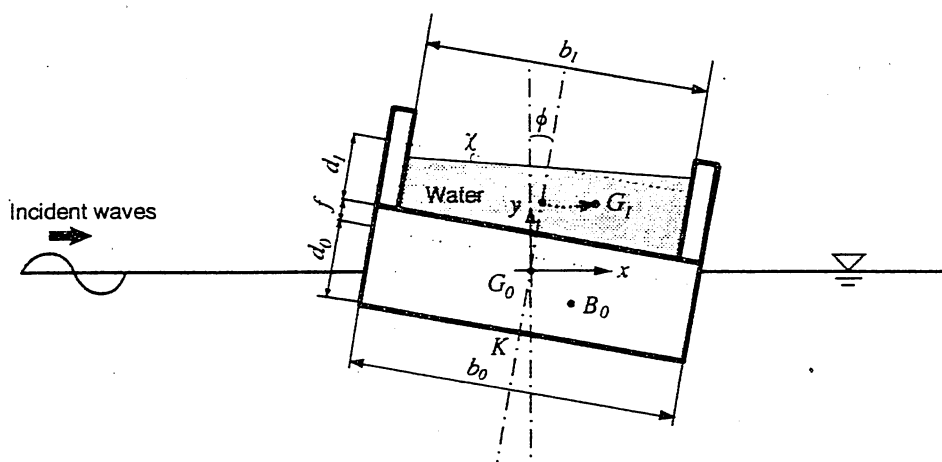

Fig.3 Roll motion of a box-shaped floating body in beam sea

We assume that 1) the coupling of roll motion and water-on-deck is dominant, and sway and heave modes can be neglected, 2) the surface of water-on-deck is flat with the slope χ, 3) the motion of water-on-deck can be approximated by that of a material particle located at the center of gravity G_1, 4) the exciting roll moment varies sinusoidally with the same angular frequency as the incident waves Ω, and 5) the damping forces on a ship and water-on-deck vary linearly with $\dot{\phi}$ and $\dot{\chi}$, respectively. Set the origin at the center of gravity of the floating body G_0 and take the coordinates as shown in fig.3. In order to derive equations of the coupled motion, it may be convenient to use Lagrange's equations of motion with the kinetic energy K, the potential energy P, and the dissipation energy D as follows:

$$\frac{d}{dt}\left(\frac{\partial L}{\partial \dot{\phi}}\right) - \frac{\partial L}{\partial \phi} + \frac{\partial D}{\partial \dot{\phi}} = 0 \ ,$$
$$\frac{d}{dt}\left(\frac{\partial L}{\partial \dot{\chi}}\right) - \frac{\partial L}{\partial \chi} + \frac{\partial D}{\partial \dot{\chi}} = 0 \ ,$$

(1)

where the Lagrangian $L = K - P$. The kinetic energy K and the potential energy P are given by sums of them of each system, namely $K = K_0 + K_1$ and $P = P_0 + P_1 + P_e$ where the subscripts $_0$, $_1$, and $_e$ denote the floating body, the water-on-deck, and the exciting roll moment, respectively. They can be written in the form

$$K_0 = \frac{1}{2}(I + \delta I)\dot{\phi}^2 = \frac{1}{2}M\kappa^2\dot{\phi}^2 \ , \quad K_1 = \frac{1}{2}m\left(\dot{x_{G_1}}^2 + \dot{y_{G_1}}^2\right) \ ,$$

$$P_0 = -\rho V g y_{B_0} = -(M + m)g y_{B_0} \ , \quad P_1 = mg y_{G_1} \ , \quad P_e(\phi,t) = -\phi A_m \sin(\Omega t + \psi) \ , \quad (2)$$

$$D = \frac{1}{2}s_0\dot{\phi}^2 + \frac{1}{2}s_1\dot{\chi}^2 \ ,$$

where I and δI denote the moment and the added moment of inertia about the axis of roll, M and m the masses of the body and of the water-on-deck, κ the radius of gyration, $x_{G_1} = (x_{G_1}, y_{G_1})$ the position of the center of gravity of the water-on-deck G_1, $x_{B_0} = (x_{B_0}, y_{B_0})$ the position of the center of buoyancy of the floating body B_0, A_m the amplitude of the exciting roll moment, ψ the phase difference between the incident waves and the exciting roll moment, and s the damping coefficent, respectively. The positions of G_1 and B_0 can be geometrically obtained as follows:

$$
\begin{cases}
x_{B_0} = \overline{G_0 M_0}\sin\phi + \dfrac{1}{2}\overline{B_0 M_0}\tan^2\phi\sin\phi \\[2mm]
y_{B_0} = -\dfrac{1}{2}\overline{B_0 M_0}\tan\phi\sin\phi - (\overline{B_0 M_0} - \overline{G_0 M_0})\cos\phi
\end{cases}
\quad \text{for } |\phi| < \phi_1
$$

$$
\begin{cases}
x_{B_0} = \mathrm{sgn}(\phi)\dfrac{b_0}{2}\cos\phi - \mathrm{sgn}(\phi)\dfrac{2}{3}\sqrt{b_0 d_0}\dfrac{\cos 2\phi}{\sqrt{\sin 2|\phi|}} - \overline{KG_0}\sin\phi \\[4mm]
y_{B_0} = -\mathrm{sgn}(\phi)\dfrac{b_0}{2}\sin\phi + \dfrac{2}{3}\sqrt{b_0 d_0}\sqrt{\sin 2|\phi|} - \overline{KG_0}\cos\phi
\end{cases}
\quad \text{for } |\phi| > \phi_1
$$

$$\text{(3)}$$

$$
\begin{cases}
x_{G_1} = \overline{B_1 M_1}\tan\chi\cos\phi + \left(\overline{G_0 B_1} + \dfrac{1}{2}\overline{B_1 M_1}\tan^2\chi\right)\sin\phi \\[2mm]
y_{G_1} = -\overline{B_1 M_1}\tan\chi\sin\phi + \left(\overline{G_0 B_1} + \dfrac{1}{2}\overline{B_1 M_1}\tan^2\chi\right)\cos\phi
\end{cases}
\quad \text{for } |\chi| < \chi_1
$$

$$
\begin{cases}
x_{G_1} = \mathrm{sgn}(\chi)\dfrac{b_1}{2}\cos\phi - \mathrm{sgn}(\chi)\dfrac{2}{3}\sqrt{b_1 d_1}\dfrac{\cos(\phi+\chi)}{\sqrt{\sin 2|\chi|}} \\[3mm]
\qquad + (d_0 + f - \overline{KG_0})\sin\phi \\[4mm]
y_{G_1} = -\mathrm{sgn}(\chi)\dfrac{b_1}{2}\sin\phi + \mathrm{sgn}(\chi)\dfrac{2}{3}\sqrt{b_1 d_1}\dfrac{\sin(\phi+\chi)}{\sqrt{\sin 2|\chi|}} \\[3mm]
\qquad + (d_0 + f - \overline{KG_0})\cos\phi
\end{cases}
\quad \text{for } |\chi| > \chi_1
$$

$$\text{(4)}$$

where d_0 denotes the draft, d_1 the depth of water-on-deck, b_0 the width of the floating body, b_1 the width of the vehicle deck, and f the freeboard of the floating body as shown in fig.3, and $\overline{B_0 M_0} = b_0^2/(12 d_0)$, $\overline{B_1 M_1} = b_1^2/(12 d_1)$, $\tan\phi_1 = 2d_0/b_0$, and $\tan\chi_1 = 2d_1/b_1$, respectively. The center of buoyancy of free water B_1 is located at the same position as G_1. Substitution of eqs.(2)~(4) into eq.(1) produces model equations. They can be rewritten in the form of the autonomous system

$$
\frac{dx}{dt} = F(x(t)) , \tag{5}
$$

where $x = [\phi, \chi, \dot\phi, \dot\chi, \vartheta]^T$, $F = [\dot\phi, \dot\chi, F_3(x), F_4(x), \Omega]^T$, $\vartheta = \Omega t + \psi$, and ^{T} denotes the transpose.

Numerical solutions of the model equations

The model equations (5) were numerically solved using the 4th order Runge-Kutta method. Figs.4.(a),(b), and (c) represent some examples of the computed results under the conditions of T_i=1.44sec., b_0=0.681m, d_0=0.186m, κ=0.253m, $\overline{GM}$=0.069m, b_1/b_0=0.72, m/M=0.19, $A_m/(M\kappa^2)$=0.02, $s_0/(M\kappa^2)$=0.03, $s_1/(M\kappa^2)$=0.08, and ψ=0.0, and with the different initial conditions $(\phi(0),\chi(0),\dot{\phi}(0),\dot{\chi}(0))$. The time history and the phase portrait of the roll angle $\phi(t)$ and the slope of the surface of water-on-deck $\chi(t)$ are displayed. These numerical solutions indicate that different modes of motion can coexist in the system of the model equations (5). This nonlinear phenomenon is similar to the experimental result very well.
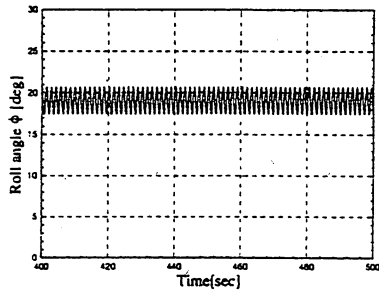

(a.1) Time history of ϕ (b.1) Time history of ϕ (c.1) Time history of ϕ
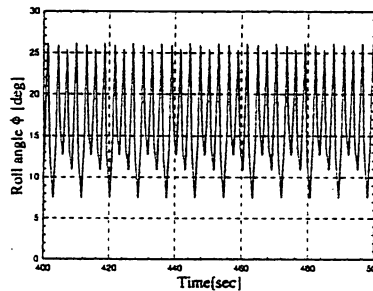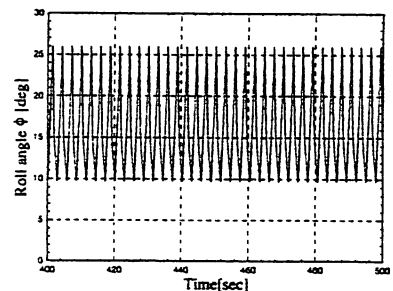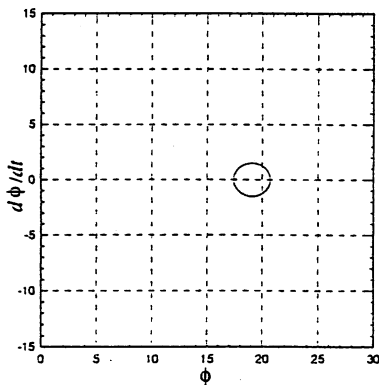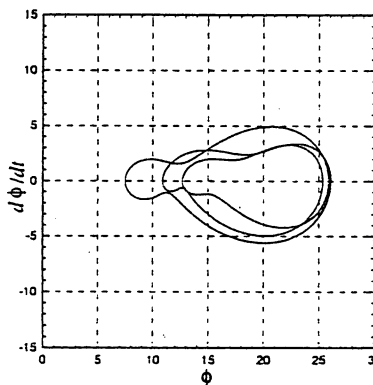
(a.2) Phase portrait $(\phi,\dot{\phi})$ (b.2) Phase portrait $(\phi,\dot{\phi})$ (c.2) Phase portrait $(\phi,\dot{\phi})$
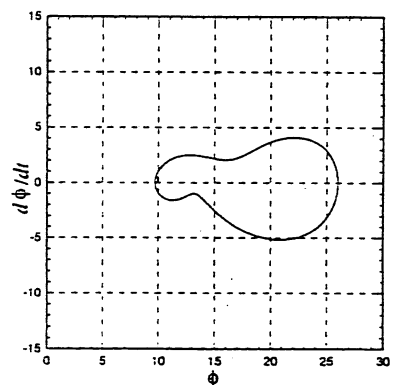
Fig.4 Computed results (ϕ:roll angle. χ:slope of the surface of water-on-deck.)
((a)$\phi(0)$=$\chi(0)$=24.0deg., (b)$\phi(0)$=$\chi(0)$=28.8deg., (c)$\phi(0)$=$\chi(0)$=28.9deg..
$(\dot{\phi}(0),\dot{\chi}(0))$=(0.0,0.0) for all.)
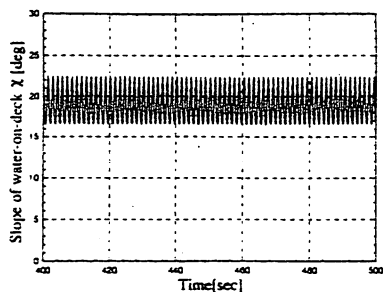
(a.3) Time history of χ (b.3) Time history of χ (c.3) Time history of χ
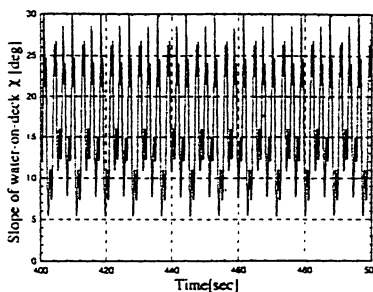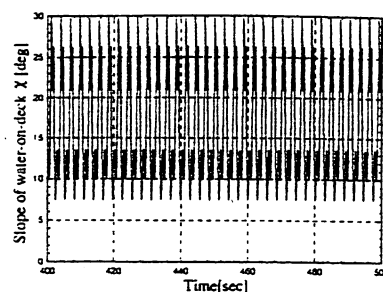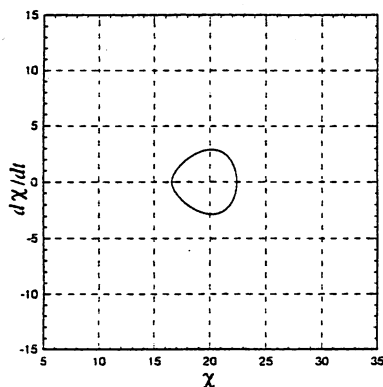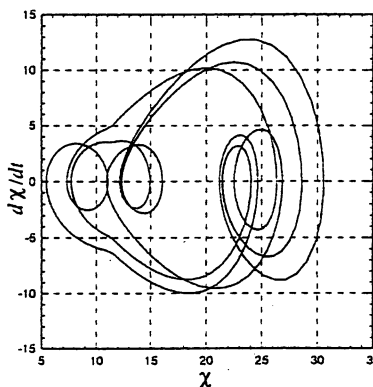
(a.4) Phase portrait $(\chi,\dot{\chi})$ (b.4) Phase portrait $(\chi,\dot{\chi})$ (c.4) Phase portrait $(\chi,\dot{\chi})$
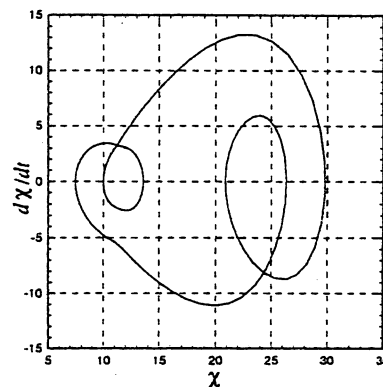
Fig.4 Continued.

((a)$\phi(0)=\chi(0)=24.0$deg., (b)$\phi(0)=\chi(0)=28.8$deg., (c)$\phi(0)=\chi(0)=28.9$deg..
$(\dot{\phi}(0),\dot{\chi}(0))=(0.0,0.0)$ for all.)

CONCLUSIONS

We investigate nonlinearly coupled motion of a ship and water-on-deck in regular beam seas. Both experimental and numerical works show coexistence of different modes of roll motion even in regular waves of moderate amplitude. Since there are some modes of large amplitude motion which may lead to capsizing, we need further studies on it and development of a technique to control it.

REFRENCES

1. Paulling, J.R. and Rosenberg, R.M. : On Unstable Ship Motions resulting from Nonlinear Coupling, J. Ship Res., Vol.3, 1959, pp.36-46.

2. Nayfeh, A.H., Mook, D.T., and Marshall, L.R. : Nonlinear Coupling of Pitch and Roll Modes in Ship Motions, J. Hydronautics, Vol.7, No.4, 1973, pp.145-152.

3. Nayfeh, A.H. : On the Undesirable Roll Characteristics of Ships in Regular Seas, J. Ship Research, Vol.32, No.2, 1988, pp.92-100.

4. Francescutto, A., Contento, G., and Penna, R. : Experimental Evidence of Strong Nonlinear Effects in the Rolling Motion of a Destroyer in Beam Sea, Proc. 5th International Conference on Stability of Ships and Ocean Vehicles, Vol.1, 1994.

5. Virgin, L.N. : The Nonlinear Rolling Response of a Vessel including Chaotic Motions leading to Capsize in Regular Seas, Applied Ocean Research, Vol.9, No.2, 1987, pp.89-95.

6. Kan, M. and Taguchi, H. : Capsizing of a Ship in Quatering Seas (Part 2. Chaos and Fractal in Capsizing Phenomenon), J. Soc. Naval Architects Japan, Vol.168, 1990, pp.211-220. [in Japanese]

7. Rainey, R.C.T. and Thompson, J.M.T. : The Transient Capsize Diagram-A New Method of Quantifying Stability in Waves, J. Ship Res., Vol.35, No.1, 1991, pp.58-62.

8. Soliman, M.S. and Thompson, J.M.T. : Transient and Steady State Analysis of Capsize Phenomena, Applied Ocean Research, Vol.13, No.2, 1991, pp.82-92.

9. Thompson, J.M.T., Rainey, R.C.T., and Soliman, M.S. : Mechanics of Ship Capsize under Direct and Parametric Wave Excitation, Phil. Trans. R. Soc. Lond. A 338, 1992, pp.471-490.

10. MacMaster, A.G. and Thompson, J.M.T. : Wave Tank Testing and the Capsizability of Hulls, Proc. Roy. Soc. Lond. A, Vol.446, 1994, pp.217-232.

11. Murashige, S., Aihara, K., Yamada, T., and Ishida, S. : Chaotic Motion of a Flooded Ship [in preparation].

12. Dillingham, J. : Motion Studies of a Vessel with Water on Deck, Marine Technology, Vol.18, No.1, 1981, pp.38-50.

13. Caglayan, I. and Storch, R.L. : Stability of Fishing Vessels with Water on Deck: A Review, J. Ship Res., Vol.26, No.2, 1982, pp.106-116.

14. Vasta, J., Giddings, A.J., Taplin, A., and Stilwell, J.J. : Roll Stabilization by means of Passive Tanks, Soc. Naval Arch. and Marine Eng., Vol.69, 1961, pp.411-460.

A Study on Capsizing Phenomena of a Ship in Waves

S. Y. Hong, C. G. Kang and S.W. Hong

Korea Research Institute of Ships and Ocean Engineering

P.O. Box 101, Yusong, Taejon, 305-600, Korea

SUMMARY

After the disastrous accident of Seohae Ferry at Korean West Sea in 1993, a numerical and experimental study on the capsizing of the ferry was carried out to investigate the cause of the accident. Righting moments for various loading condition are calculated both in still water and in wave conditions. Capsizing simulations are performed with hydrodynamic coefficients obtained from strip method and nonlinear restoring moments considering relative motion using Runge-Kutta fourth-order method. It is found out that deterioration of designed righting moment causes ships to capsize in severe wave conditions. Nonlinear effects such as hydrodynamic forces due to change of attitude of a ship, effects of green water and freeing ports which are not considered in the calculation are investigated through model tests.

INTRODUCTION

Capsizing of a ship in waves may be the last disaster which she could experience through her life. That kind of accident usually results in tremendous loss and casualties. So, it is important to examine the mechanism of capsizing in waves for the prevention of the accident. Energetic research activities have been made by Hamamoto, Kan, Iwashita and others on this hot issue during past years[2,3,4,5,6].

In this paper, numerical and experimental stability analysis is performed for Seohae Ferry[1]. Restoring moment is calculated both in calm water and in following waves for various loading conditions and capsizing simulations are performed to examine the possible cases for capsizing. Experiments are also performed to measure restoring moments in waves and the nonlinear hydrodynamic effects are investigated.

THEORETICAL ANALYSIS

Static analysis

Generally, righting moment of a ship in waves has its minimum value when the wave crest is at middle of the ship, while maximum value is obtained when the wave trough approaches the same location of the ship. Which can be explained by

the geometrical property of ships; it has noticeable change of sectional shapes at stem and stern as the change of waterline, while it does not at middle body. The righting moment of a ship is calculated as following procedures;

1) Search equilibrium waterline for a given heeling angle.
2) Search center of buoyancy for submerged part.
3) Calculate moments due to buoyancy and gravity.
4) Finally restoring moment is obtained by subtracting gravity effect from the moment due to buoyancy.

Capsizing Simulation

Lateral righting moment($GZ \cdot W$) is one of most important factors which have influence on the capsizing of ships in waves. Where, W is the displacement of the ship. For large rolling motion, righting arm is governed by nonlinear effect as shown in Fig. 1, while GZ is usually approximated by linear function of rolling angle in linearized ship motion equation. Since the examination of capsizing phenomenon is focused in this study, all the hydrodynamic coefficients except for lateral righting moment term are obtained from STF(Salvesen, Tuck and Faltinsen) strip method[7]. Lateral righting moment is calculated accurately considering relative motions between ship and incident waves at each stations. Time-domain simulation of rolling motion is performed using Runge-Kutta fourth-order scheme with the hydrodynamic coefficients and the righting moment.

MODEL EXPERIMENTS

Loss of stability of a ship is regarded as one of major causes to capsizing phenomena in waves. Hence, many simulation models have been developed to investigate the role of nonlinearity of righting moment in waves and the focus is paid on the accurate estimation of righting moment in waves. Experimental study can give more information which theoretical approach may miss real physical phenomena such as green water on the deck, the effect of green water flow, the effect of freeing port, nonlinear hydrodynamic forces due to change of attitude of a ship and so forth. A series of model experiments were performed at KRISO towing tank equipped with a flap-type wave maker under the following conditions.

-scale ratio : 1/12
-heading : following sea
-ship type : ferry
-ship speed : 10 knots
-draft : 106 condition(departure condition)

-wave height : 0, 1, and 2m

-wave length : 35m

-measured items : heeling angle, sinkage for freely floating model

heeling angle, rolling moment for captive model

Two methods are adopted to get more accurate righting moment in waves. The one is a freely floating model method which gives more accurate value of heeling angle and sinkage for a given heeling moment. The other is a captive model method which gives change of righting moment in waves for a fixed heeling angle. The former method is applied first to find out realistic attitude for a given heeling angle and to investigate the effects of Kelvin wave induced by ship advance. Restoring moment in waves is essentially nonlinear as shown in Fig. 2. However, measured restoring moment signal shows periodic and almost repeated amplitudes. The peak value is important in stability sense, that analysis is made on the basis of peak to peak value approach. Fig. 3 shows schematic diagrams for both experimental methods used in this study.

RESULTS AND DISCUSSIONS

In order to investigate as many as possible capsizing conditions, restoring moments for various loading conditions are examined as shown in Fig. 4 - Fig. 6. Loading conditions are classified as numbers in the figure as follows:

Legend   Description

Design : Full load departure condition at design stage

102   : Departure condition(October 10, 1993) assuming without overloads such as pickled anchovies, excessive passengers, cargos on upper deck, gravel

103   : In addition to 102 load condition, 7.3 tons of gravel are loaded at steering gear room

104   : In addition to 103 load condition, cargos(pickled anchovies) are loaded on the upper deck

105   : In addition to 104 load condition, 143 excessive passengers are on board

106   : In addition to 105 load condition, 4 ton passengers' cargos are loaded (departure condition on Oct. 10, 1993)

107   : 7.3 tons of gravel are removed from 106 load condition

Fig. 4 denotes the righting moment in still water condition. Fig. 5 shows the minimum righting moment in stern quartering wave condition when wave height is 2m and wave length is 30m. Fig. 6 shows the maximum righting moment for the same wave condition as Fig. 5. As loads on the deck increase, righting moments

decrease. It is believed that increase of draft due to cargos results in decrease of freeboard, which consequently causes water level approaches upper deck earlier. Though gravel is loaded under the center of gravity location, it has bad influence on the righting moment except for small heeling angle range. Comparing load conditions 104 and 105, it can be seen that excessive passenger is one of decisive factors for loss of stability. When the crest of wave locates at the middle of ship, righting moments dramatically decrease due to excessive passengers and gravel. Among considered load conditions, the worst case is obtained for loading condition 106 which is assumed for departure condition at accident. From these investigations, excessive passengers and gravel are main factors for the loss of stability.

In order to investigate the possibility of capsizing under design and departure loading conditions considered and wave condition, the simulation is made for the following conditions:

Ship speed : 10 knots

Average wind speed : 5.5 m/sec.

Max. wind speed : 10.5 m/sc.

Wave height : 2.0 m

Wave length : 30 m

Wave incidence angle : 30 and 45 degrees (head sea = 180 degrees)

Loading condition : Design load and departure condition(106)

Fig. 7 and 8 show the simulation results for design load condition when wave incidence angle is 45 degrees and 30 degrees, respectively. These results show that capsizing does not occur for design load condition for all wave incidence angles. Fig. 9 and 10 show the simulation results for departure load conditions. These results show the significance of wave incidence angle on capsizing of a ship. Within a minute after simulation, capsizing occurs when wave incidence angle is 30 degrees. This result demonstrates that the deterioration of designed righting moment causes the ship to capsize in severe wave conditions such as the case when the high wave and stern wave direction occur simultaneously.

Fig. 11 compares the measured and calculated righting arm. Free model method is used in this measurement and good agreement is obtained between them. Fig. 12 presents the effects of ship speed on the change of heeling angle and sinkage for given heeling moments. It can be found that the sinkage slightly increases and the heeling angle slightly decreases as ship advances in still water. This implies that steady Kelvin wave pattern plays a role to increase righting moment and it can be explained that steady wave pattern generally has crests at bow and stern and trough at midship. This effects could be also found in righting moments measured in

following wave condition for the captive model as shown in Fig. 13. Calculation predicts that loss of stability occurs at heeling angle of about 16 degree while experiment shows that it occurs at heeling angle over 26 degree under the same condition of which wave height of 2m, wave length of 35m and ship speed of 10 knots in following wave. Fig. 14 shows the effects of wave heights on righting moment. Increase of maximum righting moment is not so significant as wave height increases, while decrease of minimum righting is noticeable as wave height increases. This tendency is similar to that obtained from the calculation. The quantitative discrepancy between measurements and calculations could be found from the following reasons that calculation did not consider:

-the effect of steady wave pattern which contributes to increase of righting moment

-the nonlinear effects of green water and its floodlike flows on the deck

-the effects of freeing port

-the other effects such as experimental errors.

CONCLUSIONS

From the investigation on the stability of a passenger ship in waves through numerical and experimental study, following conclusions can be drawn.

1. Deterioration of initial GM could lead dramatic decrease of restoring moment in waves, which may cause a ship to capsize in severe following or stern quartering sea condition.

2. Motion simulation in following and stern quartering waves could be used to examine capsizing situation of ship in waves.

3. Measurements of restoring moment in following waves show that numerical estimation of restoring moment in waves overestimates loss of stability. Steady wave flow seems to an important factor to resist the decrease of righting moment in waves.

REFERENCES

[1] Lee, J.T. et. al, "Stability and Safety Analysis of a Coastal Passenger Ship", KIMM Report UCK020-1812.D, 1994(in Korean).

[2] Hamamoto, M. and Tsukasa, Y., "An Analysis of Side Force and Yaw Moment on a Ship in Quartering Waves", J. of Soc. of Naval Arch. of Japan, Vol 171, 1992.

[3] Kan, M. and Taguchi, H., "Capsizing of a Ship in Quartering Seas(Part 4, Chaos and Fractals in Forced Mathieu Type Capsize Equation)", J. of SNAJ, Vol. 171, 1992.

[4] Hamamoto, M., Kim, Y.S., Matsuda, A. and Kotani, H., "An Analysis of a Ship Capsizing in Quartering Sea", J. of SNAJ, Vol. 172, 1992.

[5] Iwashita, H., Ito, A., Okada, T., Ohkusu, M., Takaki, M. and Mizoguchi, S., "Wave Forces Acting on a Blunt Ship with Forward Speed in Oblique Seas", J. of SNAJ, Vol. 171, 1992.

[6] Hamamoto, M., Matsuda, A. and Ise, Y., "Ship Motion and the Dangerous Zone of a Ship in Severe Following Seas", J. of SNAJ, Vol. 175, 1994.

[7] Salvesen, N., Tuck, E.O. and Faltinsen, O., "Ship Motions and Sea Loads", SNAME Trans. 78, 1970.
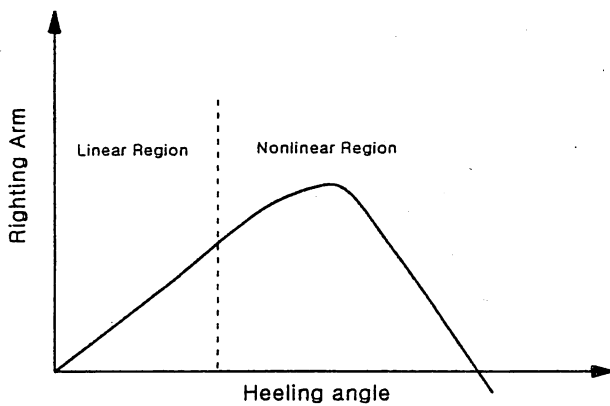
Fig. 1 Righting Arm vs. Heeling Angle

Fig. 2 Measured Restoring Moment in Following Waves

(a) Free Model Method

(b) Fixed Model Method
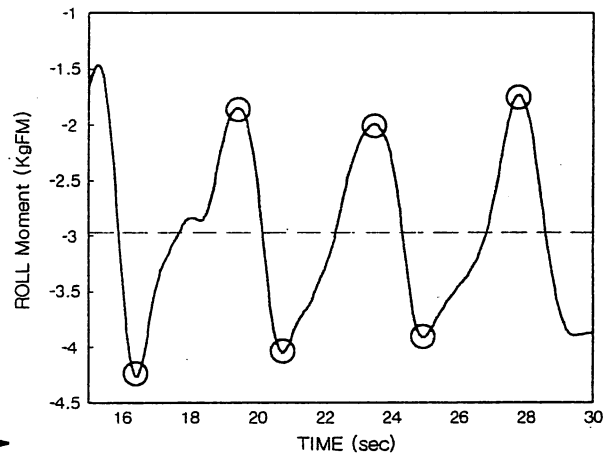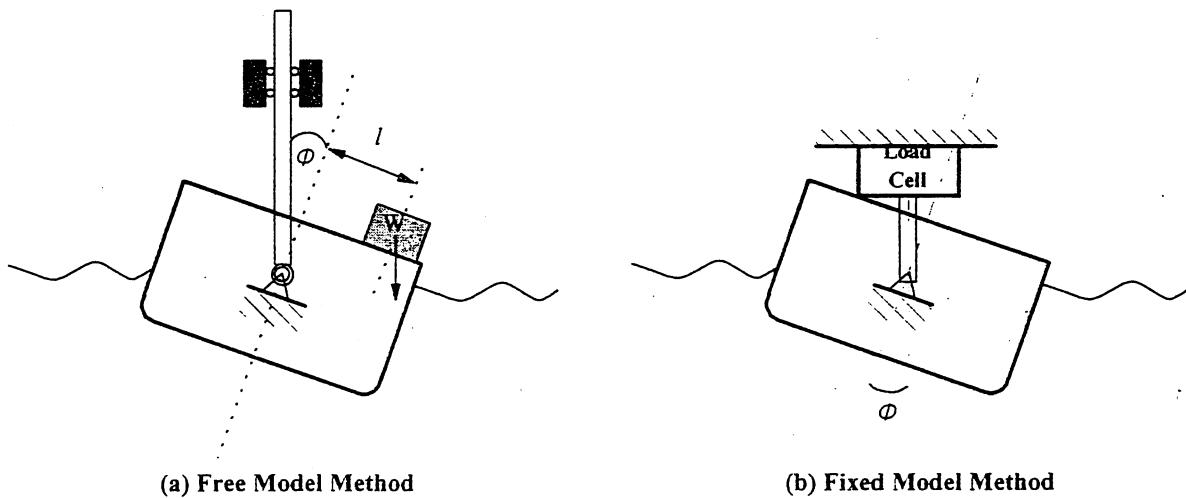
Fig. 3 Test setup for measurement of Heeling Angle and Restoring Moment
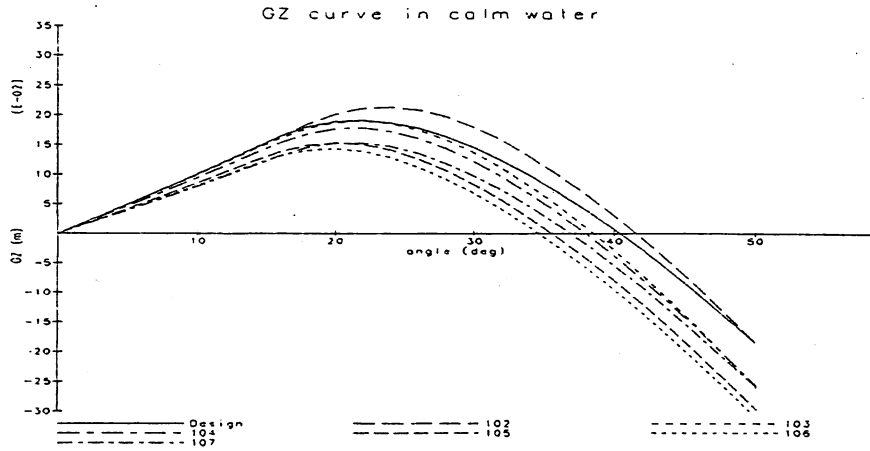
Fig. 4 Righting Arm Curve of a Passenger Ship for Various Loading Condition in Calm Water
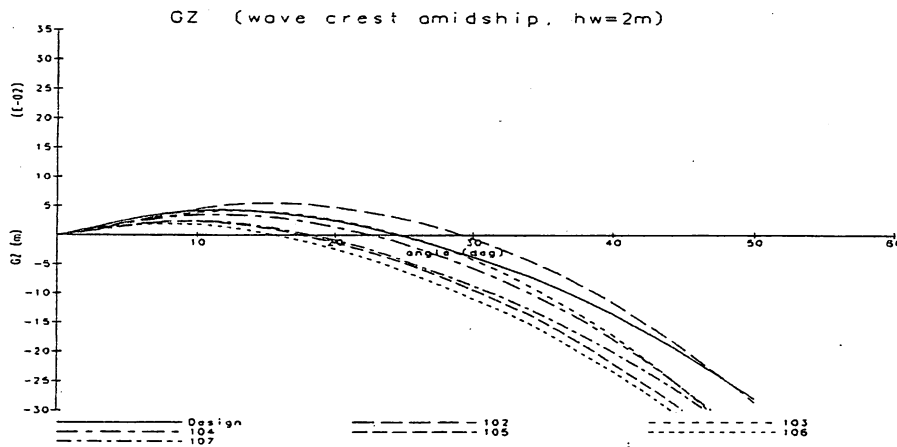
Fig. 5 Minimum Righting Arm Curve of a Passenger Ship for Various Loading Condition in Waves
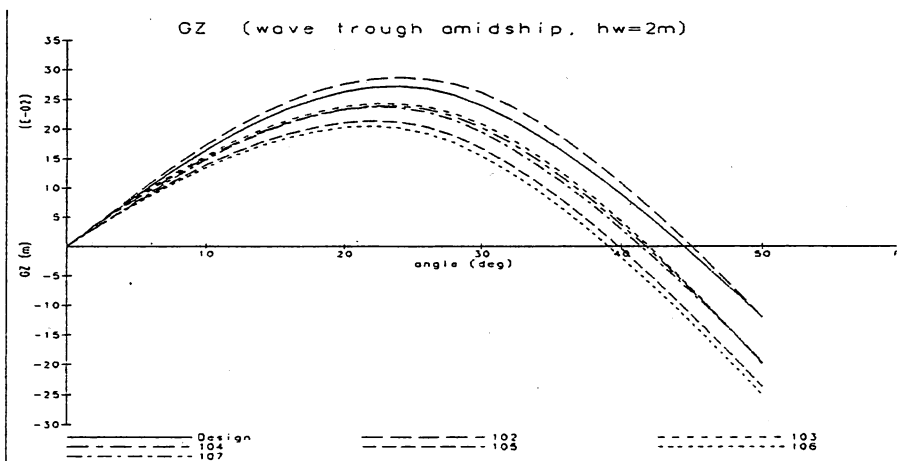
Fig. 6 Maximum Righting Arm Curve of a Passenger Ship for Various Loading Condition in Waves

Time Simulation in 2m Waves (Design)
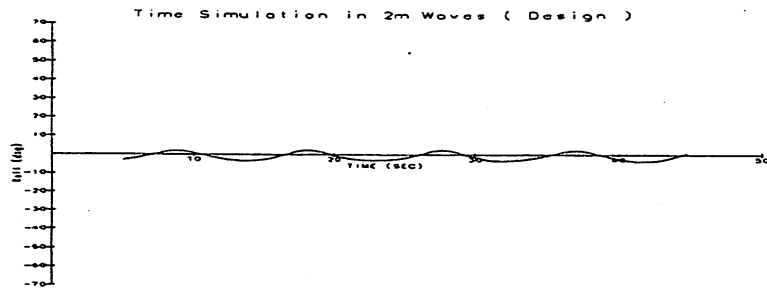
Fig. 7 Time Simulation of Roll Motion in 2m Waves
(Design, $\beta=45°$)

Time Simulation in 2m Waves (Design)
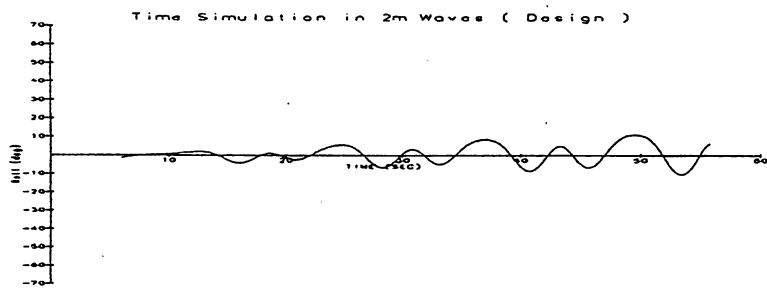
Fig. 8 Time Simulation of Roll Motion in 2m Waves
(Design, $\beta=30°$)

Time Simulation in 2m Waves (106)
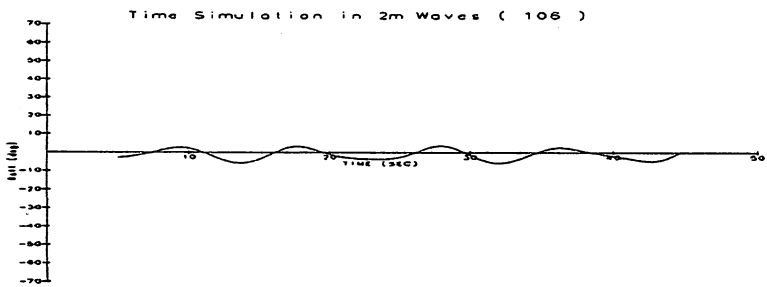
Fig. 9 Time Simulation of Roll Motion in 2m Waves
(Departure, $\beta=45°$)

Time Simulation in 2m Waves (106)
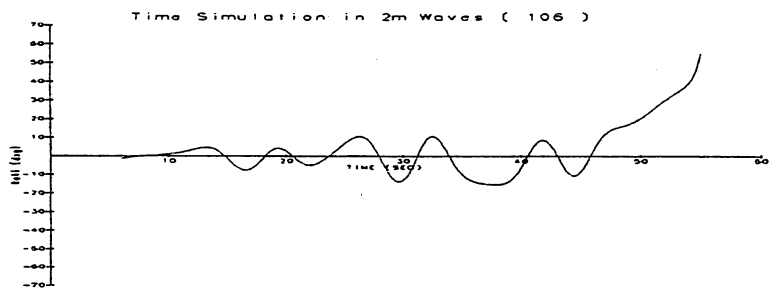
Fig. 10 Time Simulation of Roll Motion in 2m Waves
(Departure, $\beta=30°$)
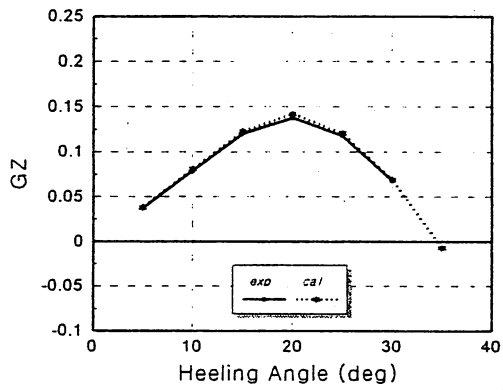
Fig. 11 Comparison of Righting Moment Curve in Calm Water
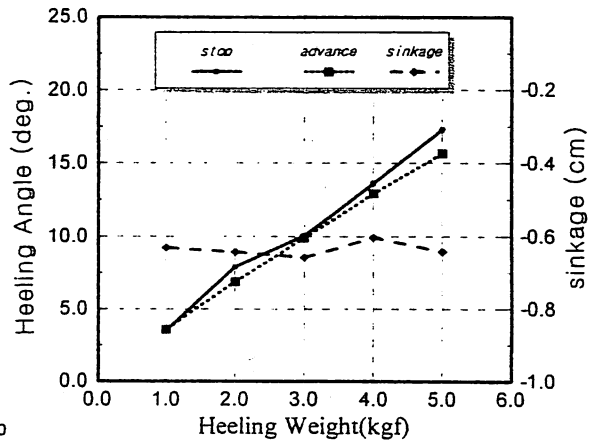
Fig. 12 Effects of Steady Waves on the Heel Angle and Sinkage in Still Water(Vs = 10 knots)

(wave height=2m, fixed model, departure condition)
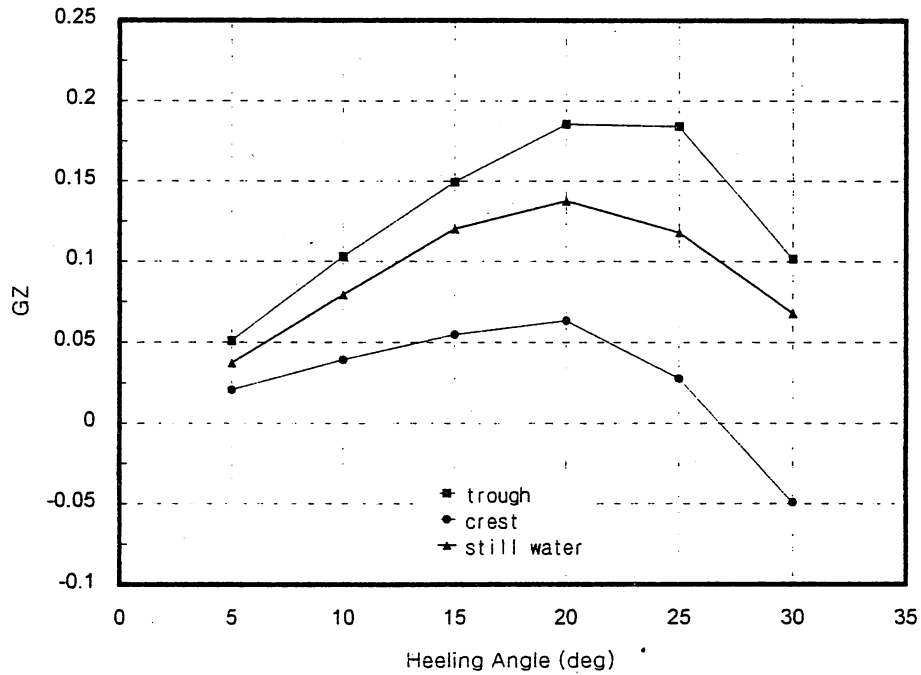
Fig. 13 Righting Moment Curve in Following Regular Wave

(H=2m, λ=35m, Vs = 10knots)

(crest, fixed model, departure condition)
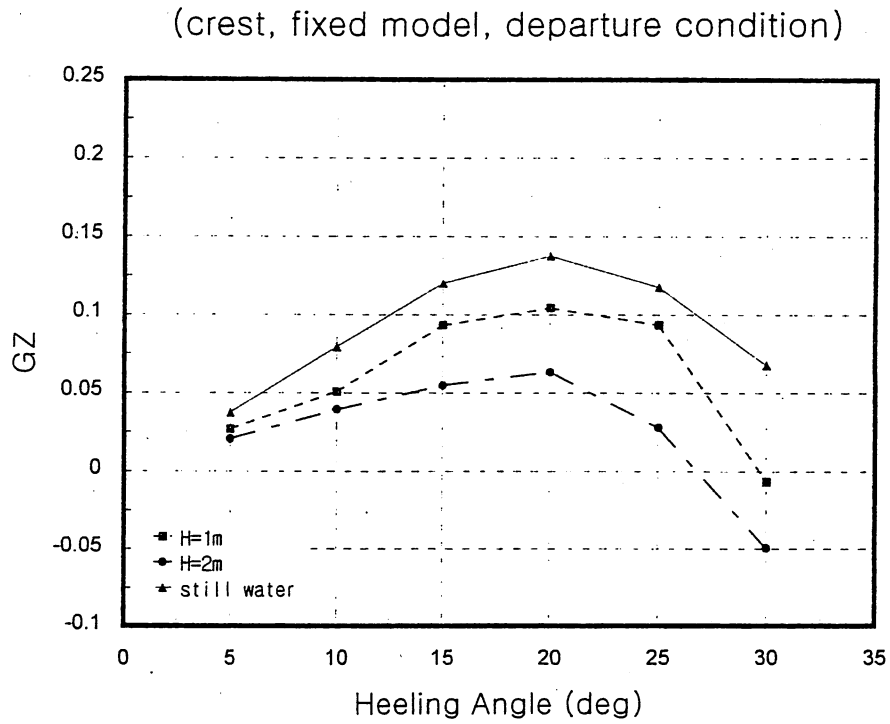
Fig. 14a Effects of Wave Height on the Maximum Restoring Moment in Following Regular Wave (λ=35m, Vs = 10 knots)

(trough, fixed model, departure condition)
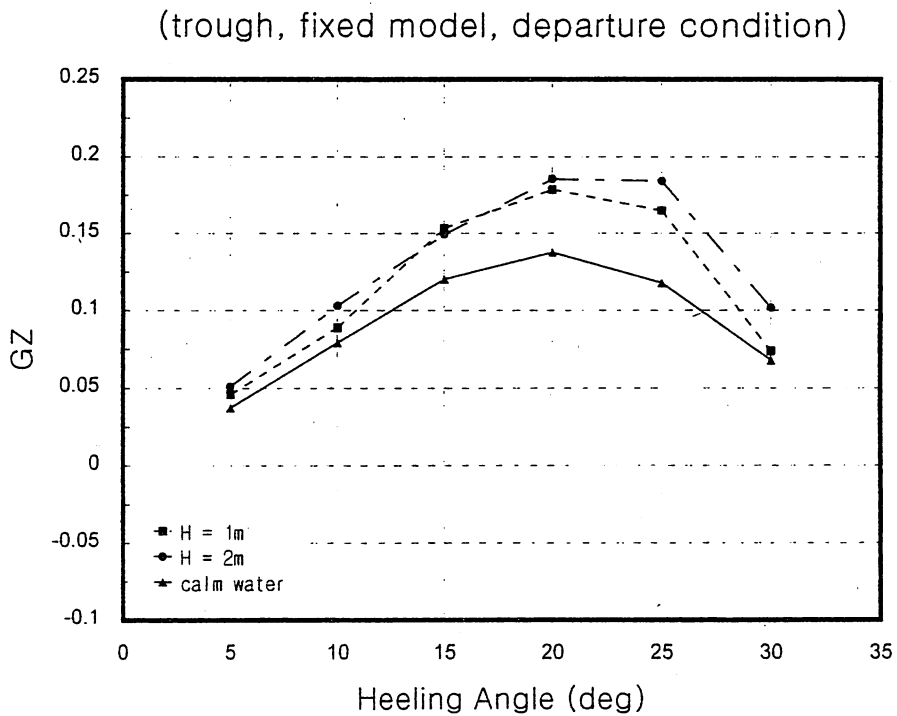
Fig. 14b Effects of Wave Height on the Maximum Restoring Moment in Following Regular Wave (λ=35m, Vs = 10 knots)

DAMAGE STABILITY WITH WATER ON DECK
OF A RO-RO PASSENGER SHIP IN WAVES

Shigesuke ISHIDA,　Sunao MURASHIGE,　Iwao WATANABE,
Yoshitaka OGAWA,　Toshifumi FUJIWARA

SHIP RESEARCH INSTITUTE, Ministry of Transport
6-38-1, Shinkawa, Mitaka, Tokyo 181, Japan
Fax : +81-422-41-3056,　E-mail : ishida@srimot.go.jp

SUMMARY

An experiment on the stability of a RO-RO passenger ship with side damage was conducted in beam seas.　Capsize only occurred with a small GM value, which did not satisfy SOLAS Regulation.　In non-capsize conditions the ship became a stationary condition, with constant mean values of heel angle ϕ_0 and water volume on deck w_0.　The effect of experimental parameters on these values and the capsize conditions were discussed.

The effect of resonance of roll motion was also discussed.　The importance of it was clarified because ϕ_0, w_0 and some other data often had peaks in regular waves near the resonant frequency.

The mean height of water on deck above the calm sea surface H_d, which almost kept a certain plus value, was proposed as an index for the stationary condition.　It was concluded that the possibility of capsize can be evaluated by the equilibrium curve which is calculated and plotted on the H_d-ϕ diagram without knowing the exact value of H_d.

INTRODUCTION

The safety standard of RO-RO passenger vessels was deliberated at IMO from 1994 to 1995 in order to prevent capsizing disaster like the one of Estonia in 1994.　One of the authors, I.Watanabe, joined the discussion in the expert panel.　The main topic of it was the stability standard because RO-RO passenger vessels have wide non-separated car decks. Once free flooded water is piled up on them, the large heel moment could be the cause of capsize because of this feature.

There can exist two scenarios of flooding; (1) flooding from damaged bow door but with intact main hull, (2) flooding from side damage caused by collision.　The discussion in IMO was focused on the second scenario, because that is assumed to be the worst accident in the stability regulation.

There were several papers published on this problem like Bird et.al.[1], Velschou et.al.[2], Dand[3] and Vassalos[4], but flooding, accumulation of flooded water, and the interaction of ship motion and flooded water are so complicated that much more study is necessary for clarifying this phenomena.   So we conducted an experiment using a RO-RO passenger ship with a side damage in beam seas in order to contribute to the discussion in IMO.

EXPERIMENT

Model Ship and Damage

Table 1 and Fig.1 show the model ship and damage. The damage reaches two compartments and follows the SOLAS Regulation 8.4.   A vertically movable vehicle deck is provided.   There is some space between the vehicle deck and the hull, so this model simulates a ship with side casing.   It should be noted that GM_d (GM in damaged condition) is far larger than the intact value because of the flare. Four wave gauges at the center of the damage and six water level meters are equipped in the deck.

Table 1 Principal Particulars

	Ship		Model	
	Intact	Damaged	Intact	Damaged
Lpp (m)	101.0		4.3	
B (m)	16.0		0.681	
D (m)	5.7		0.236	
d (m)	4.37	5.22	0.186	0.222
W	3821 t		272.7 kg	
KG (m)	5.87		0.25	
$GM_{(d)}$(m)	1.62	3.12	0.069	0.133
Tr (sec.)	9.40	8.43	1.94	1.74
f (m)	1.17	0.33	0.050	0.014
H (m)	4.84		0.206	

f : freeboard,   H : RO-RO deck height

Experiment

The experiment was conducted in irregular waves with JONSWAP spectrum and duration time of 30 minutes in ship scale.   Basically significant wave height ($H_{1/3}$) was 4.0m and peak period (T_p) was 8.0sec., but varied keeping the condition of $T_p [sec] = 4\sqrt{H_{1/3}[m]}$. The test was also carried out in some regular waves.   The main parameters were GM_d and wave height.   Moreover the effect of center casing (CC), height of vehicle deck and initial heel was investigated in some conditions.   The damaged side of the ship was kept to weather side.

Stability Curves

Measured and calculated gz curves plus water volume on deck w are shown Fig.2. Calculated gz curves with constant w are also shown Fig.3. $w/W=10\%$ is equivalent to the flooded water height of 39cm in upright condition.   SOLAS Regulation 8.2.3 was satisfied except the condition of $GM_d=1.27m$.

We should keep it in our minds that ship does not roll along the curves in Fig.2 because the area of the damage opening over the vehicle deck is small compared to the volume of the deck, which means the flooding velocity is not high enough to make w equal to the one drawn in Fig.2.   In a few cycles of rolling motion we should assume that w is almost constant and that the ship rolls along the stability curves shown in Fig.3.

RESULT IN IRREGULAR WAVES

Figs.4 and 5 show the time history examples of roll angle ϕ and w.   Positive roll angle

means heeling to lee side. At the last stage of experiment ϕ and w had constant mean values, ϕ_0 and w_0 respectively, in the stationary condition. The effect of experimental parameters on ϕ_0, w_0 and water ingress rate at the beginning of experiment v was investigated as follows.

(1) Effect of GM_d (see Fig.6)

When GM_d gets smaller ϕ_0 becomes greater, but w_0 and v become smaller because small GM_d leads to a large heel angle to lee side in a short time, which makes the damage opening higher up the sea surface. The effect of wave height is small. The reason seems to be the constant wave slope.

(2) Effect of Center Casing (see Fig.7)

In Fig.7 (with CC) the tendency of ϕ_0 versus GM_d is the same as Fig.6 (without CC) but the opposite direction (to weather side) because the flooded water stays mainly in the weather side compartment of the deck. The variation of w_0 is not so clear as Fig.6 because the movement of flooded water between two half-separated compartments is complicated. But in general, the tendency of w_0 is opposite to Fig.6 because heeling to weather side (lowering the damage opening) keeps flowing in and out of water. It can be seen that with the standard GM_d (3.12m) this ship almost keeps upright condition even if w/W gets as much as 40% and that it capsizes with the smallest GM_d.

(3) Effect of Freeboard (height of the vehicle deck) (see Fig.8)

ϕ_0 and w_0 gets smaller when the freeboard in damaged condition f_d becomes larger even if some loss of GM_d happens.

(4) Effect of Initial Heel

When the ship has an initial heel angle of 4 degrees by a shift of weight to weather side, the time histories of ϕ and w are similar to the ones with CC because heeling direction is the same. At the case of the smallest GM_d (1.27m) she capsized in about three minutes in model scale. So it can be concluded that heeling to weather side because of CC and/or cargo shift leads to a disastrous situation.

EFFECT OF ROLL RESONANCE

The results in regular waves with constant (wave height)/(wave length) ratio of 1/25 are shown in Fig.9, where ω_i is the angular frequency of incident wave. ω_r is calculated from free roll test result which is carried out in damaged condition, but the vehicle deck is undamaged. ω_i / ω_r is called a tuning factor.

It can be seen that not only rolling amplitude and relative water amplitude but also water on deck w_0 have peaks around tuning factor = 1. The peaks are notable with CC because the motion of the flooded water is reduced by CC. Moreover heel angle ϕ_0 have some change around the same frequency. This result suggests that irregular waves for the stability test should include significant wave component of the roll resonance frequency and that the interaction of ship motion and water on deck should not be ignored.

Looking through the figures of roll amplitude in Fig.9, the peak frequency ω_{MAX} seems to shift to low frequency side with CC and to high frequency side without CC in some cases. The factors of shifting ω_{MAX}, characteristic to the damaged RO-RO passenger ships, are listed below.

(1) Large damping

(damping in damaged condition is 5 times as large as intact condition according to the

free roll test)

(2) Static effect of the water on deck (including the sinkage of the ship)

(3) Dynamic effect of the water on deck.

It is clarified that all the effects of (1), (2) and the damping effect of (3) make ω_{MAX} shift to the low frequency side. But a calculation, modeling the ship and water on deck like a double pendulum, shows an opposite result[5], which could explain the tendency of the shift of ω_{MAX} with CC in Fig.9(a).

KEY FACTOR FOR THE BALANCE IN STATIONARY CONDITION

As mentioned in the previous section the water ingress velocity from damage opening is not so high that in a few cycles of rolling motion the damaged ship moves almost along a stability curve shown in Fig.3, with a constant volume of water on deck w. When w increases by flooding it transfers to another stability curve with less stability. At last when the rolling energy overtake the dynamic stability the ship will capsize, but if this transference stops in a stationary condition under *a certain balance* she will survive. This *balance* will be discussed.

The mean heel angle ϕ_0 and the mean water volume on deck w_0 in the stationary condition are shown in Fig.10. When the model capsized the values just before capsize are plotted. The solid lines show the equilibrium angles calculated from the stability curves in Fig.3 for a given w/W. But if the stability curve is almost parallel to the horizontal axis near the equilibrium point and if some moment like a wind moment works, the equilibrium angle can easily change from the exact one. So quasi-equilibrium angles, the crossing points of the stability curves with the lines of $gz = \pm 0.0624m$ (2% of GM_d of the standard condition), are also calculated and drawn by broken lines in Fig.10. The zone between these two broken lines will be called a equilibrium zone hereafter.

It can be seen from Fig.10 that the non-capsized experimental results are in or near the equilibrium zones and that capsized results are away from the zone with surplus water on deck. According to Fig.3 gz is always negative with these GM_d and w/W values, so it is a natural result that she capsized.

It is necessary to know another key factor or key quantity which decides the balance in stationary conditions. As the key quantity we propose H_d, the mean height of the water surface on deck from the calm sea surface. If H_d has a large positive value at a moment the water on deck will flow out and vice versa, so H_d must be within a certain range. Fig.11 shows experimental results of H_d vs. GM_d. It can be seen that H_d have a value between -0.26m ~ 0.78m in ship scale when the freeboard height in damaged condition f_d is standard (0.33m).

It should be necessary to investigate the variation of H_d as a function of ϕ and w before proceeding with the discussion on the experimental results. The calculated H_d in calm water is shows in Fig.12. As long as ϕ is small the water surface on deck is a little higher than the freeboard (0.33m) and is almost constant regardless of w because the flooded water spreads over the whole deck. On the other hand when ϕ_0 becomes large H_d tends to vary widely according to w because flooded water concentrates at the corner of the deck. So, when H_d keeps a certain positive value in waves after the ship heels, that inevitably leads to a large value of w and to a less stable condition.

Returning back to Fig.11, the black and single marks show low H_d values when GM_d is small because the ship heels to lee side and the flooding stops in a short time. As long as

wave height is small H_d is also small like the circles in Fig.11. But in other cases in which water is still coming in and out of the deck, H_d keeps a high values in a small range between 0.4 and 0.8m, regardless of wave height. So if GM_d is very small and the ship heels to weather side by the effect of CC or cargo shift in high waves, the ship will be capsized by much flooded water on deck. It should be noted that the stability curves of the damaged condition in Fig.2 is calculated under the assumption that $H_d = 0$. This ordinary calculation underestimates the amount of water on deck and the loss of stability in waves.

RISK ESTIMATION FOR CAPSIZE

The figure whose ordinate is changed to H_d from Fig.10 is shown in Fig.13. It can be seen that when GM_d becomes greater the tendency of the equilibrium zones change from right side down to right side up. From Figs.13 and the idea sketch in the right, we can see the process of the change of ship condition in waves and can estimate the risk for capsizing.

When the first flooding occurs the ship condition locates on the point of (ϕ, H_d) = (ϕ_i, f_d), where ϕ_i is the initial heel angle. If the ship heels H_d becomes small, but that encourages flooding. So the chain of "flooding", "increase of H_d", "heel (flow out of some water at the same time)", "decrease of H_d" and "flooding" will be repeated. In the dangerous condition, i.e. the wave is high and the ship has a CC or $\phi_i < 0$ (weather side), the point moves almost parallel to the right side, keeping H_d constant and increasing w.

Finally if the point comes across the equilibrium zone like a figure of $GM_d = 2.44m$ in Fig.13, the movement of the point stops and the ship starts to roll around the stable condition. But if the zone is right side down like the top figure in Fig.13, there is nothing to stop the movement of the point and the ship will capsize with much water on deck.

So the risk for capsizing can be roughly estimated from the tendency of the equilibrium zones without knowing exact H_d value. In order to make the ship capsize-resistant it seems crucial to make the gz at big heel angles large enough to make the zone right side up. It can be concluded for this ship that the minimum required GM_d is 1.79m.

CONCLUSIONS

1) The effect of GM_d (GM in damaged condition) etc. on the mean heel angle and the mean water on deck in the stationary condition, ϕ_0 and w_0 respectively, is investigated. When GM_d gets larger w_0 also becomes larger, but the ship is stable with smaller ϕ_0 value.
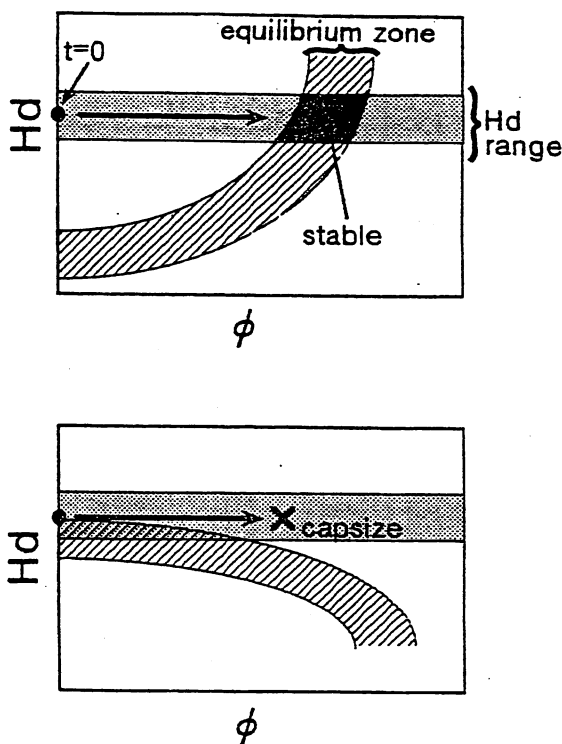
The tested ship did not capsize as long as SOLAS Regulation is satisfied.

2) When the ship heels to weather side she becomes unstable with much water on deck if GM_d is small. So cargo shift or existence of center casing might lead to a dangerous situation.

3) The test result in regular waves show that not only ship motion but ϕ_0 and w_0 have some peaks near the resonant frequency of rolling, so the waves for stability test should include that wave component.

4) The water on deck keeps a higher mean surface than sea surface as long as the damage opening of the deck is not made high by heeling to lee side. This difference of water surface, H_d, has a value in a small range in various conditions.

5) In dangerous condition, i.e. the wave is not so low and the ship has a CC or cargo shift, the ship transfers to less stable condition, repeating the chain of "flooding", "increase of H_d", "heel", "decrease of H_d" and "flooding". Finally if the rolling energy overtake the dynamic stability she capsizes.

6) By calculating the equilibrium zone and drawing it on H_d-ϕ diagram the risk of capsize can be roughly estimated without knowing the exact value of H_d.

REFERENCES

1) H.Bird, R.P.Browne : Damage Stability Model Experiments, Trans. of R.I.N.A., 1973

2) S.Velschou, M.Schindler : RO-RO Passenger Ferry Damage Stability Studies - A Continuation of Model Tests for a Typical Ferry, Symp. on RO-RO Ships' Survivability, 1994

3) I.W.Dand : Factors Affecting the Capsize of Damaged RO-RO Vessels in Waves, Symp. on RO-RO Ships' Survivability, 1994

4) D.Vassalos : Capsizal Resistance Prediction of a Damaged Ship in a Random Sea, Symp. on RO-RO Ships' Survivability, 1994

5) S.Murashige, K.Aihara, T.Yamada : Nonlinear Roll Motion of a Ship with Water-on-Deck in Regular Waves, The Second Workshop on Stability and Operational Safety of Ships, 1996

6) The Joint Accident Investigation Commission of Estonia, Finland and Sweden : Part-Report Covering Technical Issues on the Capsizing on 28 September 1994 in the Baltic Sea of the RO-RO Passenger Vessel MV ESTONIA, 1995

7) I.W.Dand : Hydrodynamic Aspects of the Sinking of the Ferry 'Herald of Free Enterprise', Trans. of R.I.N.A., 1988

8) N.Shimizu, K.Roby, Y.Ikeda : An Experimental Study on Flooding into the Car Deck of a RORO Ferry through Damaged Bow Door, Journal of the Kansai Society of Naval Architects, Vol.225, 1996 (to be published)

9) Some Results of Model Test , IMO RORO/ISWG/1/3/5, 1995

10) S.Murashige, S.Ishida, I.Watanabe, Y.Ogawa : A Model Experiment for a Relation between Flooding of a Ro-Ro Deck and Ambient Waves, 66th General Meeting of Ship Research Institute, 1995 (in Japanese)

11) T.Nimura, S.Ishida, I.Watanabe : On the Effect of Hull Forms and Other Factors on the Capsizing of Sailing Yachts, Journal of the Soc. of Naval Architects of Japan, vol.175, 1994 (in Japanese)

12) I.Watanabe : Disaster of Ro-Ro Passenger Ship "Estonia" and Safety Measure in IMO, 66th General Meeting of Ship Research Institute, 1995 (in Japanese)
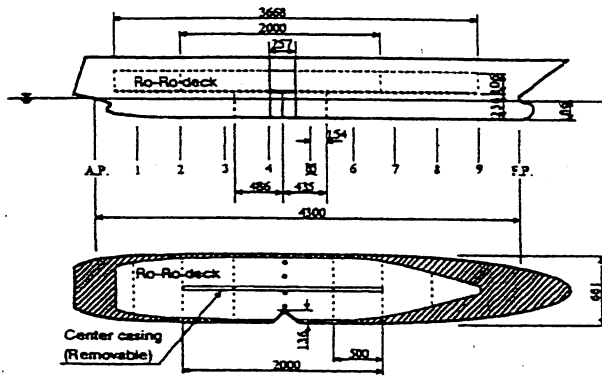
Fig.1 Model and Damage Opening (unit:mm, Broken lines and circles in the lower figure show water level meters and wave height gauges, respectively.)
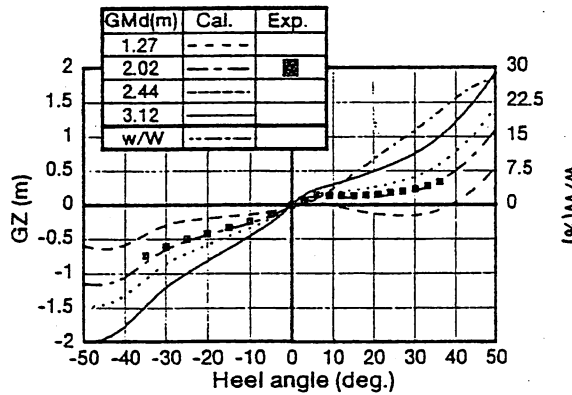
Fig.2 GZ Curves and Amount of Water on Deck in Damaged Condition
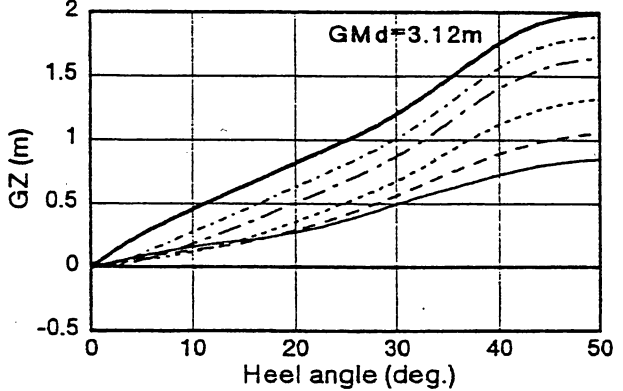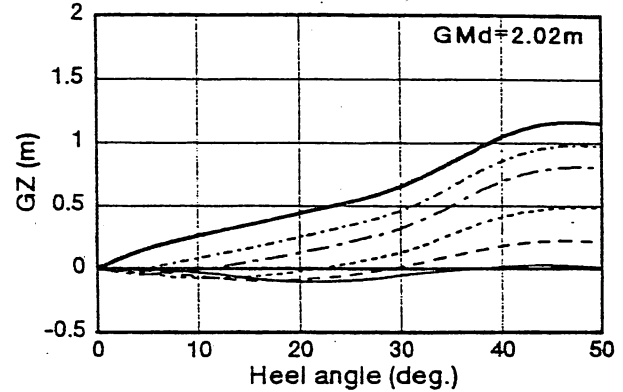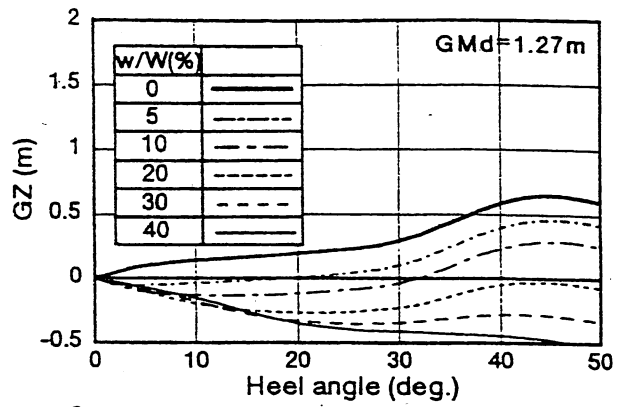
Fig.3 GZ Curves with Constant Amount of Water on Deck
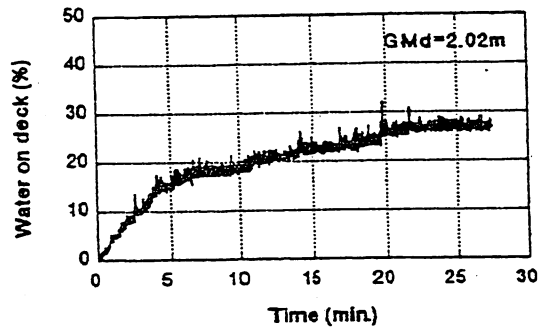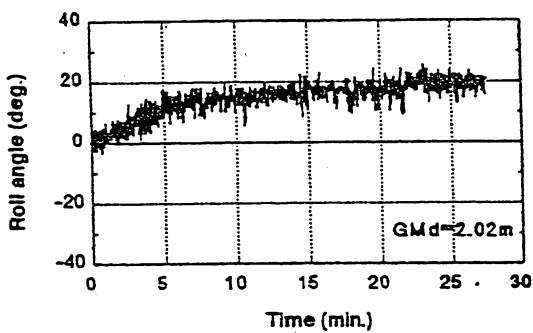
Fig.4 Time History of Roll Angle ϕ and Amount of Water on Deck w (No Center Casing)
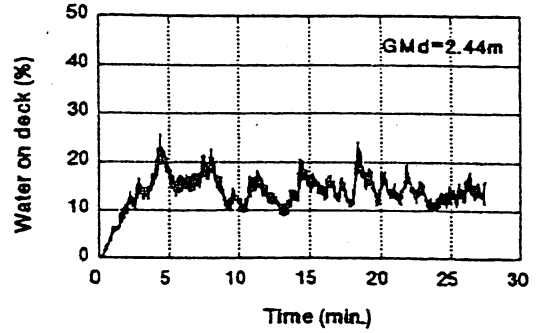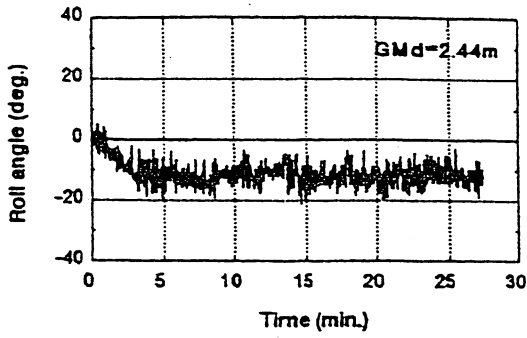
Fig.5 Time History of Roll Angle ϕ and Amount of Water on Deck w
(With Center Casing)
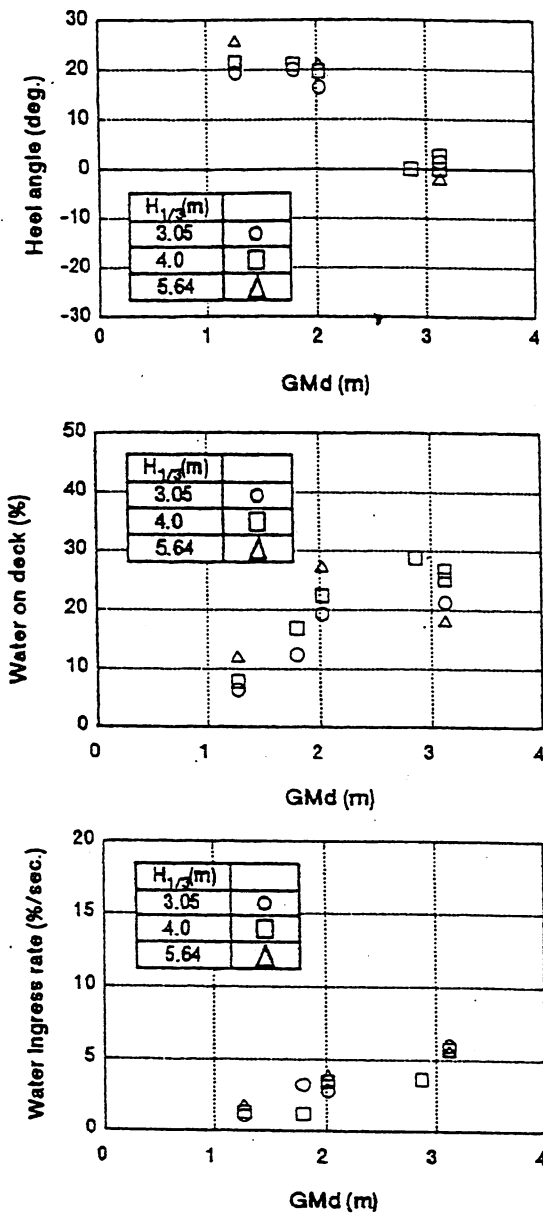
Fig.6 Experimental Results in Irregular
Waves (No Center Casing)
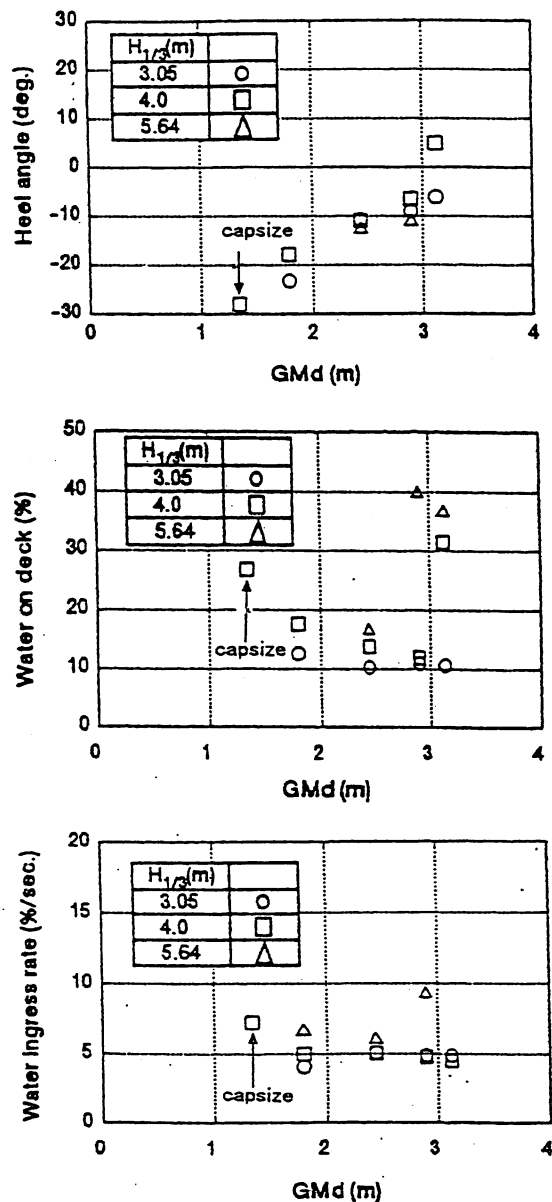
Fig.7 Experimental Results in Irregular
Waves (With Center Casing)
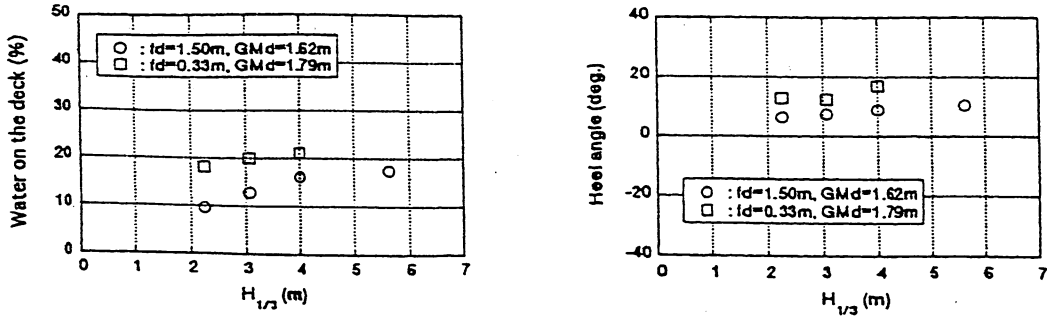
Fig.8 Effects of Freeboard on Heel Angle ϕ_0 and Amount of Water on Deck w_0
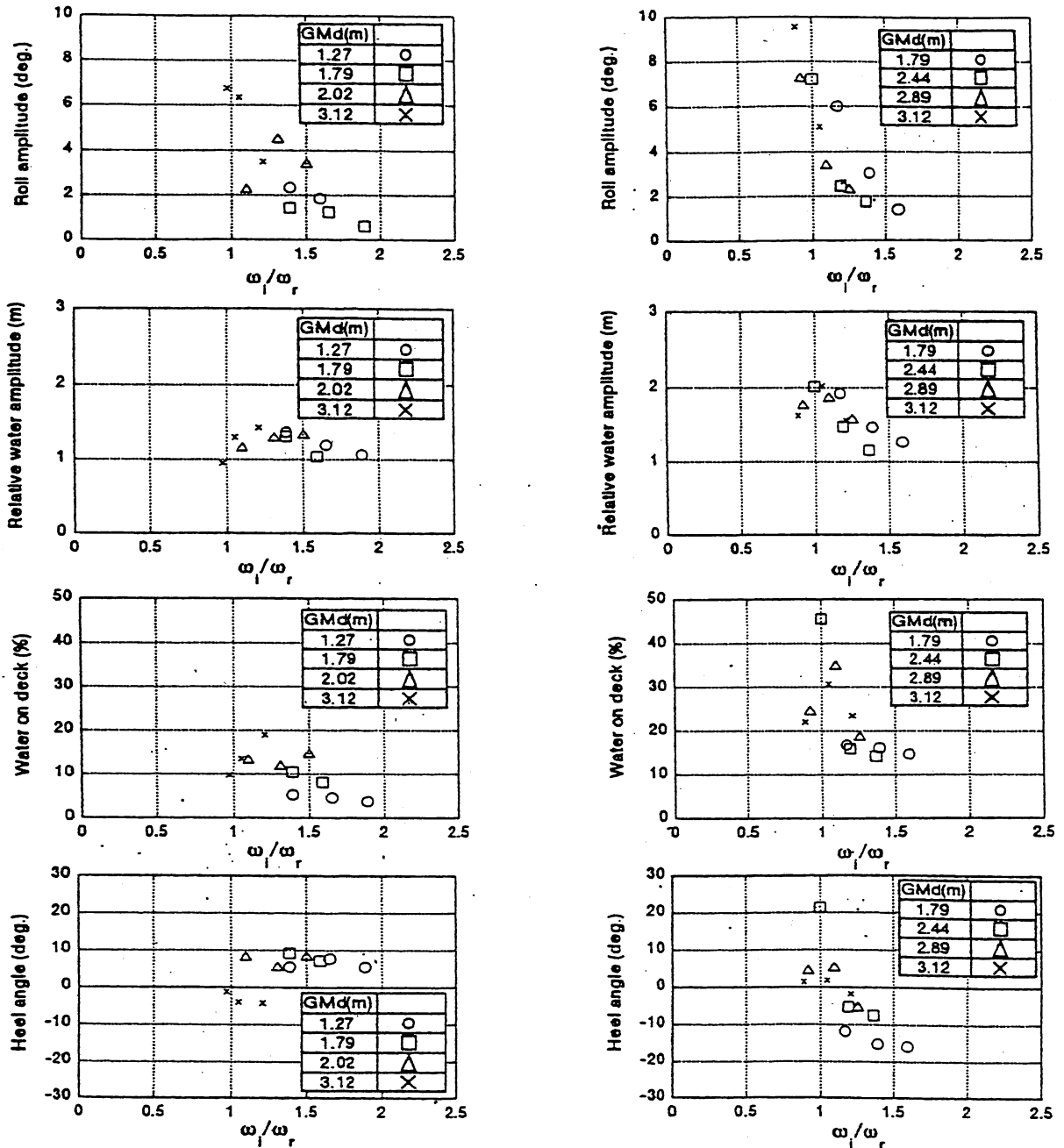
(a) No Center Casing   (b) With Center Casing

Fig.9 Frequency Responses in Regular Waves
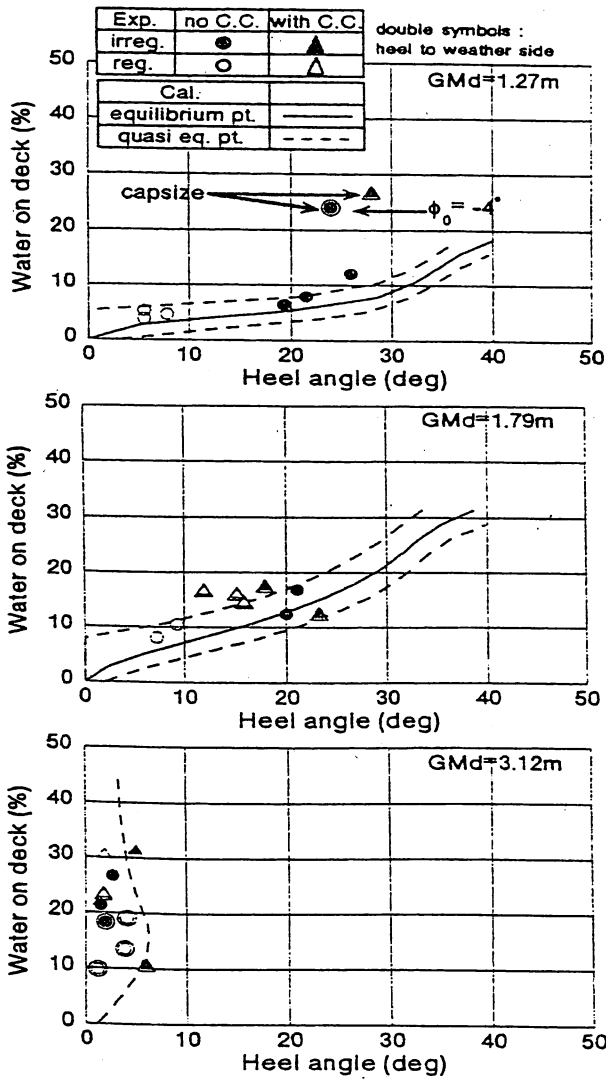
Fig.10 Amount of Water on Deck
w_0 and Heel Angle ϕ_0 in
Stationary Condition
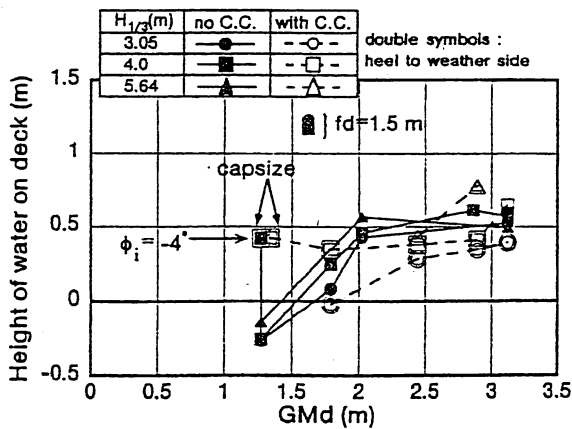
Fig.11 Height of Water on Deck H_d
in Stationary Condition
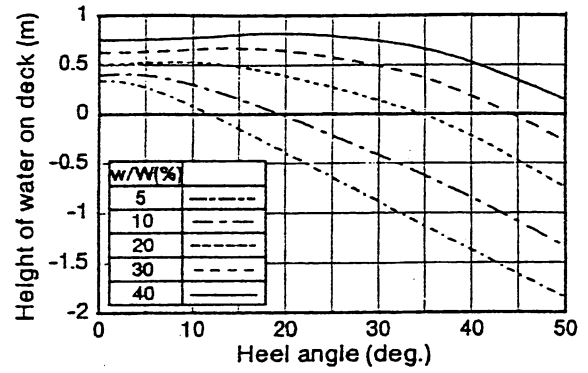
Fig.12 Height of Water on Deck H_d
in Calm Water
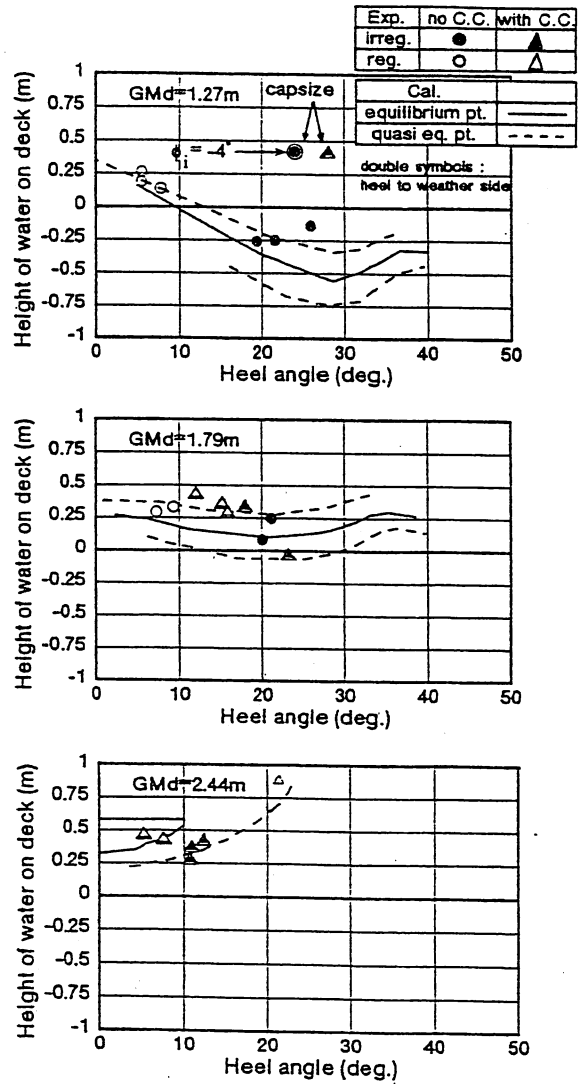
Fig.13 Height of Water on Deck H_d
and Heel Angle ϕ_0 in Stationary
Condition

CHARACTERISTICS OF ROLL MOTION FOR SMALL FISHING BOATS

Kiyoshi AMAGAI*, Kimihiko UENO** and Nobuo KIMURA*
* Hokkaido University, 3-1-1, Minato, Hakodate, 042, Japan
** Tokyo University of Tokyo, 4-5-7, Minami, Minato, 108, Japan

SUMMARY

In most of cases, it has been said that a small amount of water on deck acts as a rather effective roll damper and a roll of ship is less when a small amount of deck water exist than no deck water [1]. In our experiments, we reconfirmed the above effect of a small amount of water on deck. However, in our experiments, there were some cases that a small amount of water on deck did not act roll damper but increased the rolling motion. In addition, when damping effect by free water was enough, yaw was increased. This paper describes those cases from a view point of resonance.

INTRODUCTION

The authors classified roughly into five types of characteristic behavior of shallow water on a ship's deck, based on tests using an oscillatory rectangular tank physically simulated with sinusoidal motion[2]. Furthermore, the authors pointed out that the characteristics of roll damping of small fishing boats with projecting broadside and hard chine depend on rolling amplitude especially. Therefore, the curve of damping was simulated by using the same parameters in the nonlinear equation of free rolling, because damping coefficient were different[3].

This paper describes comparison of rolling motions between the cases when small amount of deck water present and when no deck water.

EXPERIMENT

To clarify rolling motion due to the behavior of water on deck, tank tests were performed by using two ship models (see Table 1 and Fig. 1) in beam sea, at near the resonant period. To evaluate the shipping water effect on ship's rolling motion, a tank was set on the upper deck of the ship model. The dimension of the tanks used in the experiment was shown in Fig. 2. The rise of center of gravity due to the existence of

water on deck is about 1.5 cm increase of A-maru and 0.5 cm increase of B-maru. The inclining angle of roll was measured by using Gyroscope system in free roll experiment. In experiment of forced rolling motion in regular beam waves, the angles of roll and angle of yaw were measured without restriction.

TABLE 1 PRINCIPLE DIMENSIONS OF MODEL SHIP

		MODEL		FULL SCALE	
		A-maru	B-maru	A-maru	B-maru
Lpp	(m)	2.000	1.291	15.20	14.20
B	(m)	0.500	0.330	3.80	3.63
D	(m)	0.195	0.181	1.48	1.25
Disp.	(ton)	0.137	0.066	60.14	8.78
GT	(ton)			19.9	7.9
GM	(m)	0.067	0.031	0.509	0.341

A-maru: salmon drift net boats
B-maru: scallop-farming boats

CHARACTERISTICS OF ROLL DAMPING WITH WATER ON DECK

Considering the bulwark height, water depth of a tank on deck was set at in the range from 0.0 cm to 6.0 cm.

Fig. 3 shows the results of free roll experiment when the damping effect on ship's rolling motion was the most notable in the case when the beginning rolling period was near natural period of water in a tank. As is evident from Fig.3, ship's rolling period tends to get shorter as roll angle decrease, in the case that natural period of water in a tank is longer than ship's rolling period (water depth h=1cm, 2cm). On one hand side, when natural period is shorter than ship's rolling period (h=4, 5, 6 cm), ship's rolling period tends to get longer. It is similar that in the case free water does not exist on deck (h=0 cm).

THE EFFECT OF RESONANCE BETWEEN FREE WATER ON DECK AND FORCED WAVES

Fig. 4 shows a comparison of roll amplitude between free water exist on deck and do

not exist. Here, the horizontal axis means water depth in tank and the vertical axis means the value which roll angle with free water divided by roll angle without free water. When $\phi / \phi o$ is less than 1.0, the effect of damping due to free water can be seen and when $\phi / \phi o$ is greater than 1.0, roll angle is increased. In many cases, the effect of damping due to free water can be seen as former report [1] until now. However, it was confirmed that roll angle was promoted in the case that period of forced wave is a little shorter than the second resonant period (one half of natural period of water in a tank). The value of $\phi / \phi o$ may be taken its maximum at the second resonant. An example in the case of a depth of 1 cm is shown in Fig. 4.

The time series of roll angle corresponding to this case is shown irrespective of a phase in Fig. 5. The behavior of water in a tank is shown in Fig. 6. There were two transient waves which proceeded in opposite directions as in Fig. 6. This behavior appears close to the second resonant period[2]. Therefore, furious shock wave was decreased and then the effect of damping due to free water was controlled.

Fig. 7 shows the roll response by existence of free water on deck. Mark ●symbolizes the result in the case of empty tank and mark ▓ symbolizes the result in the case of existence of free water in tank. The roll response without free water is resonant at natural frequency 4.13 rad/sec. The roll response with free water is greater than it without free water at two frequency (ω ; 2.85 rad/sec, 5.86 rad/sec). When frequency of forced waved ω is 2.85 rad/sec, first resonance occurred because natural frequency of roll ω_n was changed into 2.85 rad/sec from 4.13 rad/sec by free water in tank. When ω is 5.86 rad/sec, this phenomenon is called one of subharmonic resonance and in this case it is second resonance ($\phi / \phi_n = 2.05$) .Fig. 8 shows this effect. It was confirmed that there were two components of natural period of roll and double the period of forced waves. As seen from these example, the existence of free water is sometimes dangerous for the stability of ship.

OCCURRENCE OF YAW DUE TO THE FREE WATER

When we consider coupling of roll and yaw, the effect of yaw is looked upon as slightness compared with the coupling of roll and sway. Therefore, yaw is sometimes neglected. However, it is recognized that the effect of yaw is not neglected when damping effect by free water is enough. A typical example is shown in Fig. 9. The effect of yaw for roll is small and phase difference is short in the case of no free water. When free water exist in the tank even though roll is controlled yaw is increased and can not be neglected as ship's behavior. Still more the phase difference between roll and yaw become large. Fig. 10 shows the cross correlation between roll and yaw. It became clear that roll goes ahead of yaw as time was plus. This increased yaw was caused by the

existence of free water and its location and its behavior.

RESULTS

(1) When natural period of free water is shorter than ship's rolling period, ship's rolling period tends to be longer.

(2) It was confirmed that the roll response with free water is greater than it without free water at the first and the second resonant period of free water.

(3) When free water exist in the tank even though roll is controlled, yaw is increased as compared with it without free water.

REFERENCE

1. Jeff. Dillinghm; Motion Studies of a vessel with water on deck, Marine Technology, Vol. 8, No.1, 38-50, 1981.

2. K. AMAGAI, N. KIMURA and K.UENO; On the practical Evaluation of shallow Water Effect in large inclinations for small fishing boats, Fifth International Conference on Stability of Ships and Ocean Vehicles, USA, Vol.3, 1994.

3. K. UENO, K.AMAGAI, et al.; On the Characteristics of Roll Damping and its Estimation for Small Fishing Vessels, The Journal of Japan Institute of Navigation, 93, 149-161, 1995.
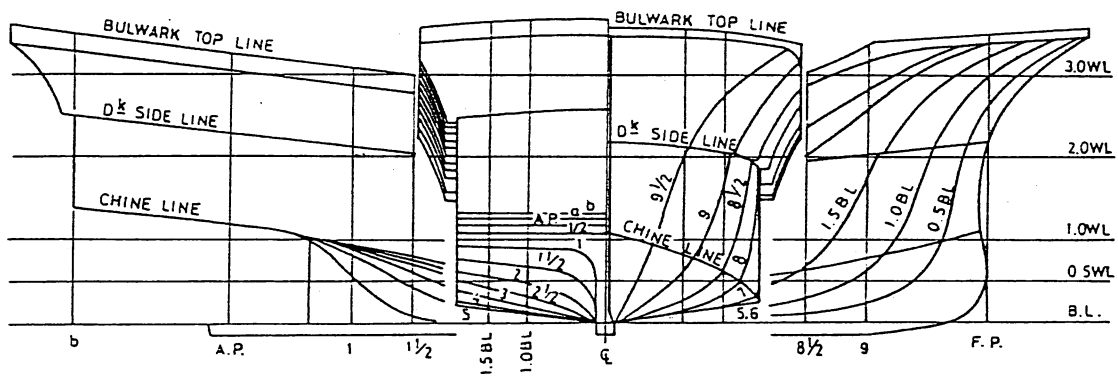
A-maru 19.9 GT
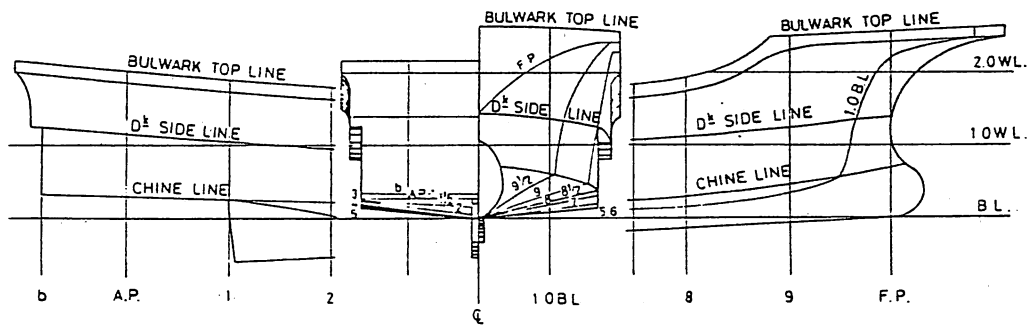
B-maru 7.9 GT

Fig. 1 Lines of model ships
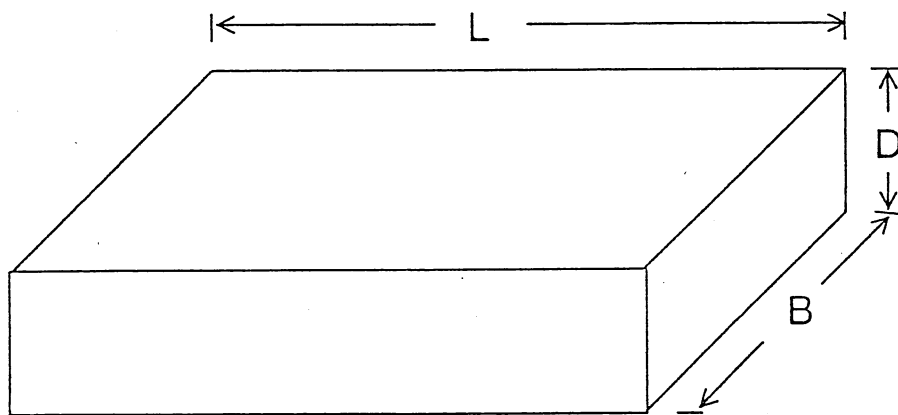
L=50cm, B=20cm, D=10cm (set on A-maru)
L=31cm, B=22cm, D=11cm (set on B-maru)

Fig. 2 Dimension of tanks
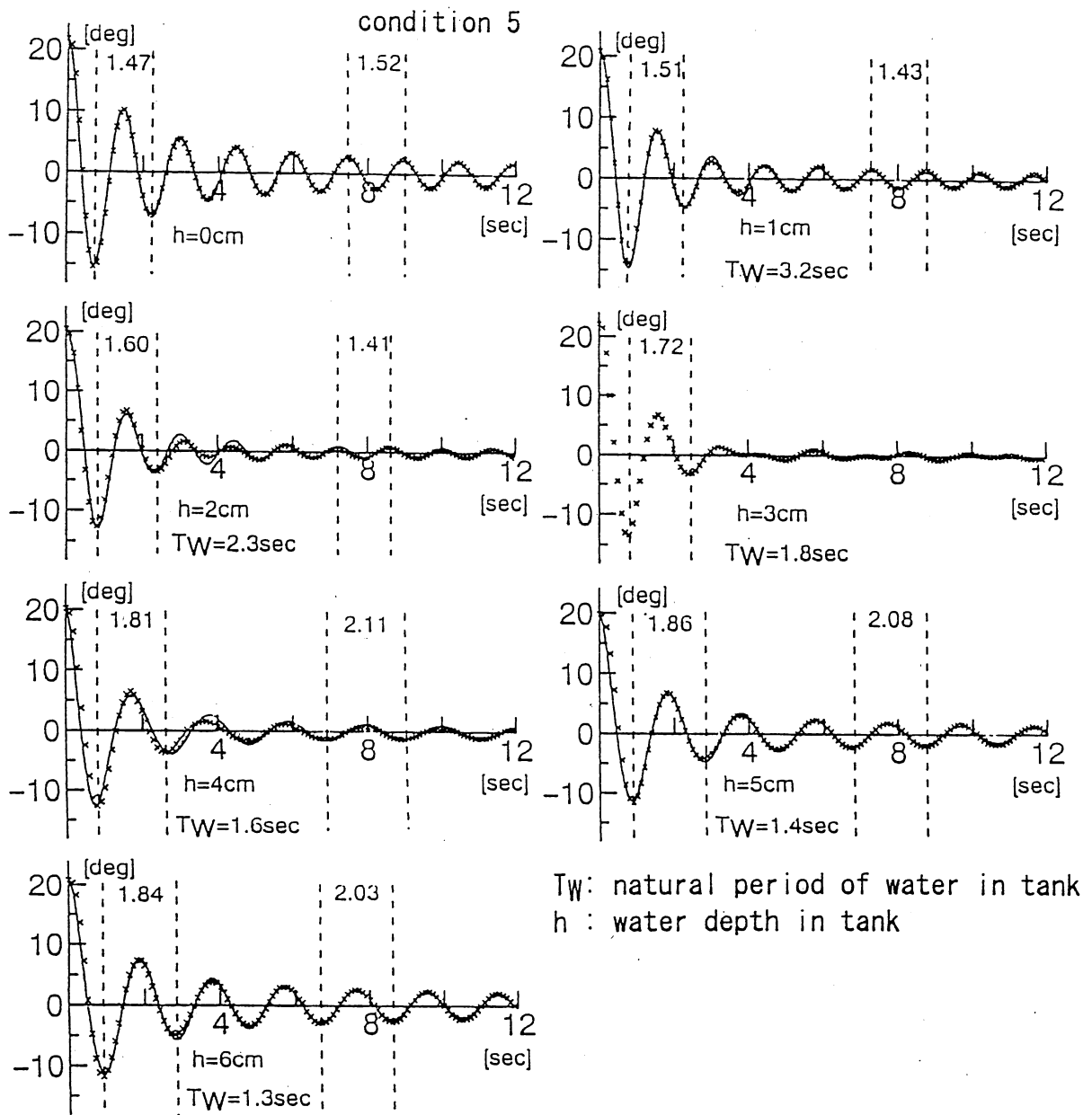
Fig. 3 The results of free roll experiment
with free water, —; Estimate, ×;Experiment

ϕ_h/ϕ_0

period of forced wave   1.3 sec
wave height of forced wave 6.0 cm

1

0.5

water depth in tank 0   1   2   3   4 [cm]

natural period of water   3.2   2.3   1.8   1.6 [sec]
in tank
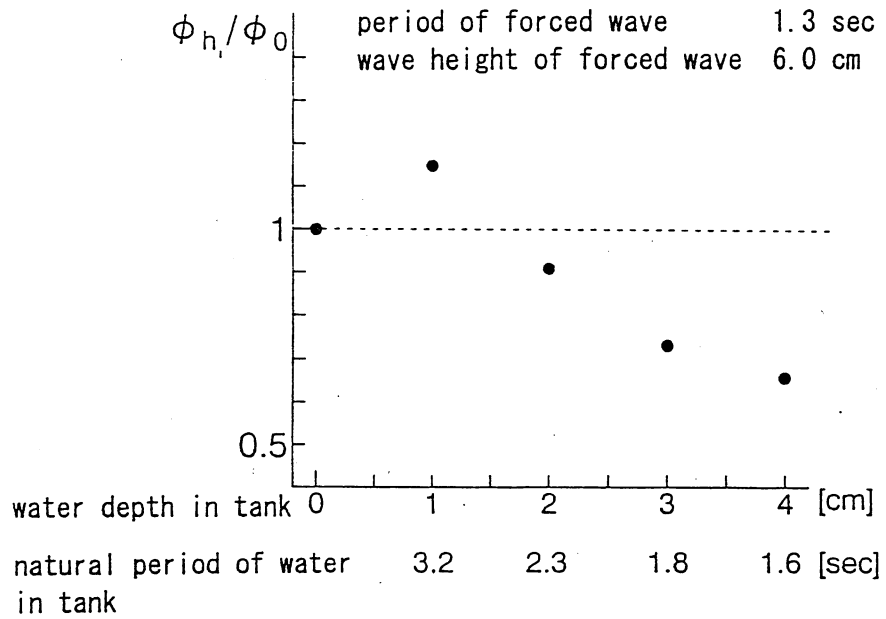
Fig. 4 The comparison of roll amplitude between
free water exist on deck and do not exist

[rad]

0.1

0

2   4   6   [sec]

-0.1

———— empty in tank

--------- water depth in tank 1 cm

natural period of water in tank = 3.2sec,
period of forced water = 1.3sec
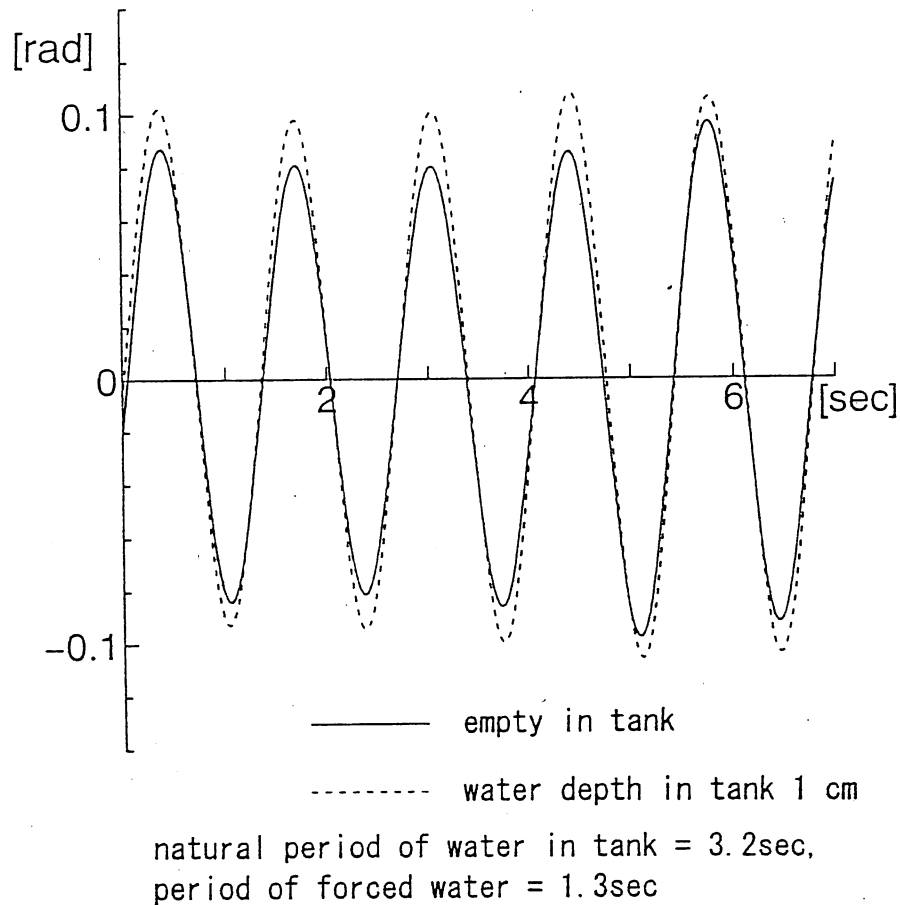
Fig. 5 The time series of roll angle
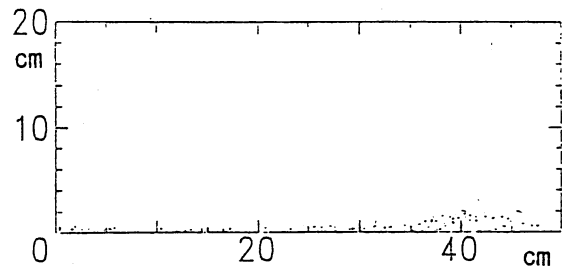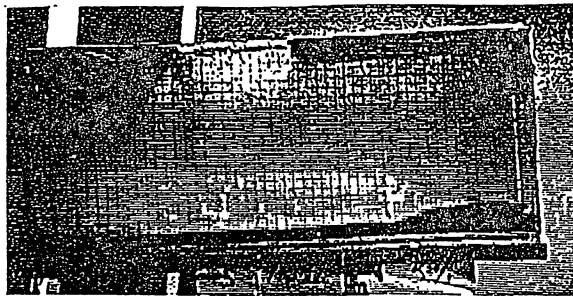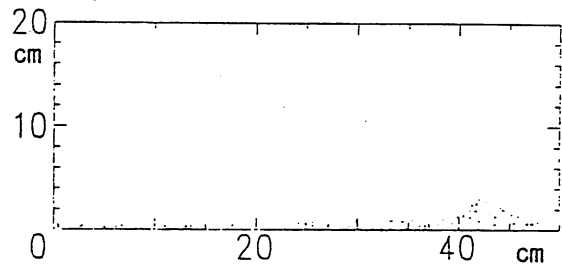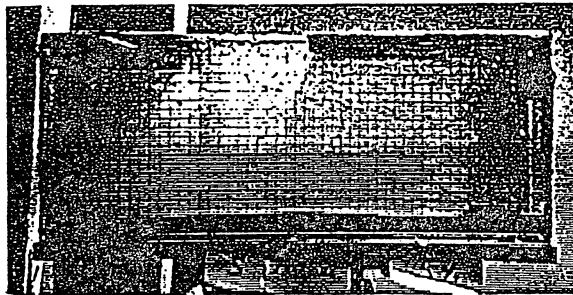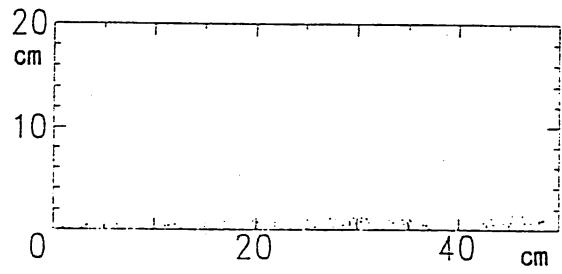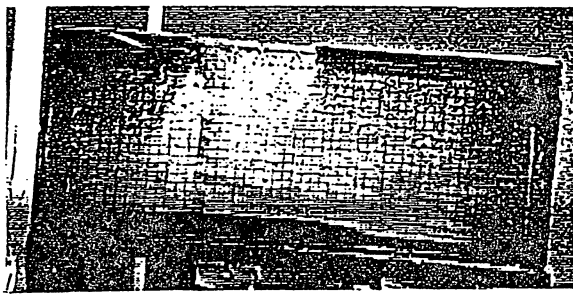
Fig. 6 The behavior of water in tank

● : in the case of empty tank

■ : in the case of existence of free water (water depth 4 cm)

frequency of forced wave

Fig. 7 The roll response

in the case of empty tank

in the case of existence of free water

natural period of roll

period of forced waves
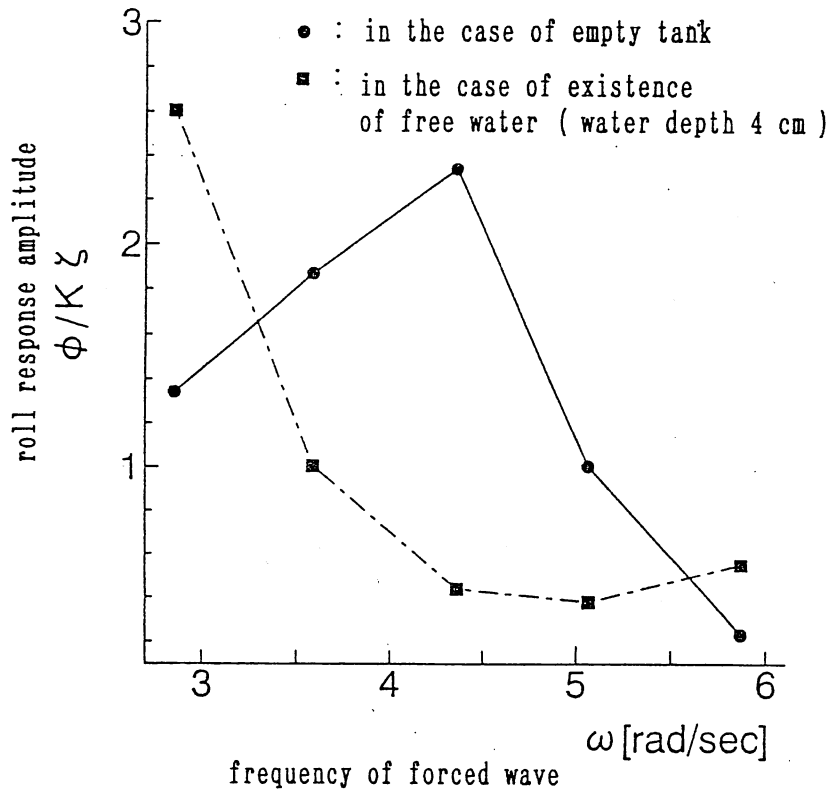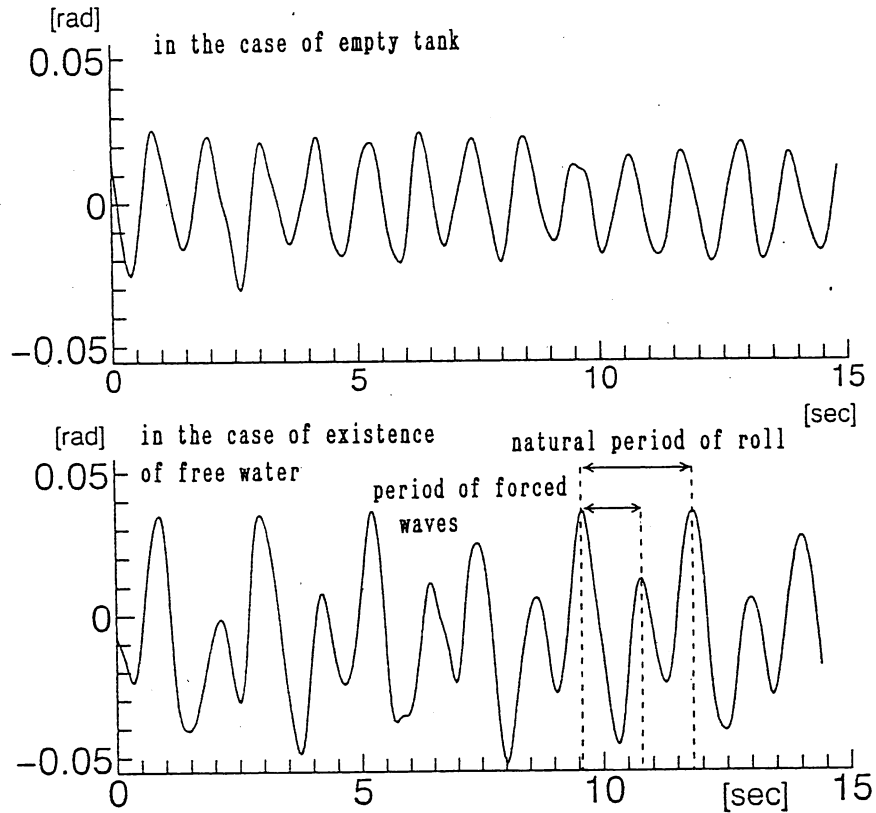
Fig. 8 Time series of roll angle in the case of subharmonic resonance
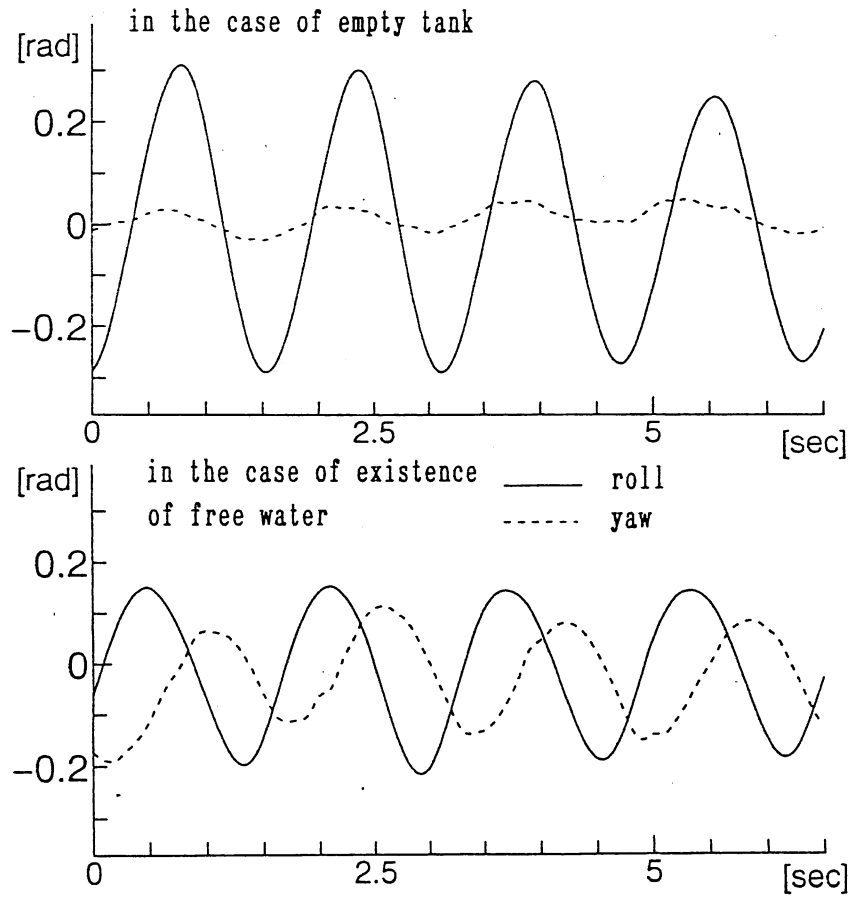
Fig. 9 A typical example of occurrence of yaw
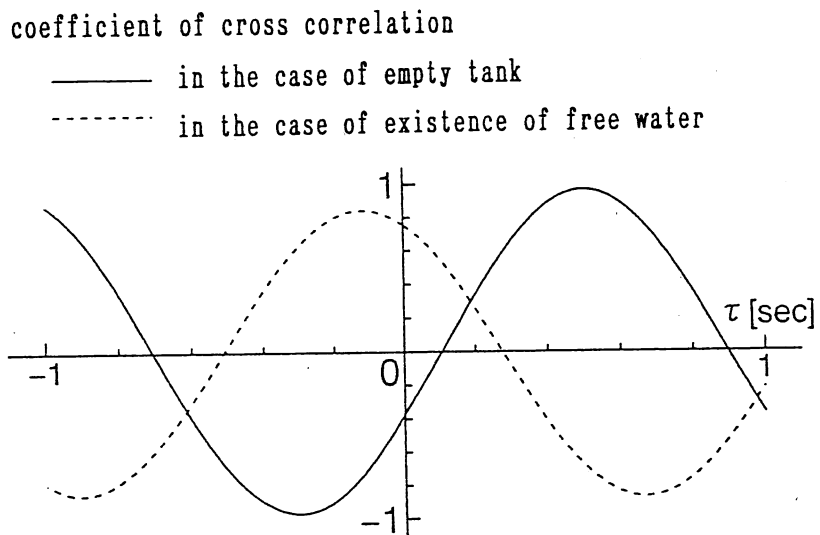
Fig. 10 A coefficient of cross correlation
between roll and yaw

Assessment of Survival Time for Damaged Passenger/Ro-Ro Vessels

by

Dracos Vassalos

University of Strathclyde

NOT AVAILABLE AT TIME OF PRINTING

Dynamics of a Ship with Partially Flooded Compartment

by

Jan O de Kat

Marine Research Institute Netherlands

The Use of Physical Models to Predict the Capsize of Damaged Ships in Waves

by

David Molyneux

National Research Council Canada

Abstract

The hydrodynamics of wave action flooding a damaged ship are complex, and difficult to analyze. Under the wrong conditions, water can accumulate in the ship and ultimately capsize it. Physical models provide the opportunity to study the water flow in and around the hull, and the subsequent behaviour of the ship, without the risk to life or property. The resulting ship models are relatively complex because they must represent the external and internal geometries of the ship and require measurements of body motions, wave amplitudes, and more recently water flow inside the hull. This paper briefly traces the development of this type of modelling, with particular reference to RO-RO ferries. Two types of damage scenario are identified, one as a result of a collision and one as a result of loss or damage to the bow door. The paper then discusses the state of the art for modelling the capsize survivability of damaged ships, based on experience with this type of testing. The minimum technical requirements for the construction of the model, the generation of waves, the conduct of the experiments and the presentation of the results are discussed in detail. Some suggestions for areas of further research in this extremely important area of ship hydrodynamics are also given.

<TITLE>

by
Robert Tagg
Herbert Engineering Co., USA

NOT AVAILABLE AT TIME OF PRINTING

ABOUT SAFETY ASSESSMENT OF DAMAGED SHIPS

Roby Kambisseri and Prof. Yoshiho Ikeda
Osaka Prefecture University, JAPAN.

SUMMARY

In this paper, a new approach to ensure the after damage survivability of ships is discussed. Severity of damage is measured by the size of damage opening. Required safety depends on the value lost if the ship sinks. A safer ship will be the one that can survive a larger damage opening, anywhere over its hull. In impact damage, size of damage opening will be influenced by the strength of structure at the region of impact. Survivability after damage, in a sea state, is to be assessed by a Capsizing Probability, considering also the effect of water shipped into the damaged region and the fluctuating restoring ability of the ship in waves.

Notations

L_s = maximum length on or below subdivision waterline.

INTRODUCTION

A block diagram of safety level, damage and damage stability is shown Fig. 1, which will give a broad outline of the parameters involved in them [1].

Required safety of a ship should be related to the (equivalent - financial - value) loss that can be caused by the sinking of that ship. The more the value involved in a ship, the more safer it should be against sinking. In the case of damage stability, more valuable ship should be able to withstand severe or larger size of damage (opening) on its hull or in other words should be able to withstand larger damages or heavier collision. The size of the opening caused on the hull of a ship will depend on the impact load and the strength of the structure in and around the location of collision. For the same damage opening, size of the space open to sea (i.e., damage space) will depend on the subdivision of the ship and the location of damage. Weakest region, or the smallest damage opening for which a
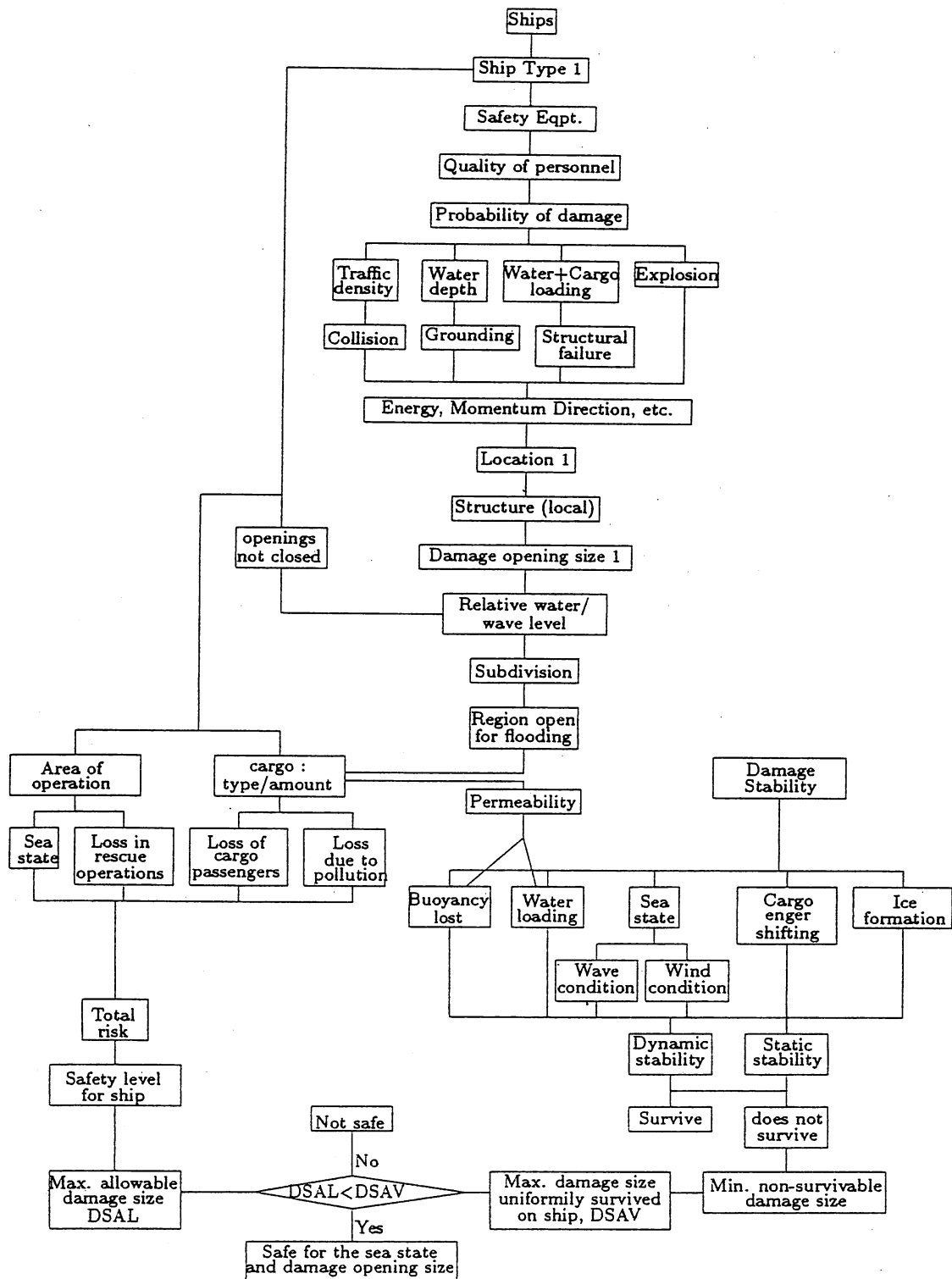
Figure 1: Block diagram of safety level, damage and damage stability

Values in figure are the probability of damages
occuring between the two transverse bulkheads

Crossed regions shows the damages not survived

R=0.5815   A=0.6595

0.0	.0024	.0004	0.0	.0004	.004	0.0		
.0024	.0063	.035	.0032	.0035	.043	.01	.01	
.032	.044	.024	.032	.08	.038	.031	.065	.07
.0229	.0437	.0357	.007	.08	.087	.0088	.0474	.06	.072

0   17   47   70   79.   110   141   150   172   197 216.2

◄————Bulkhead positions (m)————►
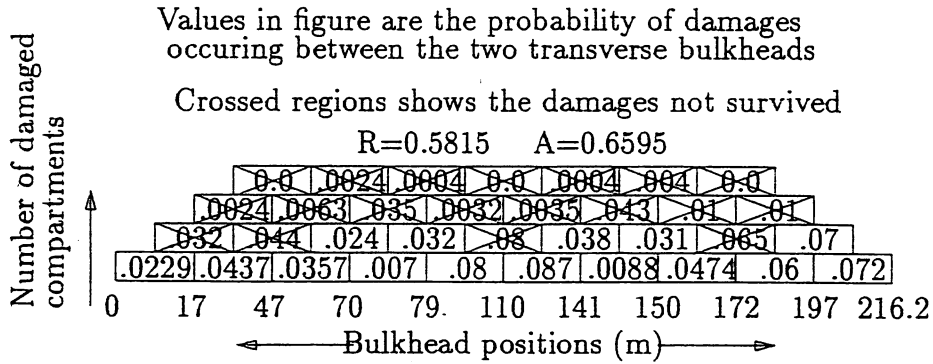
Figure 2: R, p_i and A for D=16 m

Values in figure are the probability of damages
occuring between the two transverse bulkheads

Crossed regions shows the damages not survived

R=0.5815   A=0.8782

0.0	.0024	.0004	0.0	.0004	.004	0.0		
.0024	.0063	.035	.0032	.0035	.043	.01	.01	
.032	.044	.024	.032	.08	.038	.031	.065	.07
.0229	.0437	.0357	.007	.08	.087	.0088	.0474	.06	.072

0   17   47   70   79   110   141   150   172   197 216.2

◄————Bulkhead positions (m)————►
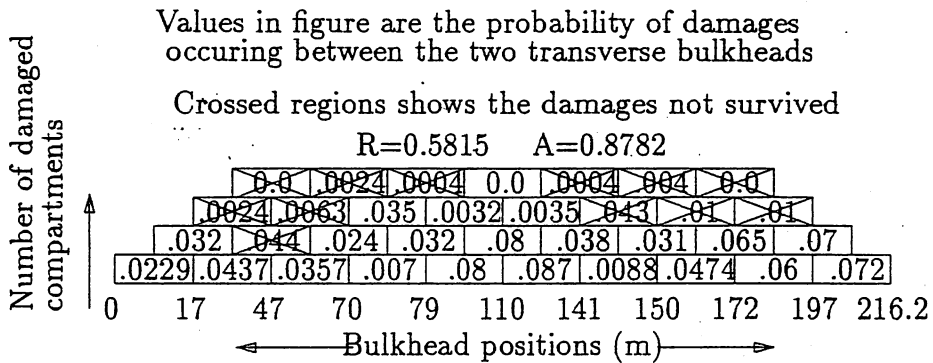
Figure 3: R, p_i and A for D=18 m

ship become unsurvivable, should determine the actual safety or damage surviving ability of that ship. Strength of the structure of a ship can be included if the size of damage opening is determined from impact load. Loss caused by the sinking of a ship or it mapped into a safety scale can be used to determine the size of the damage opening or the damage opening caused by an impact load which should be survived by the ship. The ship should achieve this in the sea states it has to operate. Survivability in a sea state is assessed by a capsizing probability study of the ship taking also into account the righting ability in the sea condition as well as the change in the righting ability due to the presence of water in the damaged region.

DEFECTS OF PROBABILISTIC RULES [2] [3] [4]

Minor damage

Figs. 2 and 3 show the probabilities of collision damages of a ship with different depths[1]. All non-survivable cases of damages ($s_i = 0$) are shown crossed. Both the cases satisfy the present criteria based on probabilistic approach (i.e., Attained subdivision index, A is not less than Required subdivision index, R), but can be lost by minor damage/s. The smallest damage that can sink these ships, with different A values, is the same. i.e. A higher A value doesnot ensure a higher level of safety.
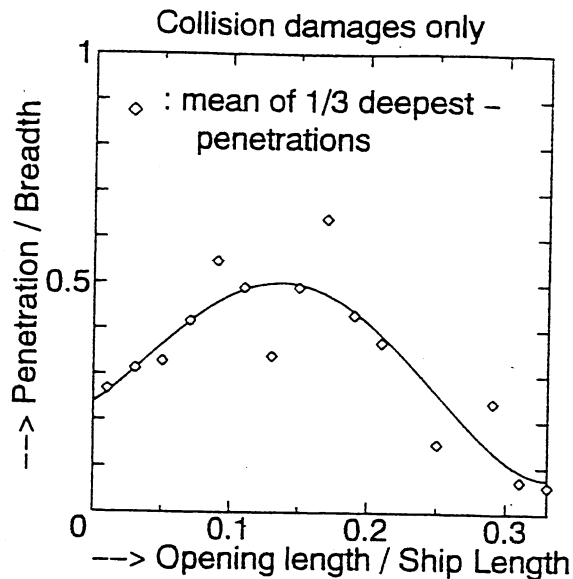
Figure 4: Change of damage penetration with damage opening length

Structural strength

In the present damage stability rules, extent of damage opening is determined on the basis of statistical data of (collision) damage. Real damage opening size, however, depends on many factors like strength of struck and striking ships, mass, velocity and bow shape of striking ship, striking angle and yawing velocity, etc. So, for the same collision, damage opening could vary with the variation in strength of local and global structure of ships.

Damage Penetration

In the probabilistic rules, damage penetration is assumed to increase with the damage length. Variation of damage penetration with the damage opening length is given in Fig. 4 [1]. This is drawn using the means of the $1/3^{rd}$ deepest penetrations of collision damage data used in the probabilistic rule. Very long damage openings may not be deep and such damages can be survived using longitudinal subdivisions [5]. Damage penetration significantly depends on the structural strength of struck ship.

Survivability criteria

Present stability criteriae is based on calm water righting ability curve and without considering the additional loading due to free water in damaged spaces. [2] [3].

A new approach

The deficiencies of the present damage stability rules, which is mentioned above, call for a new criteria and a method for its application[1]. In future, developments and new ideas in ship technology should be reflected in the damage stability rules. In the following sections, a concept of a new approach to future damage stability rules will be proposed.

SURVIVABILITY

How to determine whether a ship can survive a sea with a portion of its hull damaged ? For this, the remaining intact portion of the hull, the damaged space with or without water which is or not flowing in and out of it and the water (waves) supporting the ship and their contributions are to be included into the intact stability analysis of ships.

A possibility that may not occur to intact ships is that the damaged ships may capsize due to loss of longitudinal stability[6].

The contribution from the water in the damaged space may increase or decrease the restoring ability. Studies shows that when a ship is flooded, the ship rolls about the heel angle caused by flooding [7]. This is because if the ship heels then the water gets trapped between two slanting planes without much scope for flowing and the amount of energy required to move the water over this sloped surface to the other side of the ship is much greater than the energy contribution of the exciting forces. When the ship rolls, the motion of inside water lags behind the rolling motion and the energy of flow and the impact on the sides of the ship will have a damping effect on the rolling and will be on the safer side. So, the static effect seems to be critical to the damaged stability of ships. However, further studies are needed to see if there is any adverse dynamic effect.

For any sea state a capsizing probability[8] can be predicted considering all the factors that contribute to the stability of a ship. A required minimum value of capsizing probability can be used to classify the survivability after damages. The capsizing probability will determine whether a ship with a damage is survivable or not.

The variation in the methods employed in the estimation of motion in waves, effect of damage water, etc., may result in different values of capsizing probability for a ship. A rule-software could be used to standardise the calculation of capsizing probability and to ascertain the safety level of ships.

SAFETY PARAMETER

How to grade the after damage safety of ships ? If there is more than one design, meeting the same requirements, how to determine which one has the best damage stability ? Figs. 5 and 6 shows two subdivisions based on the same floodable length curve. The first one can survive a largest damage opening of size $.38L_s$ and the smallest damage opening size it cannot survive is $.077L_s$. The second one can survive a largest damage opening of size $.45L_s$ and the smallest damage opening size it cannot survive is $.20L_s$. The second subdivision is safer against any damage caused by damage openings of size upto $0.20L_s$ where as the first one can be sunk by an opening of size $.077L_s$. The second subdivision will be more safer from the point of view of damage stability, since it will not be sunk even by a collision or impact much heavier than the one which will capsize the first. Safety level of damaged ships can be graded using the minimum damage opening size that the ship cannot survive. i.e., the parameter which defines damage safety is the size of the damage opening. Damage opening size depends also on the strength of the structure. To include it, safety parameter is to be changed to the impact load and the ship should survive all the damages caused by the damage openings created by that impact. This will help to identify and strengthen structurally weak locations on a ship.
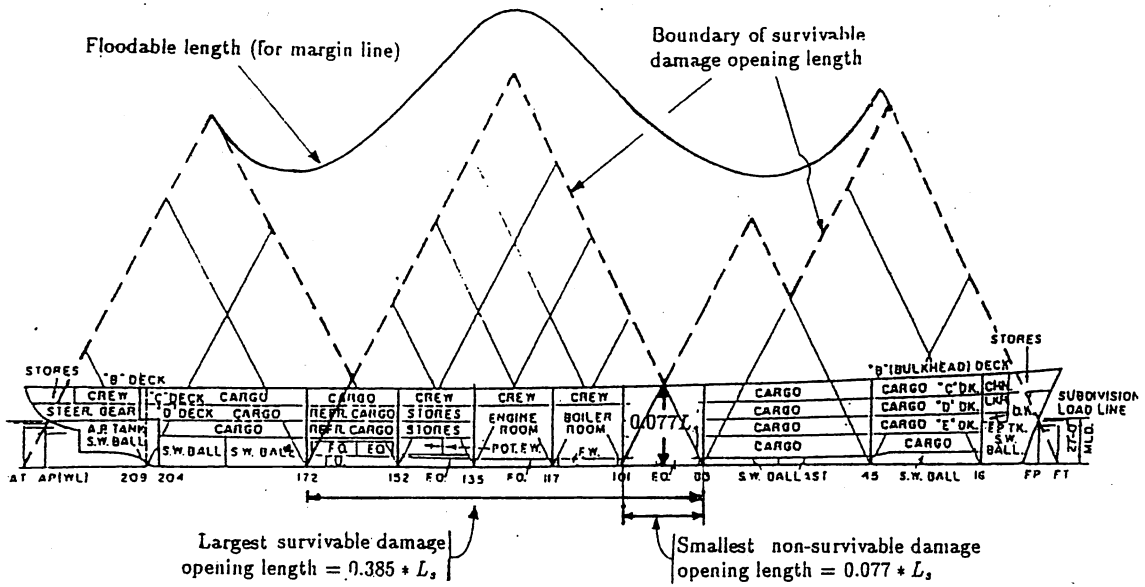
Figure 5: Survivable damage opening length boundary - A
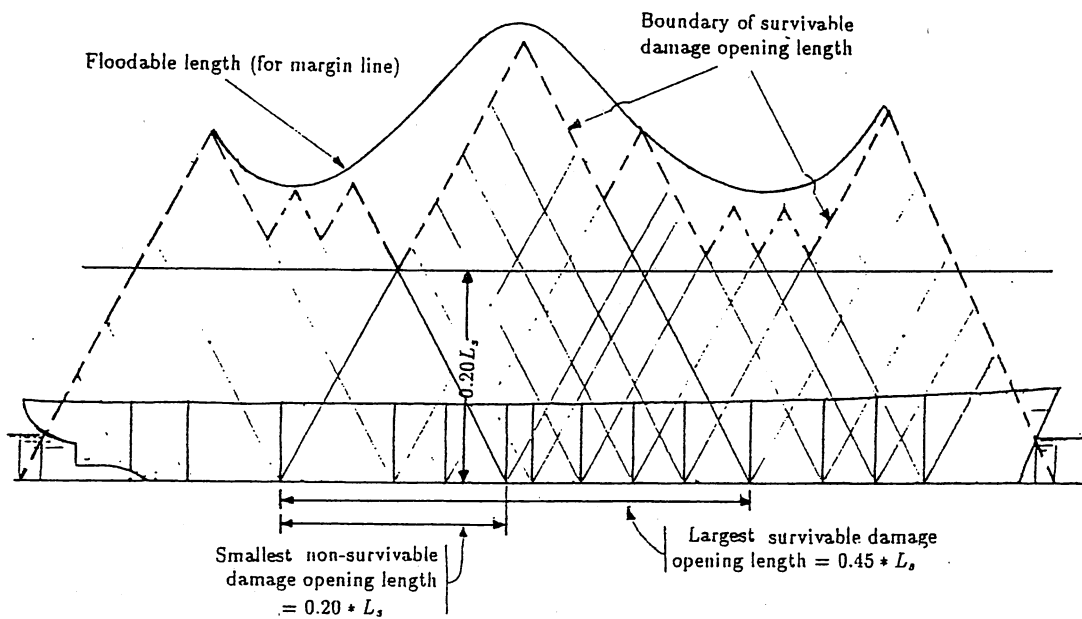
Figure 6: Survivable damage opening length boundary - B
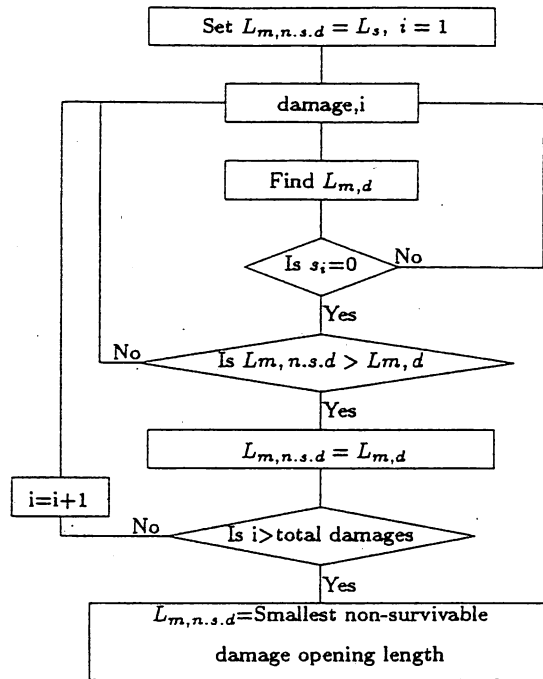
Figure 7: Flow chart to find the smallest non-survivable damage opening length

Algorithm to find minimum non-survivable damage opening size

The maximum survivable damage opening, damages caused by which can be survived anywhere on a ship, can be found by the following method[1].

Select the minimum damage opening length ($L_{m,d}$) which can cause a damage as follows :

a. If one compartment damage (no bulkheads damaged), we can assume, $L_{m,d} = 0.1m$

b. If two compartment damage (one bulkhead damaged), we can assume, $L_{m,d} = 0.5m$

c. If three or more compartment damage (two or more bulkheads damaged), $L_{m,d}$ = distance between foremost and aftmost of the bulkheads damaged.

The Flow chart in Fig. 7. will give the smallest damage opening length ($L_{m,ns.d}$), some of the damages caused by which cannot be survived by the ship.

If $L_{m,ns.d}$ is $0.1m$ then the ship is non-survivable for at least one damage in which no bulkhead is involved. If $L_{m,ns.d}$ is $0.5m$ then the ship can survive all cases where bulkheads are not damaged and is non-survivable atleast for a one bulkhead damage. If $L_{m,ns.d} > 0.5m$ then the maximum damage opening length survivable over the hull will be little less than $L_{m,ns.d}$.

FIXING SAFETY LEVEL

It is always difficult to define the safety level required for each transportation system. It may be relative, and vary from time to time. The required safety level, however, depends on each ship, and has to be measured by the loss generated by accident, including pollution of marine environment in addition to the loss of ship including its passengers, crew and cargo, loss in rescue operation, etc. Economic aspects of ship's operation also

have significant effect on the required safety level. Therefore it depends on ship type, size, capacity, missions, region of operation, etc.

The more valuable or the more dangerous an object is, it is to be given better protection so as to avoid it from loosing or to avoid it causing destruction. The level of protection given should be in commensurate with the value of the object or the loss it could cause. The same is also applicable to ships. Level of safety of a ship should depend on the value of the ship including its cargo and passengers and the loss it could cause by way of pollution, etc. Shipping is a profit oriented operation. The cost required to prevent the loss of a ship should not be disproportionate with the value loss causable by the loss of ship. Here comes the conflict between the shipping and regulating agencies. Shipping agencies eyeing at profit and regulators aiming at safety. So, it is appropriate to have regulations which will allow safety within the economic feasibility.

A ship should be designed to have enough capsizing probability for all damages caused by damage openings upto a certain size; the size is determined for each ship to match its required safety level. It need not survive larger damages, since the risk involved may not be sufficient enough to bear the cost of ensuring survival of a bigger damage.

Three models are given for determining the damage opening size required to be survived by a ship. Perfect survivability or a certain survival probability is assumed to be guaranteed for all damages caused by the damage openings upto this size; the survival probability decreases with the increasing damage opening size.

Model 1

In this model[1], $(Persons\,on\,board)/(L * B * d)^{1/3}$ is assumed to give the safety level. The following relation maps the safety level and damage opening size.

$$Percentage\,damage\,opening\,size = K * \frac{Persons\ on\ board}{(L * B * d)^{1/3}} \qquad (1)$$

where L is the length, B is the breadth and d is the draft of the ship. K is 0.25 for the data in Table 1, assuming a maximum possible damage opening size of $0.24L_s$, which is same as that in the present rules. This is a very simple model, and suitable functions for safety level, damage opening size and their mapping is to be found.

Model 2

In this model [1] a safety level is to be fixed using probable loss due to the sinkage of the ship. Using computer simulations of structural damage, damage experiments and damage statistics, the probability for each damage opening size can be fixed. A relation mapping the required safety level or risk involved, to the size of damage opening could be used to ensure a survivability standard varying with safety. A graph similar to Fig. 8, showing the relationship between the safety level and the damage opening length, can be used to find the damage opening length required to be survived by a ship. Initial part of the graph is the probability distribution of (collision) damage - maximum probable damage opening length of which is around $0.35L_s$ - which is modified and extended so that the damage opening length is the length of the ship when the safety level is the maximum. This graph and the ranges of both its axes could be different for different types of ships and could vary even between different ships of a type. This model has

L	B	d	P	$\frac{P}{L}$	$8(\frac{P}{L})^{.5}$	$\frac{0.25P}{(LBd)^{\frac{1}{3}}}$
166.0	27.2	8.7	341	2.05	11.47	2.51
211.9	32.2	7.5	2621	12.37	28.14	17.65
105.0	19.5	4.7	7	6.67	20.66	8.23
157.7	23.4	5.8	114	0.72	6.80	1.03
118.5	24.0	7.7	16	0.14	2.94	0.14
150.0	29.0	6.6	2	1.33	9.24	1.63
285.0	40.0	8.0	37	12.98	28.83	20.55
155.8	21.4	5.2	306	1.96	11.21	2.96
256.0	32.2	12.0	27	0.11	2.6	0.15
320.0	58.0	20.8	36	0.11	2.68	0.12
156.0	26.7	9.7	28	0.18	3.39	0.20
174.3	32.2	11.2	34	0.2	3.53	0.21
176.0	32.0	11.3	25	0.14	3.02	0.16
143.0	23.0	6.2	415	2.90	13.63	3.8
126.8	18.4	3.6	1606	12.67	28.47	19.75
107.0	19.5	5.3	473	4.42	16.82	5.31
185.0	30.8	7.5	2866	15.49	31.49	20.49
320.0	58.0	20.8	4	0.13	2.83	0.14
177.0	26.3	7.0	1887	10.66	26.12	14.77
183.0	28.0	7.5	2394	13.08	28.94	17.74
190.8	28.0	7.5	2566	13.45	29.34	18.75
224.0	31.5	7.8	3554	15.87	31.87	23.41
177.0	26.3	6.8	1396	7.89	22.47	11.03
190.8	28.0	7.5	1896	9.94	25.22	13.85
171.6	32.0	6.8	3313	19.31	35.15	24.78
170.0	27.8	6.0	14	8.24	22.96	11.48
163.1	26.8	6.7	1669	10.24	25.6	13.54
103.0	18.9	5.0	138	13.40	29.28	16.168
170.0	25.5	6.6	711	4.18	16.36	5.81
103.8	19.2	4.7	75	7.23	21.50	8.9
101.8	20.7	5.3	417	4.1	16.19	4.66

P is the number of passengers.

Table 1: Trial relations for safety level
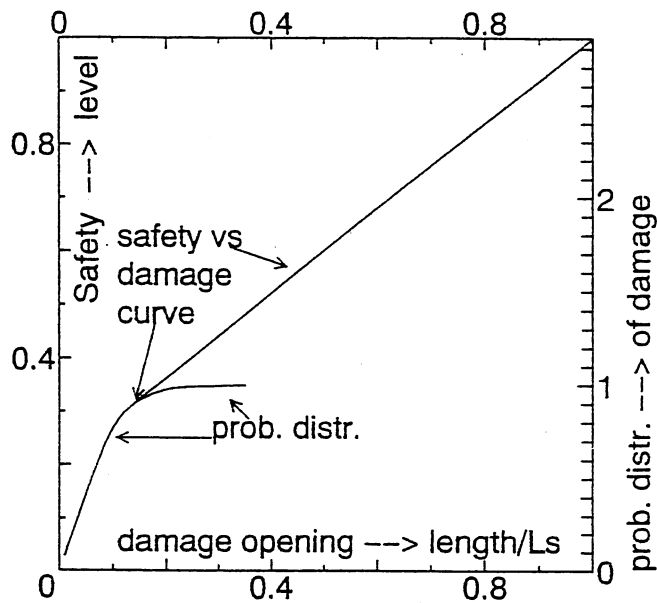
Figure 8: Required survivable damage opening length (model 2)
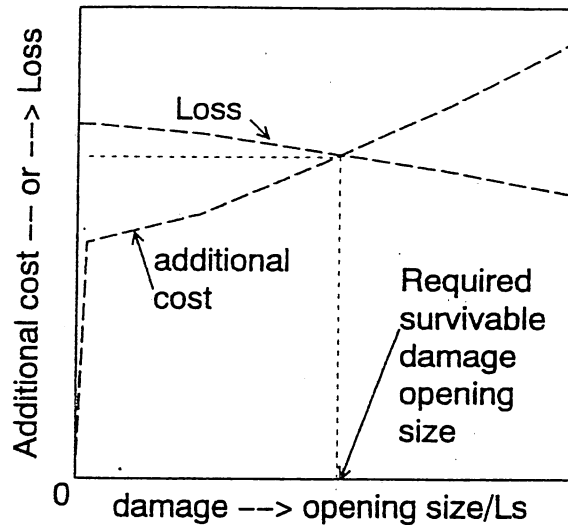
Figure 9: Required survivable damage opening size (model 3)

some flexibility in accommodating the changes in the concept of safety, changes in the structural strengths of ships and the changes in mapping between safety level and damage opening. Relation to determine the safety level and the mapping should be fixed only after careful study.

Model 3

This is a complex model. In this the damage opening size that a ship is required to survive can be found using the relation shown in Fig. 9. This figure could be made for each ship. The additional cost is the cost required to make a ship which cannot survive any damage to one which can survive all damages caused by a damage opening size. Loss is the loss or a proportion of the loss involved in the loss of the ship due to a damage caused by the damage opening size. It must be taken into account that the probability of collision and a capsize due to that is very small.

Comparision of Rules and New Concept

The salient features of the present rules and the new approach is given in Table 2 for comparision and better understanding.

CONCLUSION

The stability criteria and the method to vary safety level of ships applied in the present damage stability rules are not sufficient for ensuring safety of damaged ships as well as to grade the relative safety of ships. On the basis of recent studies a new way of arriving at a realistic survivability criteria is proposed in this paper, which is used to estimate a capsizing probability. Safety level of a ship is connected to the value loss that can occur with the sinking of the ship. Size of a damage opening is identified as the

Sl. no.	Features compared	Deterministic Rule	Probabilistic Rule	Present Conceptual proposal
1	Safety parameter	Factor of subdivision, F	Required subdivision Index R	Survivable damage opening size
2	Safety parameter depends on	Length of ship, No. of passengers	Length of ship, No. of passengers, Life boat capacity	Probable loss or risk due to capsize of ship
3	Damage space considered	all damages whose length not greater than floodable length	all damages caused by damage openings of upto $\frac{48}{L_s}$ but $\not> 0.24$	all damages caused by damage openings of a certain size
4	Damage opening size based on	Floodable length (in effect)	Collision damage statistics	Probable loss due to capsize of the ship
5	Damage survivability	all damages should meet after damage stability requirements	only a percentage of the above damages need be survived	all the above damages to meet survival criteria
6	Ship structure	not considered	not considered	survivable damage opening size to depend on structure
7	Defect of the approach	for same damage opening, survivability decreases with increase of required safety	minor damage non − survivability could be present	?
8	Survivability Criteria	based on calm water GZ curve	based on calm water GZ curve	based on restoring ability in Sea and Capsizing Probability
9	Loading due to flood water	not considered	not considered	to be included
10	Survivable sea state	not specified	not specified	sea state to be specified

Table 2: Salient features of present damage stability rules and new proposal

parameter that should define the safety level. All the damages caused by openings upto this size is to be survived by a ship. Three models to determine the damage opening size that should be survived by a ship is also shown in this paper.

REFERENCES

[1] Roby Kambisseri and Yoshiho Ikeda : A New Approach to Damage Stability Rule (1st Report) - Discussion on the Present Rules and the Concept of the New Approach -, J. of Kansai Society of Naval Architects, Japan, No. 226, Sept., 1996.

[2] SOLAS consolidated edition, 1992.

[3] IMO Resolution A.265 (VIII), 1973.

[4] Roby Kambisseri and Yoshiho Ikeda : A Comparative Study of the Probabilistic Damage Stability Rules and Proposals, Contemporary Ideas on Ship Stability, Univ. of Strathclyde, 1995.

[5] Roby Kambisseri and Yoshiho Ikeda : Compartmentation - Best Guide for Damage Stability or What is Wrong with the Floodable Length Approach of Subdivision, Contemporary Ideas on Ship Stability, Univ. of Strathclyde, 1995.

[6] Nobuyuki Shimizu, Roby, K. and Yoshiho Ikeda : An Experimental Study on Flooding into the Car Deck of a RORO Ferry through Damaged Bow Door, J. of Kansai Society of Naval Architects, Japan, No. 225, March 1996.

[7] John T. Stubbs, Peter van Diepen, Juan Carreras and Joseph H. Rousseau : (Draft report) TP12310E Flooding Protection of RO-RO Ferries, Phase I (Volume 1), Transportation Development Centre, Policy and Coordination, Transport Canada. March 1995.

[8] Umeda N. and Ikeda Y. : Rational Examination of Stability Criteria in the Light of Capsizing Probability, Vol. 2, STAB'94.